2013

Investigation of deterioration of joints in concrete pavements

Jiake Zhang
Iowa State University

Investigation of deterioration of joints in concrete pavements

by

Jiake Zhang

A dissertation submitted to the graduate faculty

in partial fulfillment of the requirements for the degree of

DOCTOR OF PHILOSOPHY

Major: Civil Engineering (Geotechnical Engineering)

Program of Study Committee:
David J. White, Co-Major Professor
Peter C. Taylor, Co-Major Professor
Kejin Wang
Halil Ceylan
Tom Rudolphi

Iowa State University
Ames, Iowa
2013

DEDICATION

This dissertation is dedicated to my parents for their unconditional love and support, and it is their support, encouragement, and constant love have sustained me throughout my life.

TABLE OF CONTENTS

LIST OF FIGURES

LIST OF TABLES

ABSTRACT

Premature deterioration of joints in concrete pavements is reportedly a problem in cold weather regions. Distress is often first observed as shadowing when microcracking near joints traps water followed by loss of materials around the joints. It is also seen as cracks parallel to the saw cut. Although not all pavements are distressed, the problem is common enough to warrant attention.

The goal of this study was to improve understanding of the mechanisms behind premature joint deterioration in concrete pavements. Objectives of this study were to (1) conduct laboratory freeze-thaw tests to investigate the effect of concrete interfacial zone to the deterioration, (2) evaluate the influence of pore structure of cement paste to the freeze-thaw durability using mercury intrusion porosimetry (MIP) tests, and (3) use of a borehole permeameter to conduct a field study to assess the influence of the permeability of subsurface layers on joint performance.

Laboratory freeze-thaw tests results revealed that the concrete interfacial zone likely contributes to the accelerated deterioration of concrete pavement joints. MIP tests results showed that hardened cement paste with a w/cm ratio typically used in pavements has a pore size distribution similar to that of aggregates prone to D-cracking. The field investigation showed that impermeable base layers are likely contributing to joint deterioration. The field investigation indicated that subsurface layers of concrete pavements in winter are significantly less permeable than in summer because when water that is trapped in the subsurface freezes, excess water cannot drain out of the pavement so increasing concrete saturation and so risk of freezing related damage. Both laboratory and field studies indicate

that a combination of multiple factors (e.g., materials, design, and construction) causes the deterioration of concrete.

CHAPTER 1. GENERAL INTRODUCTION

Joint deterioration has been reported in a number of locations in cold weather states. Damage to concrete pavement joints is often observed as cracking and spalling at joints and eventually reduces the service life of pavement systems including highways, city and county streets, and parking lots (Taylor et al. 2012). No single mechanism can account for all occurrences of joint deterioration. Spragg et al. (2011) documented that the factors that contribute to this damage include chemical reactions, inadequate air voids, poor mix design, inadequate constituent materials, or poor construction practices. This study explored these and other factors that contribute to joint deterioration in concrete pavement.

Research Objectives and Anticipated Benefits

The primary objectives of this research are to improve understanding of the mechanisms behind premature joint deterioration and to develop guidance to produce durable concrete structures.

The findings from this research are expected to benefit pavement engineers on how to make durable joints in concrete pavements, and what to do about repairing and /or slowing the distress in existing pavements.

Background

Concrete is a mixture of glue (cement, water, and air) binding together fillers (aggregate). But other materials, such as supplementary cementitious materials (SCMs) and chemical admixtures are added to the mixture (Figure 1) (Taylor et al. 2006). The paste, comprised of portland cement and water, binds the aggregates (usually sand and gravel or crushed stone) into a rocklike mass as the paste hardens because of the chemical reaction of

the cement and water as shown in Figure 2 (Kosmatka et al. 2002).

Figure 1. Composition of concrete

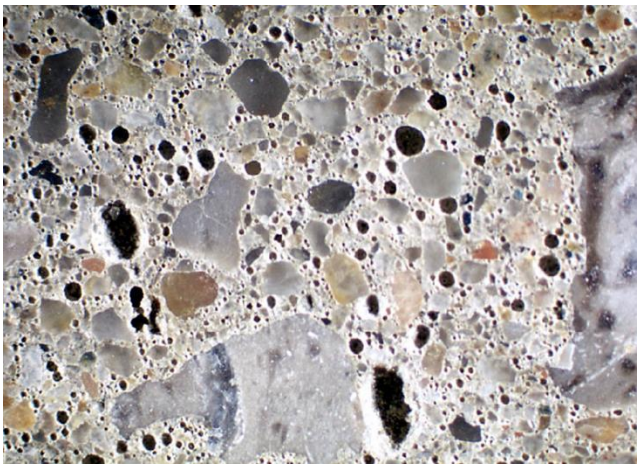

Figure 2. Rocklike hardened concrete

Hardened concrete contains relatively complicated structure which includes hydrated cement paste, aggregates, and the concrete interfacial transition zone. The hydrated cement paste mainly consists of calcium silica hydrate which takes up to 50 to 60 percent of the volume of solids in a completely hydrated cement paste (Mehta 1986). Three types of voids exist in hydrated cement paste, which are gel pores, capillary pores, and air voids, and these voids play significant role in the durability of concrete. Typical sizes and classifications of the pores in hydrated cement paste are given in Table 1 (Mindess et al. 1981). The air voids

in the hydrated cement paste exist in two forms, which are entrapped air voids and entrained air voids. Entrapped air voids can be as large as 3 mm, and entrained air voids usually range from 50 to 200 μm (Mehta 1986).

Table 1. Classification of pore sizes in hydrated cement paste (Mindess 1981)

Designation	**Diameter**	**Description**
Capillary Pores	10,000-50 nm (10-0.05 μm)	Large capillaries (macropores)
	50-10 nm	medium capillaries (large mesopores)
Gel Pores	10-2.5 nm	Small isolated capillaries (small mesopores)
	2.5-0.5 nm	micropores
	≤ 0.5 nm	interlayer spaces

Concrete expands and shrinks with changes in moisture and temperature. Joints are installed in concrete slabs to control the random slab which caused by the temperature change or by the slight contraction during cement hydration process, and joints are simply pre-planned cracks. Joints in concrete slabs can be created by forming, tooling, sawing, and placements of joint formers.

Four types of mechanisms that are responsible for the majority joint deterioration cases, which are mechanical damage, early-age drying damage, D-cracking, and frost damage. The critical factors that control joint deterioration include (Taylor et al. 2011):

- Water has to be prevented from saturating the concrete.
    - Water penetrating from the top surface must be prevented from ponding in the joint.
    - Water must be prevented from penetrating from the base.
    - Permeability of the concrete should be as low as practically feasible.
- The air-void system in the in-place concrete must be adequate.

Dissertation Organization

This dissertation contains four scholarly papers and each paper appears as a dissertation chapter and an introductory chapter provides problem statement regarding to joint deterioration and some relevant background. In addition to this introductory chapter, Chapter 2 provides comprehensive literature review regarding to some perspectives related concrete deterioration. The last chapter summarizes the conclusions from this research and some recommendations for the future research.

Chapter 3 presents the conducted research results regarding to the effect of concrete interfacial transition zone (ITZ) on joint deterioration in concrete pavements. Factors affecting the concrete ITZ were evaluated in this chapter. These, include w/cm ratio, aggregate type, and addition of silica fume. Evidences of concrete ITZ contributes to the accelerated deterioration of joint were observed from laboratory work.

Chapter 4 provides the investigation of concrete interfacial transition zone to the freezing and thawing resistance of concrete at various deicing solutions. Six concrete mixtures were prepared with different w/cm ratio and silica fume contents. Samples were saturated in seven salt solutions before being subjected to freezing and thawing. It was found that the ITZ plays an important role in the premature deterioration of joints in concrete pavements and improving the paste quality helps to reduce the risk or amount of damage.

Chapter 5 provides preliminary work on evaluating the pore structure of hardened cement pastes with different w/cm ratios and supplementary cementitious materials (SCMs) using mercury intrusion porosimetry (MIP). The findings were compared with pore sizes that may slow drying, thus increasing the risk of freeze thaw damage similar to that observed in

D-cracking aggregates. This is very preliminary work and it is premature to make recommendations based on it other than to suggest that the idea of a pessimum paste pore system for freeze thaw resistance seems to have merit, and warrants further investigation. It is notable that the pessimum appears to fall with the range of typical pavement mixtures.

Chapter 6 provides the research results of studying the relationship between joint performance and the permeability of subsurface layer. A borehole permeameter was developed in this study to measure the permeability of the subsurface layer under a core hole. Field tests were conducted on three joints (two sealed and one unsealed) and a middle panel in summer, winter, and spring on a city street in Ames, Iowa. Field tests results indicate that low permeable subsurface layer contributes to joint deterioration, especially under freezing condition. Laboratory falling head permeability tests on a selected base material under frozen and unfrozen conditions revealed that moisture content affects the permeability of base material with both frozen and unfrozen conditions. Core samples were obtained from distressed joint and sound joint for petrography analysis, and the results indicate that the distressed core sample contains higher w/cm ratio and has ettringite filled the air voids.

Chapter 7 reviews some mechanisms causing joint deterioration in concrete pavements. Both laboratory work and field investigation are covered in this chapter. Laboratory work evaluated the influences of degree of saturation, deicing solutions, concrete ITZ, and pore structure of hardened cement paste to the freezing and thawing resistance of concrete. Field investigation was conducted at multiple sites in Wisconsin, Iowa, and Minnesota to observe the various forms of distress in concrete pavements. Selected cores from three states were submitted for petrographic analysis. Besides that, this chapter also

covers some current status on investigating the joint deterioration and future needs to make durable joints in concrete pavements.

The last chapter (chapter 8) summarizes the conclusions and findings from this research and some recommendations for the future work.

References

Kosmatka, S. H., Kerkhoff, B., and Panarese, W.C., *Design and Control of Concrete Mixtures*, EB001, 14th edition, Portland Cement Association, Skokie, Illinois, USA, 2002, 358 pages.

Mehta, P. K. (1986), *Concrete: Structure, Properties, and Materials*. Englewood Cliffs, NJ: Prentice-Hall.

Mindess, S., Young. J. F. and Darwin, D., (1981). *Concrete*. Prentice-Hall, Inc., Englewood Cliffs, NJ.

Spragg, R.P., Castro, J., Li, W., Pour-Ghaz, M., Huang, P, and Weiss, J. (2011), "Wetting and Drying of Concrete Aqueous Solutions Containing Deicing Salts", *Cement and Concrete Composites*, vol. 33, page 535-542.

Taylor, P., Rasmussen, R.O., Torres, H., Fick, G., Harrington, D., and Cackler, T., (2011). *Interim Guide for Optimum Joint Performance of Concrete Pavements*, Institute for Transportation, Iowa State University, Ames, Iowa.

Taylor, P., Sutter, L., and Weiss, J., (2012). *Investigation of Deterioration of Joints in Concrete Pavements*, Final Report, InTrans Project 09-361, National Concrete Pavement Technology Center, Iowa State University, Ames, Iowa.

Taylor, P. C., S. H. Kosmatka, G. F. Voigt, M. E. Ayers, A. Davis, G. J. Fick, J. Gajda, J. Grove, D. Harrington, B. Kerkhoff, C. Ozyildirim, J. M. Shilstone, K. Smith, S. M. Tarr, P. D. Tennis, T. J. Van Dam, and S. Waalkes. (2006). *Integrated Materials and Construction Practices for Concrete Pavement: A State of the Practice Manual*. FHWA HIF-07-004. Federal Highway Administration, Washington, DC.

CHAPTER 2. LITERATURE REVIEW

This chapter reviews four subjects that are relevant to concrete deterioration, freezing thawing mechanisms, salt scaling, water movement, and the influence of concrete interfacial zone. The four subjects are linked to each other and directly related to the mechanisms causes concrete deteriorate.

Freezing and Thawing Mechanism

As temperature drops, water molecules shrink together, but they begin to expand and become less dense at temperature below 4˚C. Liquid water at zero gauge pressure will turn into ice at about 0˚C (Akyurt et al. 2002). When ice forms in saturated pores, tensile stresses built up in the paste due to the 9% volume increase when water changes from the liquid state to the solid state (Pigeon and Pleau 1995).

Freezing point of a liquid is a function of temperature and pressure. Pore structure of concrete includes a wide range of pore sizes and this influences the freezing phenomenon. Under normal pressure, the freezing temperature in concrete pores is different and it possibly decreases with the size of the pore as shown in Figure 3. Pores with a radius of 5 nm or less could remain unfrozen in temperature above -20˚C and only two-thirds of the pore water may be frozen by -60˚C (Pigeon and Pleau 1995).

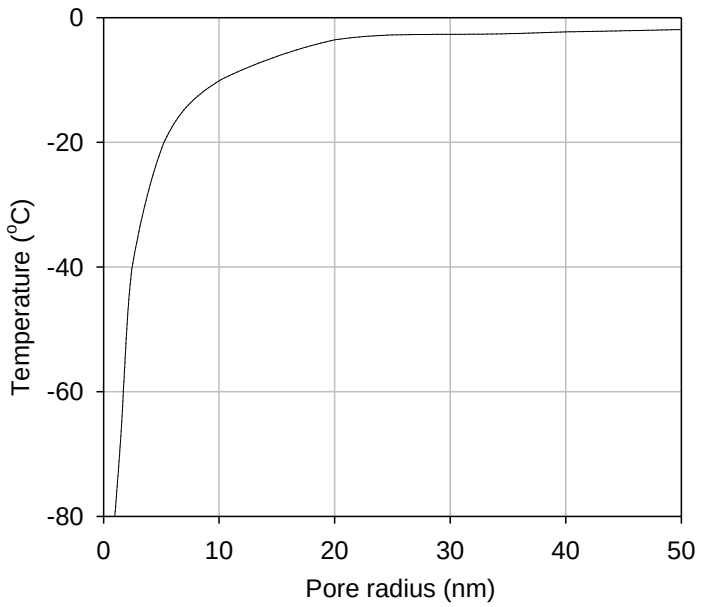

Figure 3. Relationship between capillary pore size and the freezing temperature (Pigeon and Pleau 1995)

Gel pores in concrete range in size from 1 nm to 4 nm, and water trapped in gel pores cannot rearrange itself to form ice at normal freezing temperature (Mehta 1986). The gel pores are so small that freezing cannot occur at any temperature above -78°C (Powers and Helmuth 1953).

As ice bodies form in cavities, excess unfrozen water is pushed out into the surrounding network until cavities are filled as the ice forms a moving front and pushes water ahead of it. This flow occurs under a pressure head and resistance to the flow is proportional to the length of the flow path and diameter of the pores (Pigeon and Pleau 1995). Thus, conditions may arise where the flow is impeded due to insufficient pore volume, and resistance to the flow develops hydraulic pressure. This expansive pressure may reach a level that exceeds the tensile strength of the concrete and causes cracks in the concrete. In addition, water movement during freeze thaw cycles may result in capillary water moving into microcracks. In subsequent freezing cycles this water may cause propagation of these

cracks leading to significant cumulative damage over time (Pigeon and Pleau 1995).

Degree of saturation is an important factor that affects freeze thaw damage in concrete. Closed systems with at least 91.7% saturation experience pressure on capillary pore walls and damage occurs (Page and Page 2007). Li et al. (2012) demonstrated that concrete specimens with a degree of saturation greater than the 86-88% exhibiting damage during freeze-thaw cycles (Figure 4). This critical degree of saturation appears to be independent of the air content. However, concrete that reaches or exceeds the critical degree of saturation is damaged after a few freeze-thaw cycles irrespective of the air content.

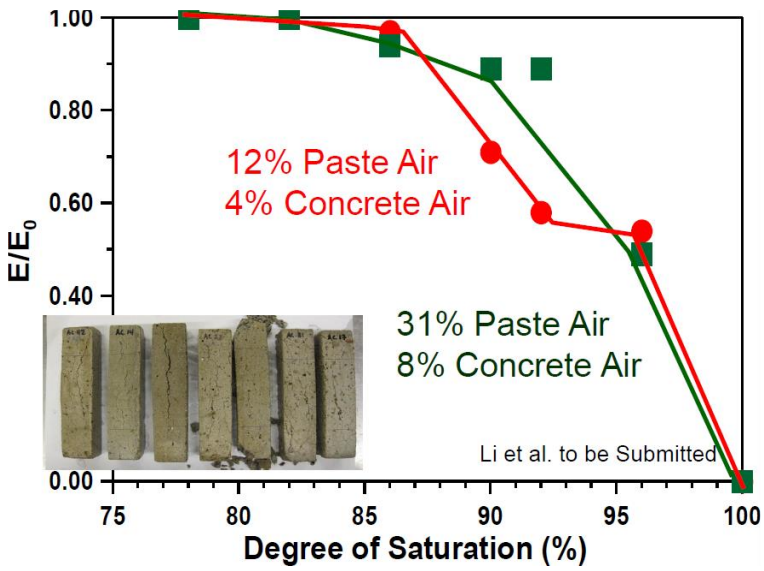

Figure 4. Relationship between degree of saturation and freeze-thaw durability (reproduced Li et al. 2012)

Capillary pore water contains solutes, such as alkalis and salts. As ice grows from the pure water, a relatively concentrated alkali solution will be introduced at the freezing site. Unfrozen water will move toward to the freezing sites due to the differences in solute concentration that introduces osmotic pressure in the capillary pores as shown in Figure 5 (Helmuth 1960). This osmotic pressure would superpose the hydraulic pressure in many

cases (Ronning 2001).

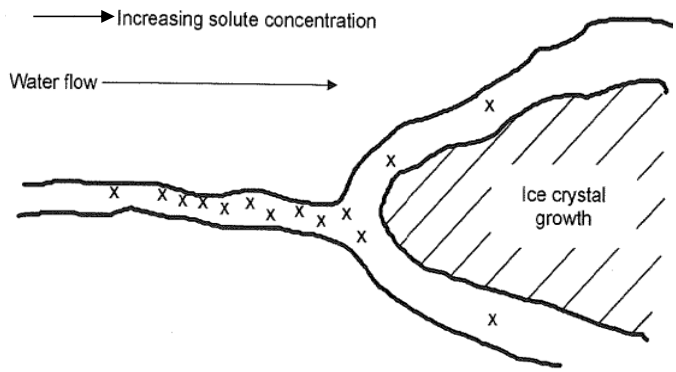

Figure 5. Conceptual illustration of the generation of osmotic pressure in concrete pores (Page and Page 2007)

During the freezing phase, air voids provides space for water to move without causing undue pressure and, on thawing, the water in the entrained voids is drawn back out into the narrower pore network by capillary forces. Figure 6 shows the SEM images of an air void in a concrete system before and after freezing (Corr et al. 2002).

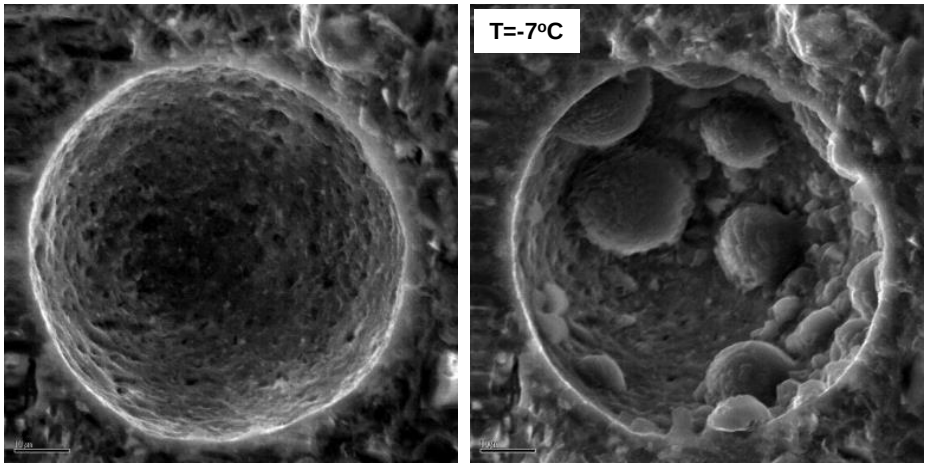

Figure 6. SEM image of air void before and after freezing occur in concrete (Corr. 2002)

Air void system delays the time for concrete to reach a critical degree of saturation. Non-air entrained concrete may reach critical degrees of saturation within 4−6 days, and air entrained concrete increases the time to reach a critical degree of saturation up to 3−6 years

(Figure 7) (Li et al. 2012). Figure 8 shows how air voids in concrete provide space to release the hydraulic pressure generated during freezing and also increases the time for concrete to reach a critical degree of saturation (Li et al. 2012; Corr et al. 2002; and Taylor et al. 2006).

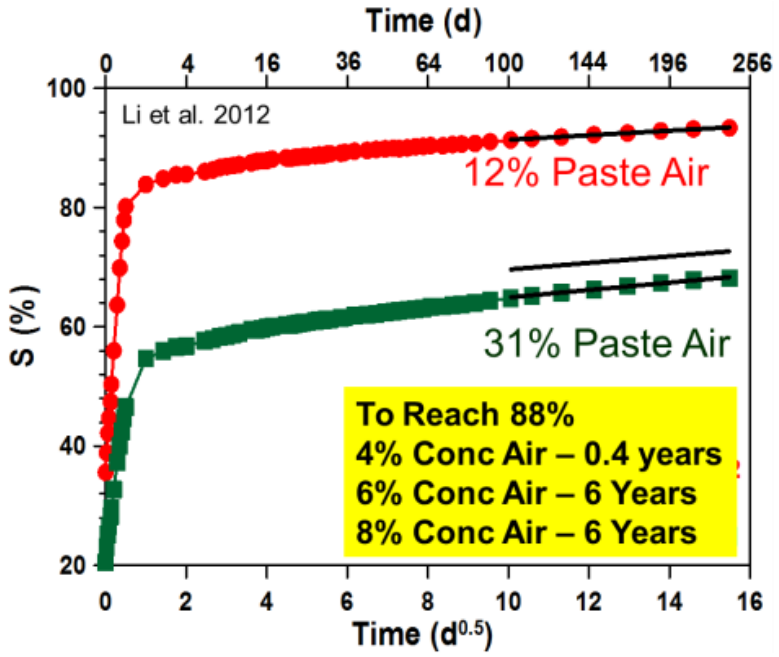

Figure 7. Time to reach the critical degree of saturation for concrete with different air contents (Li et al. 2012)

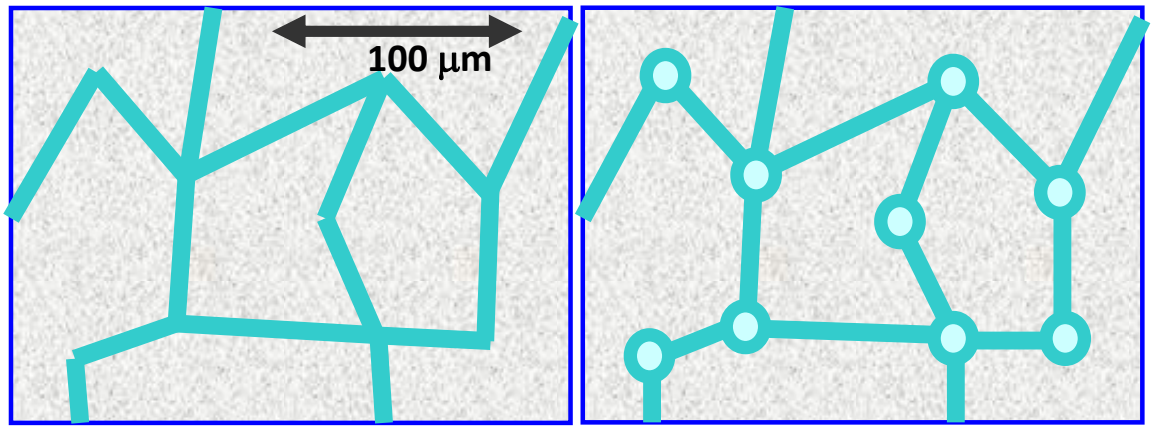

Figure 8. Air voids provide a place for expanding water to move into as it freezes

Spacing factor (L) is another key parameter that affect concrete freeze thaw durability, and it is the distance that water can flow from freezing site to the surrounding

nearest air-filled space (Li et al. 2012). Power (1954) stated that the spacing factor less than 0.200 mm (0.008 in) and the specific surface of 24 mm^2/mm^3 (600 in^2/in^3) of air void volume are required for concrete to be protected from freeze-thaw damage. For a given air content, small, closely spaced air voids provide better protection than larger, more distant voids as illustrate in Figure 9 (Klieger 1994).

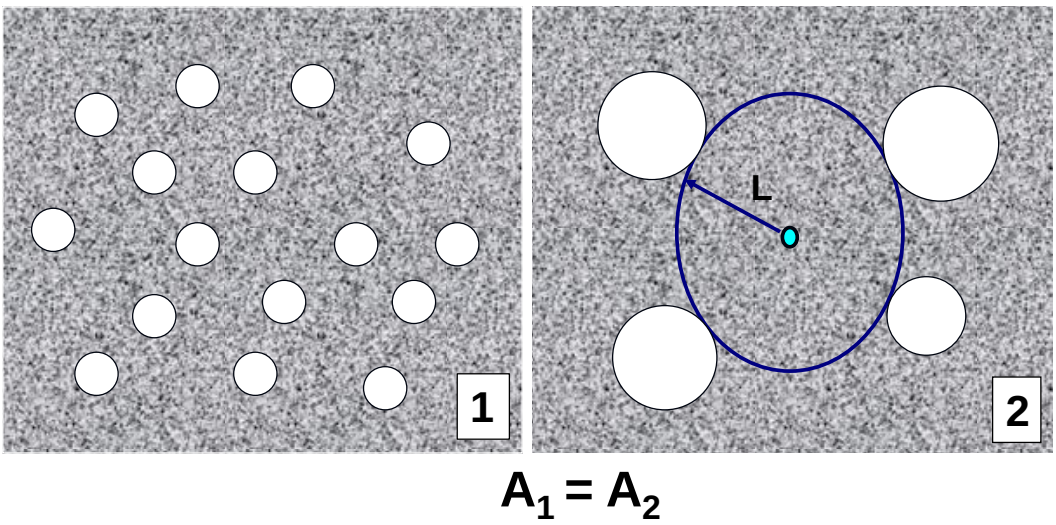

Figure 9. Total air with different spacing factor

Salt Scaling

In cold weather regions, deicing salts are applied on concrete roads to keep the roadways functional during winter. This practice leads to salt scaling, which is one of the major durability issues facing concrete in such climates. Salt scaling is the superficial damage caused by freezing a deicing solution on the surface of a concrete body. It is a progressive damage and consists of the removal of small chips or flakes of binders with very few small aggregates removed as shown in Figure 10. Salt scaling alone may not destroy a concrete structure, but it causes the concrete body susceptible to ingress of moisture and aggressive species that affects its overall durability. Moreover, salt scaling often results in the

exposure of coarse aggregates (Valenza and Scherer 2007).

Figure 10. Salt scaled concrete sidewalk

Two critical factors that contribute to salt scaling are freeze-thaw cycles and presence of de-ice salts (Shi et al. 2010). Verbeck and Klieger (1957) found that a solute with about 3% concentration brings the maximum damage to concrete, regardless of the type of solute (Figure 11). Gulati and Hagy (1982) explained that this maximum damage is caused by glue-spalling, which is a technique used to describe glass surfaces. The fundamental procedures of glue-spalling are that an epoxy spread on a sandblasted surface and stress from the thermal expansion mismatch causes the epoxy to crack into small islands. Valenza and Scherer (2006) described glue spalling related to glass (Figure 12) and the application of glue-spalling theory to concrete (Figure 13). Valenza et al. (2006) reported that (1) pure ice will not crack; (2) the stress rises faster than the strength in ice formed from a moderately concentrated deicing solution; and (3) more highly concentrated solution produce ice that has no strength in the temperature range of interest. Glue spalling occurs when the mismatch in the stresses of deicing salt and water that build from thermal expansion exceeds the tensile strength of the concrete and cracks propagate into concrete (Sun and Scherer 2010).

Moreover, the glue-spall stress is about 2.6 MPa (377 psi) for a uniform temperature change of 20°C, and that stress can damage the surfaces of cementitious materials. All these references provide clear explanation that a solute with about 3% concentration brings the maximum damage on concrete.

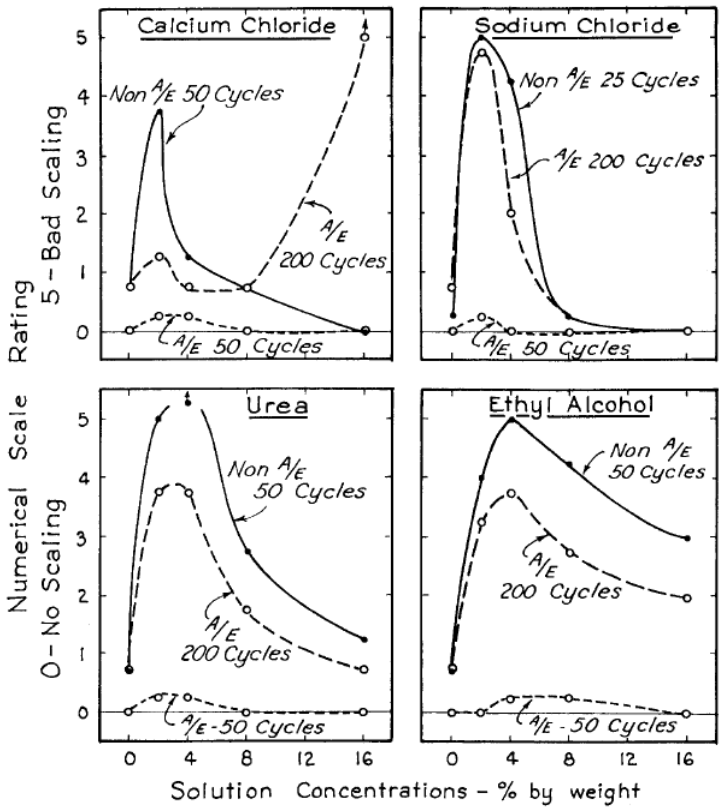

Figure 11. Effect of deicer concentration on concrete surface scaling (Verbeck and Klieger 1957)

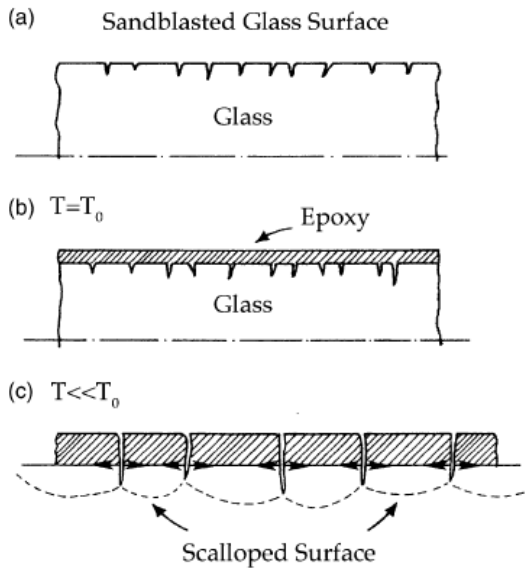

Figure 12. Schematic explanation of the glue-spall mechanism (Valenza and Scherer 2006)

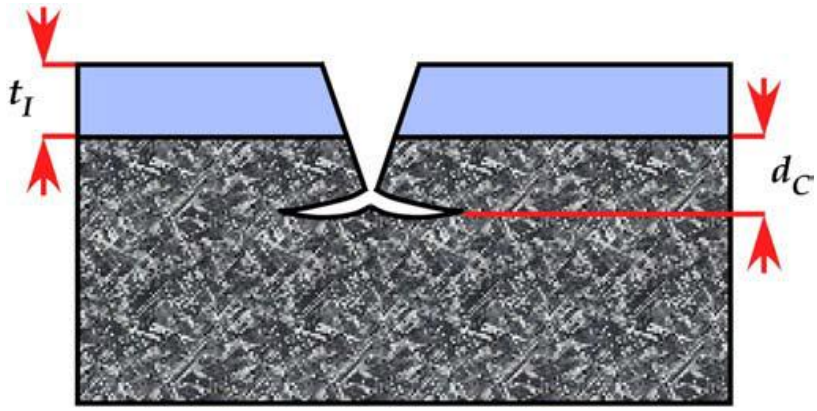

Figure 13. Schematic explanation of the glue-spalling mechanism apply to concrete (Sun et al. 2010)

Salt crystallization is also a mechanism that causes surface scaling. A supersaturated solution includes more potential energy than a corresponding saturated solution. The excess potential energy can be utilized to perform work against an external restraining pressure when the solute crystallizes out of its supersaturated solution. The state of saturation is important for crystallization to occur, and it is impossible to have crystallization in unsaturated conditions. Crystals that grow under supersaturated conditions can create enough pressure to disrupt the bulk paste in confined spaces within concrete (Thaulow and Sahu

2004). Correns (1949) provided an equation for calculating crystallization pressures:

$$\mathrm{P} = \frac{RT}{V_s} \times \ln \frac{C}{C_s} \tag{1}$$

where

P = crystallization pressure,

R = gas constant (0.082 L-atm/mol K),

T = absolute temperature in K,

V_s = molar volume of solid salt in L/mole,

C/C_s = the degree of supersaturation, and C is the existing solute concentration and C_s is the saturation concentration.

Crystallization pressures generated from supersaturated deicing salts during temperature drops are about 16 MPa (2300 psi), which is 5 to 10 times the tensile strength of concrete (Thaulow and Sahu 2004).

Evaporation of liquid also creates supersaturation which evidenced by crystallization in warm weather. Low relative humidity in warm weather leads to dehydration of salt solutions and results in crystallization (Figure 14). Salt crystals grow from deicing solution as water evaporates (Thaulow and Sahu 2004).

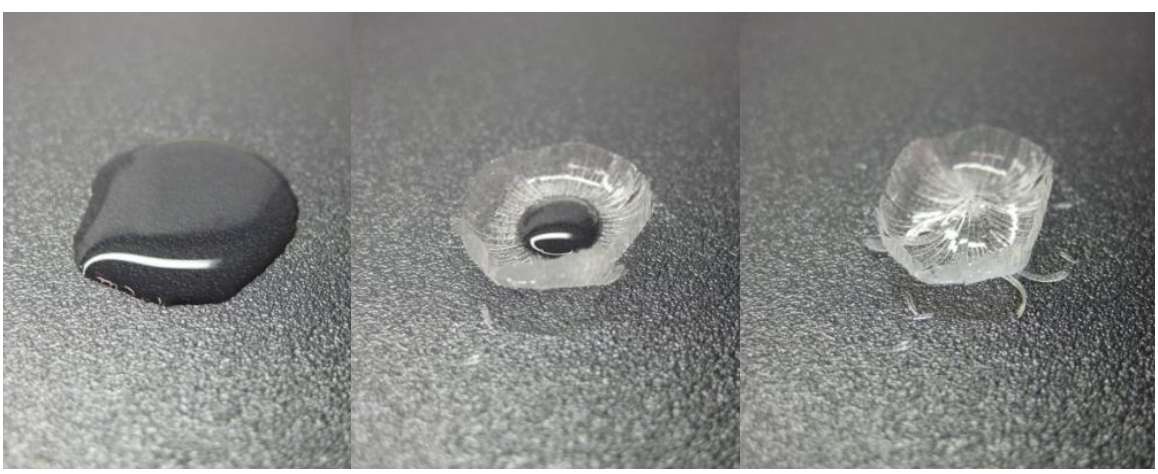

Figure 14. Salt crystallization due to evaporation of liquid

Concrete wicking is another example of salt scaling that occurs when deicing solution is brought to the surface of concrete by capillary action. Subsequently as a result of surface evaporation, the solution phase becomes supersaturated and salt crystallization occurs which results in deicing salt accumulating on dry surfaces (Figure 15 and Figure 16).

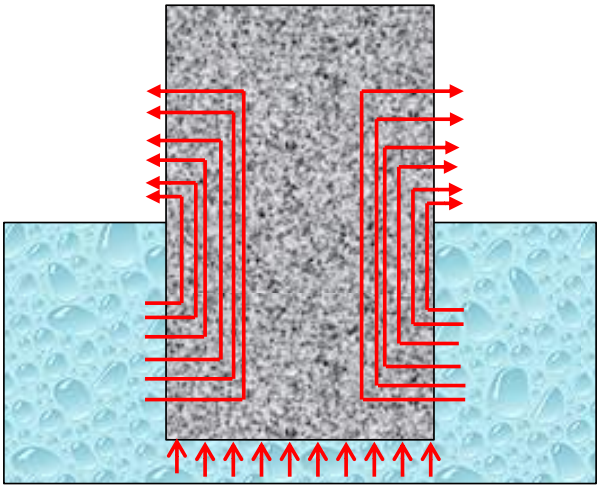

Figure 15. Schematic illustration of concrete wicking

Figure 16. Typical example of concrete wicking

Deicer scaling resistance of concrete can improved by reducing the water-cement ratio, using a moderate Portland cement content with adequate air content, applying proper

finishing and curing, and allowing an air-drying period prior exposing the concrete to deicing salts (Kosmatka et al. 2002). The most effective way to protect concrete from salt scaling is adding air entrainment to concrete. The use of air entraining agents (AEA) in concrete improves salt scaling resistance in two ways: (a) AEA reduces pore water bleeding and results in stronger surfaces; and (b) air entrained concrete can contract when it freezes, which offsets the thermal expansion mismatch with ice to reduce cracking (Valenza and Scherer 2006). Research on applying supplementary cementitious materials (SCMs) to concrete to improve salt scaling resistance indicates that most SCMs cannot significantly improve salt scaling resistance (Ahani and Nokken 2012).

Water Movement

Hardened concrete contains several types of voids that influence the properties of the concrete. The typical pore sizes in hardened concrete are shown in Figure 17 (Mehta 1986).

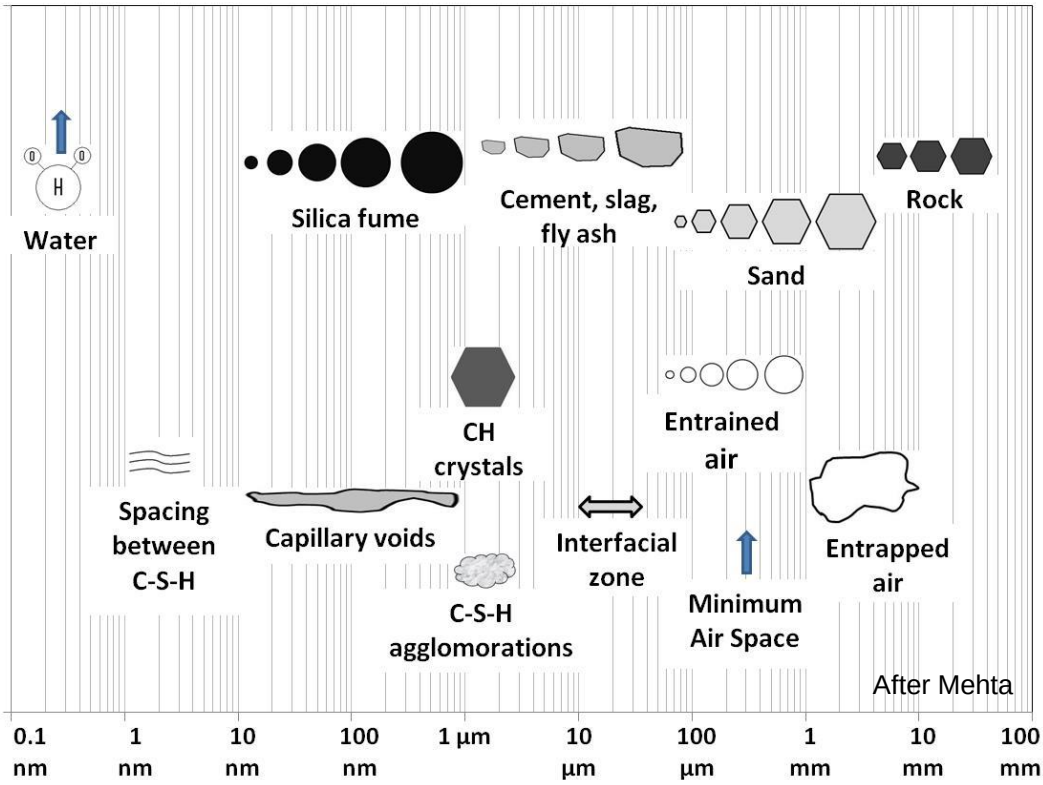

Figure 17. Size of elements in hardened concrete (after Mehta)

Two types of water exist in the voids in hydrated cement, evaporable water and nonevaporable water. Evaporable water exists in both capillary and gel pores and will be lost when the hydrated cement dries. Nonevaporable water is combined structurally in the hydration products but can be lost when the hydrated cement is heated up to 1000°C (Mindess et al. 1981). Because this high heat does not occur in natural conditions, the discussion of water movement focuses on evaporable water.

For initial unsaturated concrete, water absorption is accomplished by an initial instantaneous surface suction, a subsequent capillary suction, and a later water diffusion at the small (gel) pore level when the concrete is in contact with liquid water. Capillary porosity is primarily controlled by the water to cement ratio and the degree of hydration (Mindess et al. 1981). Capillary suction accounts for approximately 70% and diffusion causes 30% of the

overall absorbed water (Neithalath 2006). Capillary suction results in the formation of a meniscus that is convex toward the wet side (Figure 18).

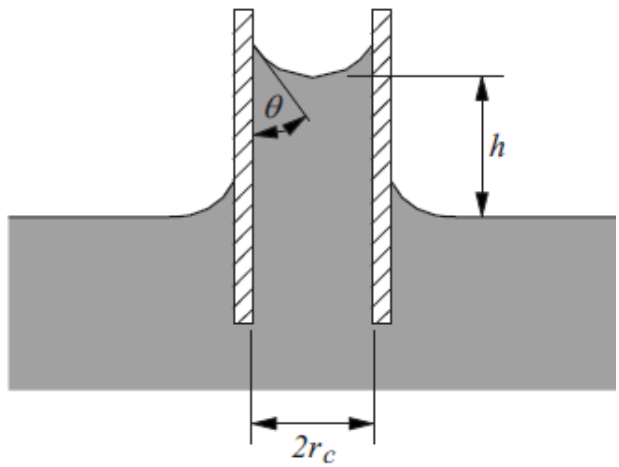

Figure 18. Schematic illustration of capillary suction on single capillary pore (Collins and Sanjayan 2010)

Capillary pressure can be calculated using the following equation:

$$\Delta P = \frac{2\sigma}{r_c} \tag{2}$$

where

σ = surface tension,

r_c = radius of the capillary (Collions and Sanjayan 2010).

Typical capillary sizes range from 0.01 μm to 1 μm (see Figure 17), and the calculated capillary pressure ranges from ($2 \times 72 \times 10^{-3} / 10^{-6}$) or 0.14×10^{8} N/m^2 to 0.14×10^{6} N/m^2. The pressure required to raise a column of water 1 m is (ρgh) 9.8×10^{3} N/m^2, which is significantly less than the capillary pressures (Chatterji 2004).

The length of the capillary filled by water can be determined by the equation:

$$l_{\mathrm{m}} = (\varepsilon/\mathrm{T}) r^{0.5} (\gamma / 4\eta)^{0.5} t^{0.5} \tag{3}$$

where

(ε/T) = pore characteristics coefficient,

r = the radius of capillary,

γ = the surface tension of water,

η = the viscosity of water, and

t = time.

Table 2 provides the depth of water penetration in concrete in one year (Chatterji 2004).

Table 2. Depth of water penetration in one year (Chatterji 2004)

Capillary radius (nm)	Water filled length at one year (m)
102	7.89
53	5.81
20	3.57
10	2.52
5	1.79
1	0.80

The interconnection of pores affects water movement in concrete. Low water/cement ratio concrete is less permeable because of smaller pores and low connectivity of the pores, which results in less water movement (Chatterji 2004; Castro-Borges and Torres-Acosta 2010). The initial moisture conditions of concrete also affects the concrete absorption. Concrete treated with low relative humidity absorbs more water than concrete treated with high relative humidity (Spragg et al. 2011).

The absorption of concrete decreases when concrete is exposed to salt solutions. Sutter et al. (2008) reported that the absorbed solution decrease with the order of water, NaCl, $CaCl_2$, and $MgCl_2$. A similar conclusion was made by Janusz (2010), and a deicing salt solution transported in concrete at lower rate than water.

Interfacial transition zone (ITZ) in concrete is the most permeable region and more

water can be transported into concrete internal through this region (Wang and Ueda 2011; Winslow and Liu 1990). Winslow and Liu (1990) demonstrated that concrete contains larger pores than plain cement paste using mercury intrusion porosimetry, and the pore volume increase with the increase of the aggregate. The probability of ITZ percolation can be reduced by improving the concrete ITZ (Winslow et al. 1990; Winslow et al. 1994).

Interfacial Transition Zone

The interfacial transition zone (ITZ) is the region (typically 10−50 μm in thickness) between aggregate and cement paste (Cwirzen and Penttala 2005). The ITZ is formed because of water film around aggregate and the so-called "wall" effect of packing cement grains against relatively flat aggregate surfaces (Figure 19). The spatial arrangements of anhydrous cement particles become loose near the aggregate surface. Even through the particles are touching, the amount of empty space approaches 100% as the "wall" is approached. As a result, the local w/cm ratio and the porosity tended to be higher, and at the same time, w/cm ratio in the bulk cement paste become lower which may lead to higher porosity in the ITZ. Besides that, the effects of "one-side" growth of hydrates also contribute to the ITZ (Maso 1996).

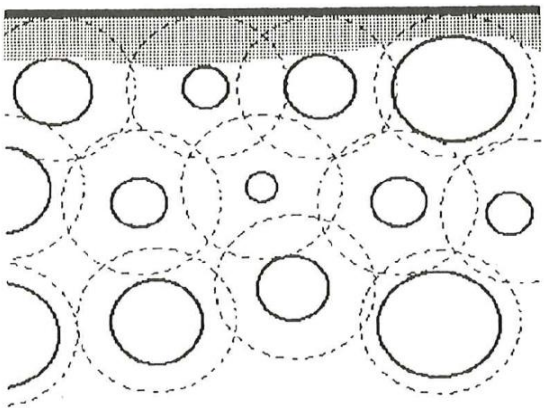

Figure 19. Hypothetical illustration of "wall" affect (Maso 1996)

In fresh placed concrete, water films that form around aggregate particles result in higher w/cm ratios closer to aggregate than away from it. Relatively higher local w/cm causes the hydration product more porous around aggregates (Maso 1980). The ITZ consists primarily of calcium hydroxide and ettringite (Figure 20) (Cwirzen and Penttala 2005; Maso 1980; Mehta 1986). Cwirzen and Penttala (2005) observed the concrete ITZ using scanning electron microscope (SEM) and more porous structure approximately 20 to 50 μm from the interface (Figure 21). The ITZ is not evenly distributed around aggregate and it is thicker and weaker below aggregate than above aggregate (Figure 22) (Maso 1996; Scrivener et al. 2004).

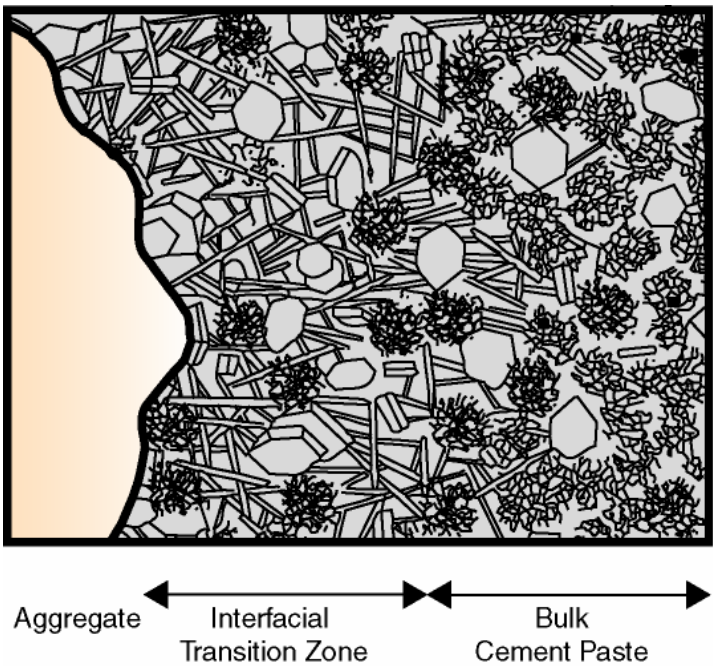

Figure 20. Schematic illustration of the structure of concrete interfacial zone (Mehta 1986)

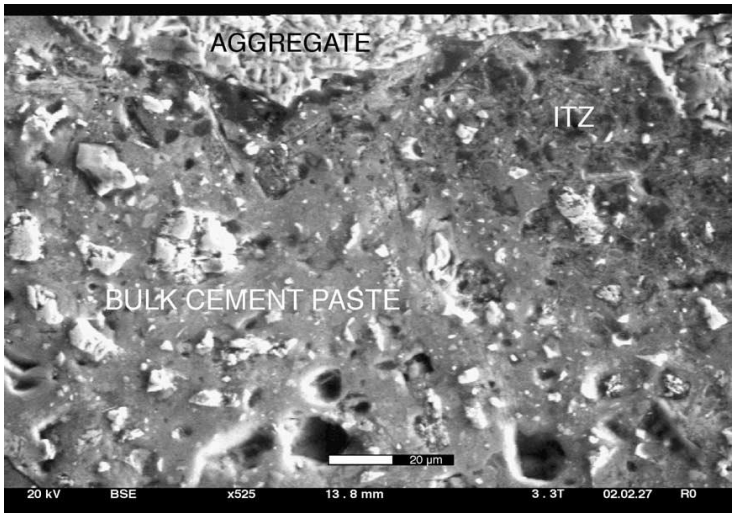

Figure 21. SEM image of concrete with ITZ around aggregate (Cwirzen et al. 2005)

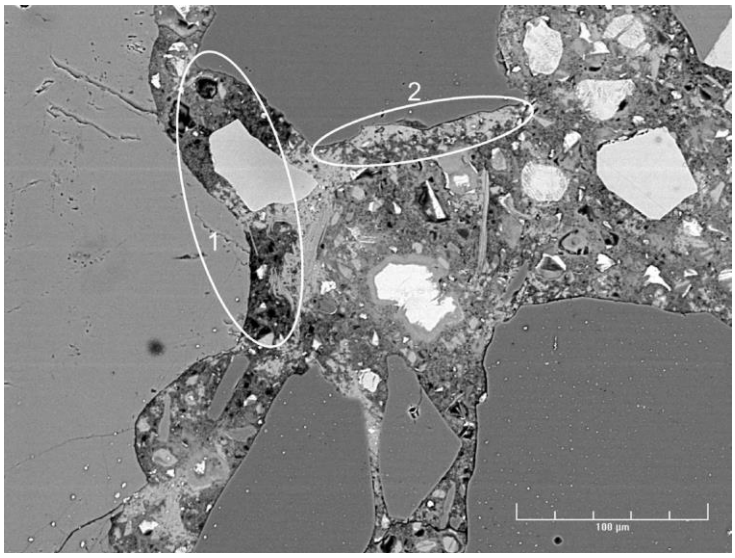

Figure 22. BSE image of concrete illustrating typical inhomogeneity (Scrivener et al. 2004)

Aggregate characteristics: aggregates with rougher surface result in slightly narrower ITZ. Because the rougher particles will have greater tendency to acquire small cement grains during mixing. In general, larger aggregate results in higher local w/cm ratio in the ITZ with everything else remaining the same, consequently, the concrete will be weaker and more permeable (Mehta 1986). The more elongated aggregate in concrete results in lower aggregate content being required for ITZ percolation than the spherical ones. Smaller aggregate particles contain more ITZ than bigger aggregate with the same aggregate volume

(Bentz et al. 1995).

Aggregate chemistry: Yuan and Odler (1987) found that calcite which is the main component of rocks can react with tricalcium aluminate of the cement and the reaction results in calcium carboaluminate phases that improves the strength of bonding. The evidence of cement etching calcite grains was also observed using scanning electron micrographs (Mehta and Monteiro 1988). Other study also shows that the use of reactive aggregate significantly affects the amount and the degree of orientation of calcium hydroxide crystals in the ITZ (Saito and Kawamura 1993). Tasong et al (1998) reported that ions are both absorbed and released by the aggregates in all the aggregate-cement solution systems, and basalt aggregate is more active than limestone, silica and quartzite materials.

Mix design: mix design had some modifying effect on the packing of cement particles and hence on the microstructure gradient in the interfacial zone. Low w/cm ratio and high aggregate/cement ratios results in efficient packing of cement particles around the aggregate and so minimized the width of the ITZ. High w/cm and low aggregate/cement permitted rearrangement of the cement grains over greater distance, which results in wider ITZ, and the microstructure gradients are shallower (Maso 1996). Cwirzen et al. (2005) found that the thickness of the ITZ reduces from 40 μm to less than 5 μm as w/cm ratio changes from 0.42 to 0.30. However, the proportion of the microstructural constituents in the first 5 μm or so adjacent to the aggregate was relatively unaffected by mix design (Maso 1996).

Supplementary cementitious materials (SCMs): apply some SCMs (e.g., silica fume) in concrete can fill the space which was occupied by water around aggregates in concrete as shown in Figure 23 (Maso 1980). It has been reported that the thickness of ITZ was reduced

as silica fume introduced into concrete (Monteiro and Mehta 1986a). Silica fume makes more efficient packing of cement particles around aggregates and less bleeding in fresh mix, as well as introducing pozzolanic reaction to form more C-S-H to improve the ITZ (Maso 1996). Toutanji et al. (1995) reported that the replacement of cement by silica fume along with a sufficient amount of superplasticizer increases the strength of mortar. Strength increases with increasing silica fume content, which can attribute to the improvement of aggregate-matrix bonding. But, silica fume has no strength effect on cement paste (Cwirzen and Penttala 2005; Toutanji and El-Korchi 1995).

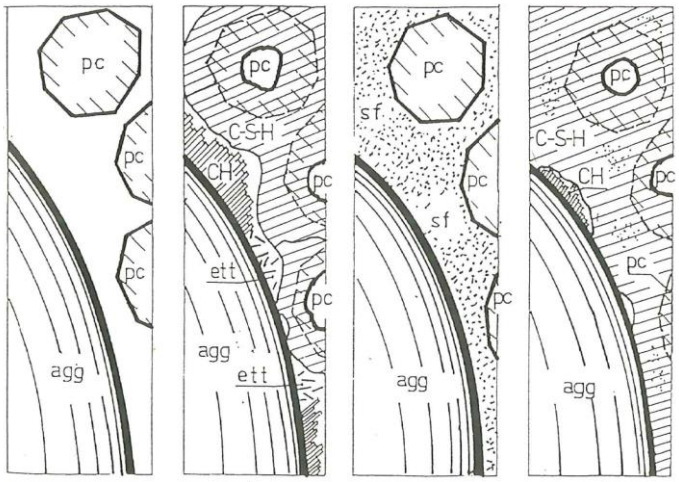

Figure 23. Schematic description of the mode and nature of formation of the interfacial zone around aggregates (Maso 1980)

Cement composition: the structure of ITZ formed in the presence of type K expansive cement was characterized by a high concentration of ettringite. The preferential orientation of calcium hydroxide crystals was reduced, which results in the increase the bond strength (Monteiro and Mehta 1985).

X-ray diffraction (XRD): XRD has been used to study the orientation of calcium hydroxide crystals in the ITZ (Maso 1996).

Surface analysis (XPS, SIMS): X-ray photoelectron spectroscopy (XPS) provides the information of concrete up to 5−10 nm deep of the surface and a chemical analysis of the surface layer can be obtained by measuring the kinetic energy of the photoelectron. It measures the C/S ratios in C3S and the cement powders which change rapidly during the first minutes of hydration. Secondary ion mass spectrometry (SIMS) uses a microfocused beam, raster across the surface, can produce chemical maps with a lateral resolution of 0.2 μm and an analysis depth of only a few nanometers (Maso 1996).

Bulk pore size distribution: mercury intrusion porosity (MIP) is a common technique to measure the porosity of concrete as well as the ITZ. It not only provides the pore sizes but also the connectivity of pores in both matrix and the ITZ (Winslow et al. 1994). Both magnetic resonance relaxation analysis (MRRA) and complex impedance spectroscopy are also used to study the porosity in cement paste. These methods can applied without drying the specimens because they rely on the presence of water in the pores (Maso 1996).

Optical microscope: optical microscope can be used to view the details of the spatial distribution of the porosity and the phases in the hardened paste in the interfacial region. Fluorescent resins are frequently used to fill the larger pores and in this way an indication of the w/cm ratio, the original mix design and the homogeneity of the porosity can be obtained (Maso 1996).

Scanning electron microscope (SEM): SEM has been used in two different modes of imaging: secondary electron imaging to study fracture surfaces where topographical features produce the contrast in the image and the large depth of focus is valuable; back-scattered electron imaging to study flat polished surfaces where differences in back-scattering

coefficient, dominated by atomic number differences, produce the contrast (Maso 1996).

Nanoindentation: nanoindentation with imaging has been used to provide the local mechanical properties of cement paste and concrete (Mondal et al. 2009). Indentation were made by using a pyramid-shaped, diamond Berkovich tip with nominal radius of 50 nm, an elastic modulus of the indenter material of 1,100 GPa, and a Poisson ratio for the indenter material of 0.07 (Garas et al. 2010).

The aggregate-cement paste ITZ is known as the weakest region in concrete and it affects both mechanical properties and durability performance of concrete (Tasong et al. 1998). Mondal et al. (2009) reported that the average modulus of ITZ is 70% to 85% of the average modulus of bulk paste depending on the aggregate type by using nanoidentation. Low strength of ITZ makes the strength of concrete between aggregate and cement paste as shown in Figure 24 (Scrivener et al. 2004). The structure of the ITZ, especially the volume of voids and microcracks present, has a great influence on the stiffness or the elastic modulus of concrete. In composite material, the ITZ serve as a bridge between mortar matrix and coarse aggregate. Even when the individual components are of high stiffness, the stiffness of the composite may be low due to the “broken bridge” (Mehta 1986).

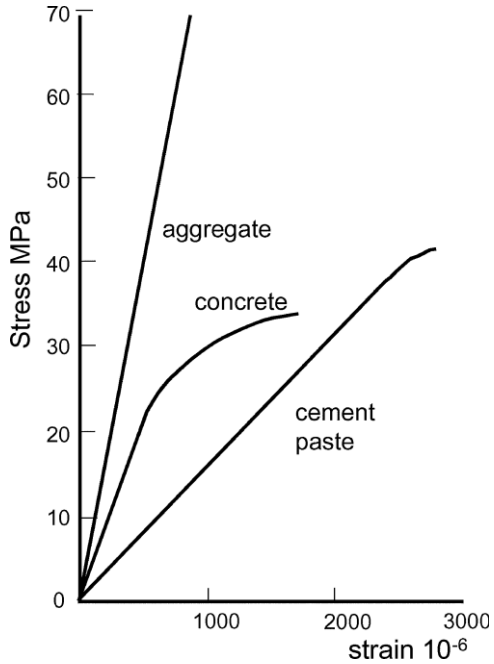

Figure 24. Comparative stress strain curves for aggregate, paste and concrete (Scrivener 2004)

High porosity of ITZ is an important factor to concrete durability, because the ITZ affects water transport in concrete (Cwirzen and Penttala 2005). The concrete ITZ includes large flat $Ca(OH)_2$ crystals which perpendicular to the surface of aggregate grains, which makes ITZ a highly porous region in concrete. Such structure favors the formation of microcracks within this layer and the propagation of microcracks under load (Prokopski and Halbiniak 2000). The diffusion coefficient of chloride ions in the ITZ can be 6–12 times higher than bulk paste, and the porosity of the ITZ is not constant, which depends on the mortar composition and the degree of hydration (Bourdette et al. 1995). The porosity of ITZ can be significantly improved by adding silica fume (Figure 25) (Scrivener et al. 1988).

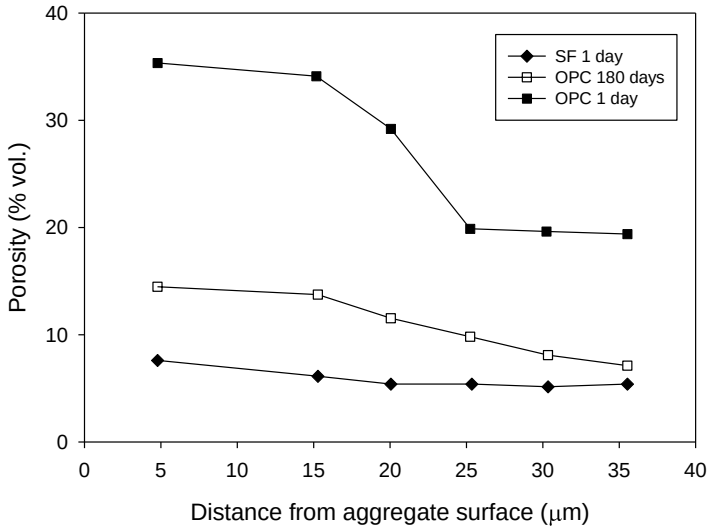

Figure 25. Effect of age and silica fume on the porosity in the ITZ (reproduced from Scrivener et al 1988)

Due to the high connectivity and porosity of ITZ, the freezing medium can easily penetrates into concrete internal system. Subsequent freezing and dissolution of the soluble calcium hydroxide in the ITZ cause cracking around the aggregate particles. Once the now-loose piece of aggregate is removed by traffic loading, the cycle is repeated (Zhang and Taylor 2012). High porosity of ITZ also enhances the transport process of pore liquids, thus allowing frequent moisture changes and permanent high water supply in the transition zone, which increased the amount of chemical ions in the ITZ for recrystallization (Cwirzen and Penttala 2005). The presence of the deicing salts causes partial transformation of monosulphate to Fridel's salts, releasing gypsum, which subsequently reacts with remaining monosulphate to form ettringite, and the high porosity of ITZ could additionally support the entire process (Stark and Bollmann 1997). The damaging processes of non-air-entrained high performance concrete are governed by the ITZ properties. ITZ enhancing transport processes within the concrete and facilitating ingress and penetration of the freezing medium and aggressive agents into the concrete microstructure. Moreover, the chemical composition and

high porosity of the ITZ enhance the secondary formation of ettringite and leaching of the portlandite (Cwirzen and Penttala 2005).

References

Ahani, R.M, and Nokken, M.R., (2012), "Salt Scaling Resistance – The Effect of Curing and Pre-saturation" *Construction and Building Materials,* Volume 26, pp. 558-564

Akyurt, M. and Zaki, G., and Habeebullah, B. (2002), "Freezing Phenomena in Ice-Water Systems," *Energy Conversion and Management*, Volume 43, Issue 14, pp. 1773-1789

Bentz, D.P., Hwang, J.T.G, Hagwood, C., Garboczi, E.J., Snyder, K.A., Buenfeld, N., and Scrivener, K.L., (1995), "Interfacial Zone Percolation in Concrete: Effects of Interfacial Zone Thickness and Aggregate Shape", in Microstructure of Cement-Based Systems/Bonding and Interfaces in Cementitous Materials, MRS Symp. Proc. Vol. 370, page 437-442.

Bourdette, B., Ringot, E., and Ollivier, J.P., (1995), "Modeling of the Transition Zone Porosity", *Cement and Concrete Research,* Vol. 25 (4), pp. 741-751.

Castro-Borges, P., and Torres-Acosta, A.A., (2010), "Capillary Absorption and Concrete Durability", *Concrete under Severe Conditions*, Taylor & Francis Group, London.

Chatterji, S., (2004), "An Explanation for the Unsaturated State of Water Stored Concrete." *Cement and Concrete Composites*, vol. 26, pp. 75-79.

Correns, C.W., (1949), "Growth and dissolution of crystals under linear pressure" *Discuss Faraday Soc* 5:267–71.

Corr, D.J, Monteiro, P, J., and Bastacky, J., (2002), "Microscopic Characterization of Ice Morphology in Entrained Air Voids," *ACI Materials Journal*

Collins, F.G, and Sanjayan, J.G., (2010). Capillary Shape: Influence on Water Transport within Unsaturated Alkali Activated Slag Concrete. *Journal of Materials in Civil Engineering,* Vol. 22, pp. 260-266.

Cwirzen, A., and Penttala, V. (2005). Aggregate-cement paste transition zone properties affecting the salt-frost damage of high-performance concretes. *Cement and Concrete Research, 35*(4), pp. 671-679

Garas, V.Y., Jayapalan, A.R., Kahn, L.F., and Kurtis, K.E. (2010), Micro- and Nanoscale Characterization of Effect of Interfacial Transition Zone on Tensile Creep of Ultra-High-Performance Concrete, *Transportation Research Board of the National Academies*, Washington, D.C., pp.82-88

Gulati, S.T., and Hagy, H. E. (1982) ‘‘Analysis and Measurement of Glue-Spall Stresses in Glass–Epoxy Bonds,’’ *Journal of the American Ceramic Society,* 65 [1] 1–5.

Helmuth, R.A. (1960) Capillary Size Restrictions on Ice Formation in Hardened Portland Cement Pastes, *Proceedings Fourth International Symposium on the Chemistry of Cement*, Washington, pp. 855-869

Janusz, A., (2010), Investigation of Deicing Chemicals and Their Interaction with Concrete Materials, Master Thesis. West Lafayette. IN: Purdue University.

Klieger, P. 1994. Air-Entrained Admixtures, *Significance of Tests and Properties of Concrete and Concrete Making Materials*. ASTM STP 169c. Eds. Paul Klieger and Joseph F. Lamond. West Conshohocken, PA: American Society for Testing and Material. pp. 484-490.

Kosmatka, S. H., Kerkhoff, B., and Panarese, W.C., *Design and Control of Concrete Mixtures*, EB001, 14th edition, Portland Cement Association, Skokie, Illinois, USA, 2002, 358 pages.

Li, W., Pour-Ghaz, M., Castro, J., and Weiss, J., (2012) “Water Absorption and Critical Degree of Saturation Relating to Freeze-Thaw Damage in Concrete Pavement Joints”, *Journal of Materials in Civil Engineering*, Vol. 24, pp. 299-307.

Maso, J.C. (1996), *Interfacial Transition Zone in Concrete*, RILEM State-of-the-art Report (E&FN Spon, London).

Maso, J.C., (1980), *The Bond Between Aggregates and Hydrated Cement Pastes*, Proc. 7th Intl. Cement Congress, 3-15.

Mehta, P. K. (1986), *Concrete: Structure, Properties, and Materials*. Englewood Cliffs, NJ: Prentice-Hall.

Mehta, P.K., and Monteiro, P.J.M., (1988), “Effect of Aggregate, Cement, and Mineral Admixtures on the Microstructure of the Transition Zone”, *Materials Research Society*, Proc. 114, 65-75.

Mindess, S., Young. J. F. and Darwin, D., (1981). *Concrete*. Prentice-Hall, Inc., Englewood Cliffs, NJ.

Monteiro, P.J.M. and Mehta, P.K., (1986a), Improvement of the aggregate-cement paste transition zone by grain-refinement of hydration products, *proceedings of the 8th International Congress on the Chemistry of Cement*, Rio de Janeiro, Vol. 3, pp.433-7

Monteiro, P.J.M. and Mehta, P.K., (1985) Ettringite formation at the aggregate cement paste interface, *Cement and Concrete Research*, Vol. 15, pp. 378-80

Mondal, P., Shah, S.P., and Marks, L.D., (2009), *Nanomechanical Properties of Interfacial Transition Zone in Concrete*, Nanotechnology in Construction 3, Springer Berlin Heidelberg.

Neithalath, N. Analysis of Moisture Transport in Mortars and Concrete Using Sorption-Diffusion Approach. *ACI Materials Journal*, Vol. 103, No. 3, 2006, pp. 209–217.

Pigeon, M. and Pleau, R., (1995), *Durability of Concrete in Cold Climates*, London, E&FN Spon.

Page, C.L. and Page, M.M., (2007), *Durability of Concrete and Cement Composites*, Cambridge, England.

Powers, T.C., (1945), "A Working Hypothesis for Further Studies of Frost Resistance of Concrete," *Journal of the American Concrete Institute*, Vol. 16, No.4, pp. 245-272.

Powers, T.C. and Helmuth, R.A., (1953), "Theory of Volume Changes in Hardened Portland Cement Paste during Freezing." *Proc. Highway Res. Board*, Vol. 32, pp. 285-295

Power, T.C. 1954. Void Spacing as a basis for Producing Air Entrained Concrete, *Research Department Bulletin RX049*, Portland Cement Association.

Prokopski, G. and Halbiniak, J., (2000), "Interfacial Transition Zone in Cementitious Materials", *Cement and Concrete Research*, Vol. 30, pp. 579-583.

Ronning, T.F. "Freeze-Thaw Resistance of Concrete Effect of: Curing Conditions, Moisture Exchange and Materials", Ph. D. dissertation, The Norwegian Institute of Technology, 2001.

Saito, M., and Kawamura, M., (1993), "Effects of Sodium Chloride on the Hydration Products in the Interfacial Zone between Cement Paste and Alkali-Reactive Aggregate", *Proceedings of the RILEM International Conference*.

Scrivener, K.L., Bentur, A., and Pratt, P.L., (1988), "Quantitative Characterization of the Transition Zone in High Strength Concrete", Advances in Cement Research, Vol. 1 (4), pp. 230-237.

Scrivener, K.L., Crumbie, A.K., and Laugesen, P., (2004). "The Interfacial Transition Zone (ITZ) between Cement Paste and Aggregate in Concrete", *Interface Science*, 12(4), pp. 411-421.

Shi, X., Fay, L., Peterson, M.M., and Yang, Z. (2010) "Freeze-thaw Damage and Chemical Change of a Portland Cement Concrete in the Present of Diluted Deicers" *Materials and Structures*, Vol. 43, pp. 933-946.

Spragg, R.P., Castro, J., Li, W., Pour-Ghaz, M., Huang, P, and Weiss, J. (2011), "Wetting and Drying of Concrete Aqueous Solutions Containing Deicing Salts", *Cement and Concrete Composites*, vol. 33, pp. 535-542.

Stark, J., and Bollmann, K., (1997), "Ettringite formation – A Durability Problem of Concrete Pavements", *Proceedings of the 10th ICCC*, Gothenburg, Sweden, Vol. IV.

Sun, Z., and Scherer, W.G., (2010), "Effect of Air Voids on Salt Scaling and Internal Freezing", *Cement and Concrete Research*, Vol. 40, pp. 260-270.

Sutter, L., Peterson, K., Julio-Betancourt, G., Hooton, D., Van, D.T., Smith, K. The deleterious chemical effects of concentrated deicing solutions on Portland cement concrete. South Dakota Department of Transportation. Final Report: 2008

Taylor, P. C., S. H. Kosmatka, G. F. Voigt, M. E. Ayers, A. Davis, G. J. Fick, J. Gajda, J. Grove, D. Harrington, B. Kerkhoff, C. Ozyildirim, J. M. Shilstone, K. Smith, S. M. Tarr, P. D. Tennis, T. J. Van Dam, and S. Waalkes. 2006. *Integrated Materials and Construction Practices for Concrete Pavement: A State of the Practice Manual*. FHWA HIF-07-004. Federal Highway Administration, Washington, DC.

Tasong, W.A., Cripps, J.C., and Lynsdale, C.J., (1998), "Aggregate-Cement Chemical Interactions", *Cement and Concrete Research*, Vol. 28, pp. 1037-1048.

Toutanji, H.A., El-Korchi, T., (1995), "The Influence of Silica Fume on the Compressive Strength of Cement Paste and Mortar", *Cement and Concrete Research*, Vol. 25, pp. 1591-1602.

Valenza II JJ, and Scherer G.W., (2006), "Mechanism for Salt Scaling", *Journal of the American Ceramic Society*, Vol. 89, Issue 4, pp. 1161-1179.

Valenza II JJ, and Scherer G.W., (2007), "A review of salt scaling: I. Phenomenology." *Cement and Concrete Research*; vol. 37(7), pp. 1007-1021.

Verbeck, G. and Klieger, P., (1957) "Studies of 'Salt' Scaling of Concrete" *Highway Research Board Bulletin No.150.* Washington, D.C.: Transportation Research Board. 1-13.

Thaulow, N. and Sahu, S. (2004) "Mechanism of Concrete Deterioration due to Salt Crystallization" *Materials Characterization*, Volume 53, pp. 123-127.

Wang, L., and Ueda, T., (2011), "Mesoscale Modeling of Water Transport into Concrete by Capillary Absorption", *Ocean Engineering*, vol. 38, pp. 519-528.

Winslow, D.N., Cohen, M.D., Bentz, D.P., Snyder, K.A., and Garboczi, E.J. (1994). "Percolation and Pore Structure in Mortars and Concrete." *Cement and Concrete Research*, 24(1), pp. 25-37.

Winslow, D., and Liu, D., (1990). "The Pore Structure of Paste in Concrete", *Cement and Concrete Research*, 20(2), pp. 227-235.

Yuan, C.Z., and Odler, I., (1987), "The Interfacial Zone between Marble and Tricalcium Silicate Paste", *Cement and Concrete Research*, Vol. 17, pp. 784-792

Zhang, J. and Taylor, P., (2012), "Investigation of the Effect of the Interfacial Zone on Joint Deterioration of Concrete Pavements", *International Conference on Long-Life Concrete Pavements*, Seattle.

CHAPTER 3. INVESTIGATION OF THE EFFECT OF THE INTERFACIAL ZONE ON JOINT DETERIORATION OF CONCRETE PAVEMENTS

A paper presented at *Internal Conference on Long-Life Concrete Pavements – Seattle, September 2012*

Jiake Zhang and Peter Taylor

Abstract

Some sawn joints in concrete pavements are deteriorating faster than desired in Midwest region of the United States. It is becoming clear that a significant factor causing the distress is the freezing and thawing of saturated concrete that contains a marginal air system and a high water to cement ratio, combined with the effects of non-NaCl deicing salts.

Typically, freeze-thaw damage is evidenced in the form of layers of small flakes, as water cyclically penetrates a few millimeters into the surface, then freezes, and expands. However, the distress in pavements is sometimes exhibited in the form of cracks that appear and grow about one inch from the free surface. These cracks are observed to go around the coarse aggregate leaving it clean with little or no cement paste adhering to it.

It is hypothesized that a mechanism for this observation is that when joints are saw cut, the cut aggregate face exposes the interfacial transition zone (ITZ) around the particle. If water is held in the saw-cuts, it can be wicked around the coarse aggregate particles through the ITZ. Subsequent freezing and dissolution of the soluble calcium hydroxide in the ITZ will cause cracking around the coarse aggregate particles until the stress field drives a vertical crack up to the surface about one inch from the sawn edge. Once the now-loose piece is removed by traffic loading, the cycle is repeated.

This paper describes an experimental program aimed at investigating this hypothesis. Factors influencing concrete ITZ evaluated in this study include w/cm, aggregate type, and addition of silica fume. A significant increase of both absorption and air permeability were observed with higher water to cement ratio (w/cm). Concrete mixture with limestone provides better durability than the mixture with gravel which results in reduce of ITZ on limestone mixture. However, the addition of silica fume increases the bonding between aggregate and paste which makes the gravel mixture has higher material loess and the limestone mixture more brittle during freezing and thawing.

Introduction

Some sawn joints in concrete pavements are deteriorating faster than expected in the Midwest region of the United States. The damage is typically observed in two different forms: one that looks like typical freeze thaw distress with small flakes being formed in the paste; and another in which vertical cracks form about an inch away and parallel to the joint face.

The freeze thaw mechanism is typically associated with pavements that contain marginal air-void systems and are exposed to abundant water – either through insufficient drainage in the base layer, or due to water being trapped in saw cavities. This mechanism has been thoroughly investigated (Li et al. 2011; Spragg et al. 2011). Their work has shown that saturated concrete is unable to resist cyclic freezing and thawing, regardless of the air content of the mixture. However, air is effective at delaying critical saturation.

The other mechanism is less well understood. While a crack is formed remote from the joint face, the concrete in between is often in good condition. Typically the crack will

form around the coarse aggregate leaving it unusually free of mortar. A possible explanation for this is that a saw cut through a piece of aggregate exposes the interfacial transition zone (ITZ) around the particle. Water or salt solution in the joint may absorb into the ITZ forming a thin layer around the aggregate. Subsequent freezing of water in the ITZ will cause expansion that will tend to separate the aggregate from the paste and drive a vertical crack up to the surface (Figure 26). Some field examples show evidence of water movement along cracks as shown in Figure 27.

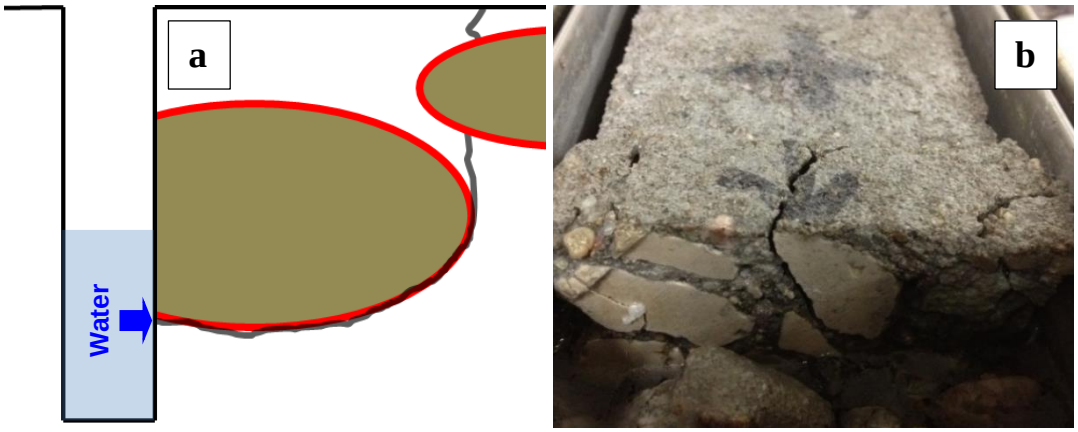

Figure 26. Crack developing out of a saturated ITZ (a: schematic sketch of the theory; b: laboratory observation for supporting the theory)

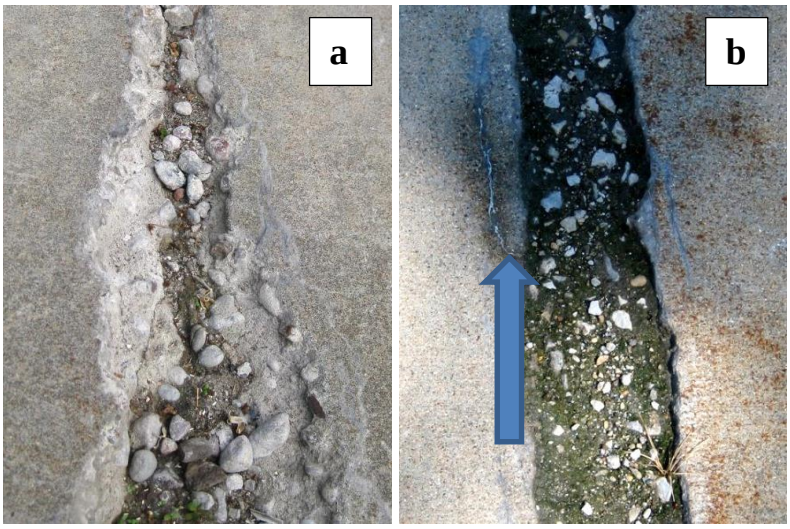

Figure 27. Field observations of joint deterioration (a: aggregates is clean and free of adhering mortar due to cyclic freeze thaw; b: water coming out of crack)

This paper discusses initial experimental work conducted to investigate the feasibility of this hypothesis.

Interfacial Transition Zone

The interfacial transition zone (ITZ) in concrete is a thin zone of paste around aggregate particles that has different characteristics from the bulk paste. According to Mehta (1986), the ITZ is typically 10 to 50 μm thick and is weaker than either of the two components of concrete. Under loading, micro-cracking will propagate more easily around the aggregate leading to reduce concrete strength. However, if the bonding between the aggregate and the paste is stronger than the aggregate, the failure surface may go through the aggregate rather than around the aggregate. The ITZ is also reportedly more permeable than the bulk paste, thus leading to reduce durability of the concrete, particularly if the aggregate is exposed to the environmental (Cwirzen and Penttala 2004).

The ITZ has a reportedly complex structure (Prokopski and Halbiniak 2000). Large flat $Ca(OH)_2$ crystals formed within this structure, perpendicular to the surface of aggregate grains, which results in the formation of a highly porous structure in the cement paste. The size and concentration of crystalline compounds such as calcium hydroxide and ettringite are larger in the ITZ than the bulk cement paste which leads to lower strength of the ITZ than the bulk cement paste in concrete (Mehta 1986). This information is consistent with the fact that the microcracks initiate within the ITZ and propagate to connect with each other when concrete is loaded.

Several factors influence the size of the ITZ. A common means of reducing the influence of the ITZ is to include silica fume in the mixture (Andrzej and Vesa, 2004). Use of

10% of silica fume in concrete reportedly results in a reduction of 36% in the thickness of the ITZ (Rossignolo, 2006). Silica fume particles strengthen the ITZ structure by consuming calcium hydroxide in a pozzolanic reaction (Vivekanandam and Patnaikuni 1997; Zhang, Lastra and Malhotra 1996). The mechanisms behind this reduction include:

- Reduced bleeding, leading to reduced water accumulation at the aggregate surface
- Presence of multiple nucleation sites for crystallization to start
- Accelerated pozzolanic reactions because of the extremely small particle sizes of silica fume.

Reducing water cementitious materials ratio will also reduce the width of the ITZ. Andrzej and Vesa (2004) reported that the width of the ITZ decreased from 40 μm to less than 5 μm as the w/cm ratio was changed from 0.42 to 0.30.

A third factor that influences performance is the aggregate. The larger the nominal maximum sizes of aggregate in concrete and the higher the proportion of elongated and flat particles the weaker the ITZ (Mehta 1986). Elongated aggregate shapes resulted in lower aggregate contents being required for ITZ percolation than spherical ones, which decreases the ITZ volume and reduces the effects of ITZ connectivity on transport coefficients (Bentz et.al. 1995). It is also likely that the mineralogy of the aggregate will affect the ITZ due to variations in surface absorption and reactivity.

Experimental Design

An experimental program was conducted to investigate whether the ITZ is a contributing factor to the premature deterioration of joints in concrete pavements. The approach was to prepare a series of mixtures with differing amounts of silica fume, w/cm, and aggregate type, and subjects them to an ASTM C666 testing freeze thaw test

environment followed by examination of the tested samples using optical and electron microscopy. The parameters that were fixed and varied are shown in Table 3.

Table 3. Design parameters

Variables	
Water cement ratio	0.40 and 0.50
Binder	0, 3 and 5% silica fume
Coarse aggregate	Round gravel (absorption=0.3%, *G_s=2.66) and crushed limestone(absorption=0.9%, G_s=2.67)
Fixed parameters	
Binder content	564 pcy
Air content	6±1%
Fine aggregate	River sand

*Gs: Specific gravity

Samples were wet cured for 14 days and then dried for 28 days prior to the start of testing, and following tests were conducted:

- Sorption according to ASTM C1585 using two specimens prepared from one cylinder: one from the finished surface and another cut from deeper in the cylinder.
- Air permeability index (API) testing was conducted using the University of Cape Town Method. Samples were similar to those used for sorption testing.
- Freeze thawing testing was conducted in accordance with ASTM C666 Procedure A. Two beams were prepared from each mixture. Two extra beams were prepared from the mixture containing gravel, high water cement ratio and no silica fume and the mixture with limestone, low water cement ratio and high silica fume content for testing in 3% sodium chloride solution.
- After freeze-thaw cycling the two beams cycled in NaCl were split and sprayed with silver nitrate to map the chloride distribution on the cross section.
- Chloride distribution was also investigated using a scanning electron microscope (SEM) on concrete beams that had been subjected to 300 freezing and thawing

cycles in calcium chloride solution. These beams were obtained from another experiment.

Results and Discussion

The initial rate of absorption and secondary rate of absorption were obtained as shown in Figure 28 and Figure 29. Samples with higher w/cm show significantly higher absorptions than those with lower w/cm. Concrete made using gravel has slightly higher absorption than the concrete with limestone, and there is no clear trend due to the influence of silica fume.

The finished surface samples have higher initial and secondary rates of absorption than the sawn surface samples. This is likely due to effects of

- Increased paste content at the surface
- Possible reduced hydration at the surface
- Increased surface area of the rough finished surface

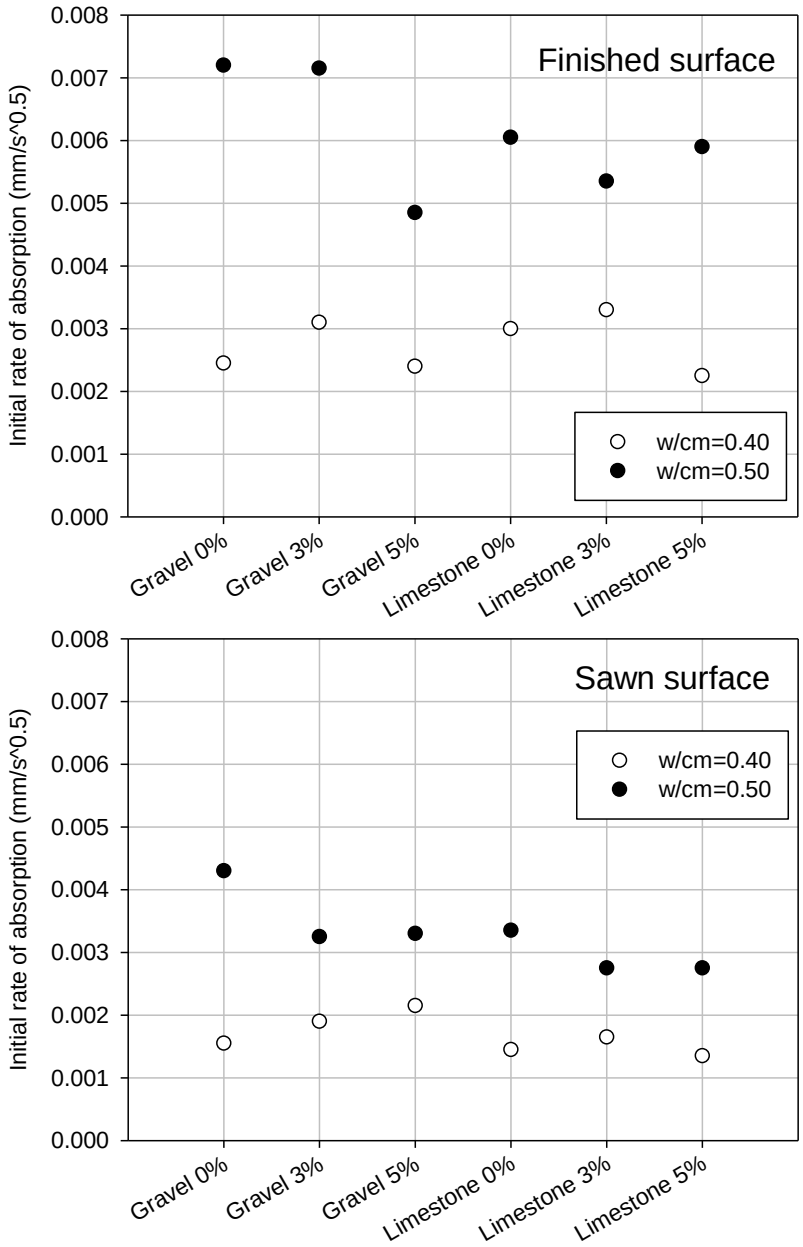

Figure 28. Initial rate of absorption for finished surface samples and sawn surface samples

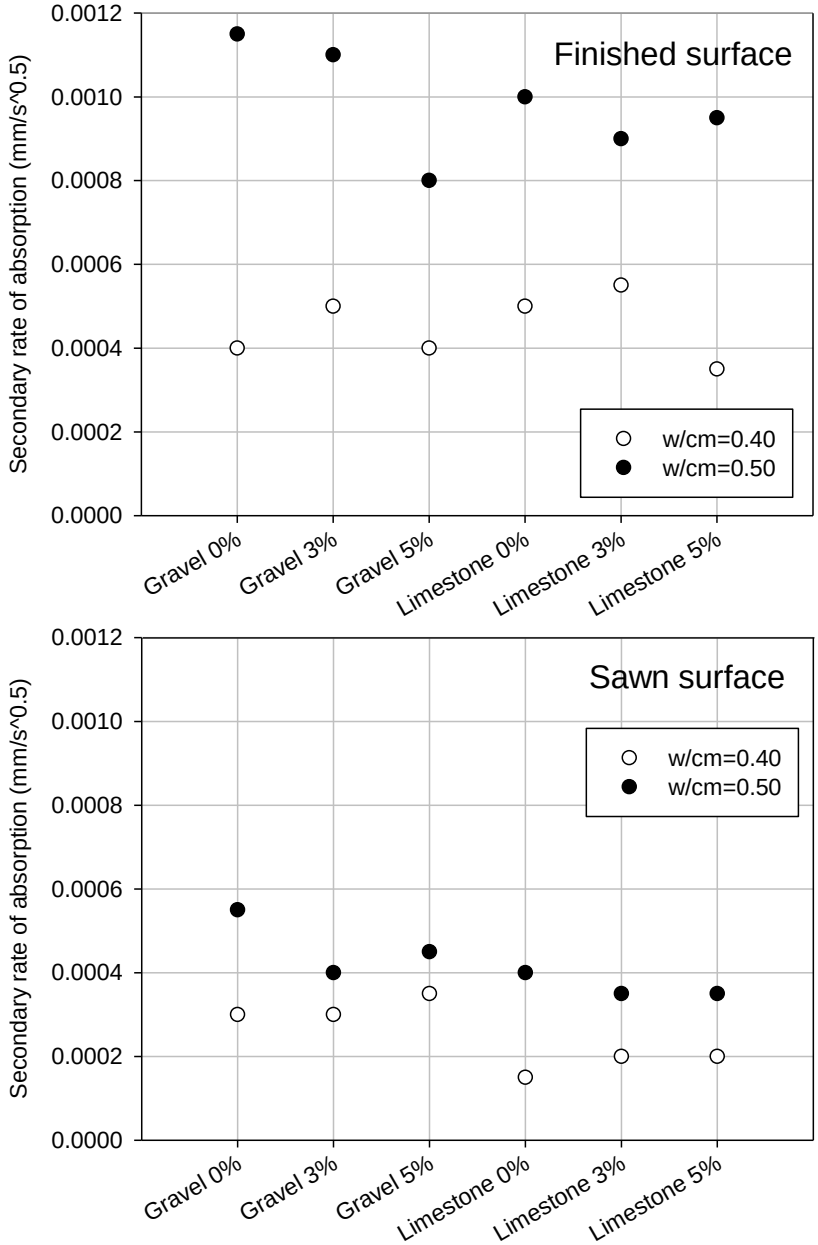

Figure 29. Secondary rate of absorption for finished surface samples and sawn surface samples

The air permeability index (API) was calculated based on the pressure decay as air passed through a concrete disk. Higher API values indicate lower permeability. The API data does not show clear trends with changing silica fume content (Figure 30). Concrete with low w/cm using limestone exhibited lower permeability than concrete with high w/cm using

gravel. The sawn surface samples indicate slight lower permeability than the finished surface samples, and that may due to the finished surface samples were obtained from the upper portion of the cylinder, which result in less dense than the sawn surface samples.

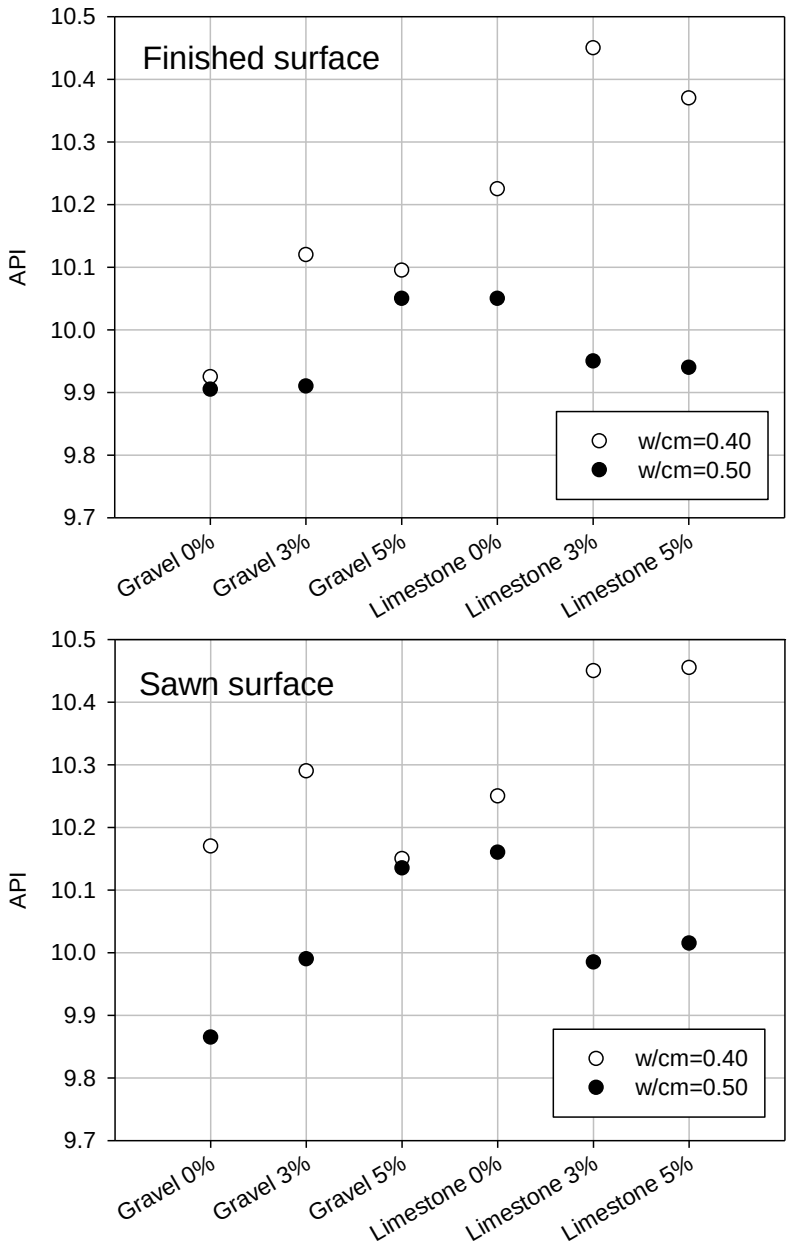

Figure 30. API of the finished surface samples and sawn surface samples

Freeze thaw tests were conducted in accordance with ASTM C666 Procedure A for 600 cycles. Both weight and dynamic modulus were measured after every thirty cycles. The

average weight and relative dynamic modulus are shown in Figure 31 and Figure 32. No significant differences, or distress, were observed for the first 300 freezing and thawing cycles, except for the beams under salt solution during freezing and thawing cycles. The change in weight of the gravel mixture is slightly higher than the limestone mixture, especially for the beams under salt solution. This is predominantly because the gravel mixture exhibited severe popouts during freezing and thawing cycles, likely due to chert in the material.

Trends from the relative dynamic modulus of elasticity were similar to the weight measurements, and no significant differences were seen during the first 300 cycles as shown in Figure 32. However, after 300 cycles, distress did start to accumulate. The limestone mixtures performed better than the gravel mixtures, and both mixtures deteriorated faster in the salt solution. The gravel mixtures exhibited more distress than those containing limestone. A possible explanation is that the gravel contained chert that lead to popouts. It also appeared that silica fume improved the bond between aggregate and paste resulting in more material loss when popouts occurred.

In contrast, the mixtures with limestone did not have the popout problem and the increased bonding between aggregate and paste likely made the beam more brittle. This would lead to single cracks forming in the samples so significantly the effects observed using RDM.

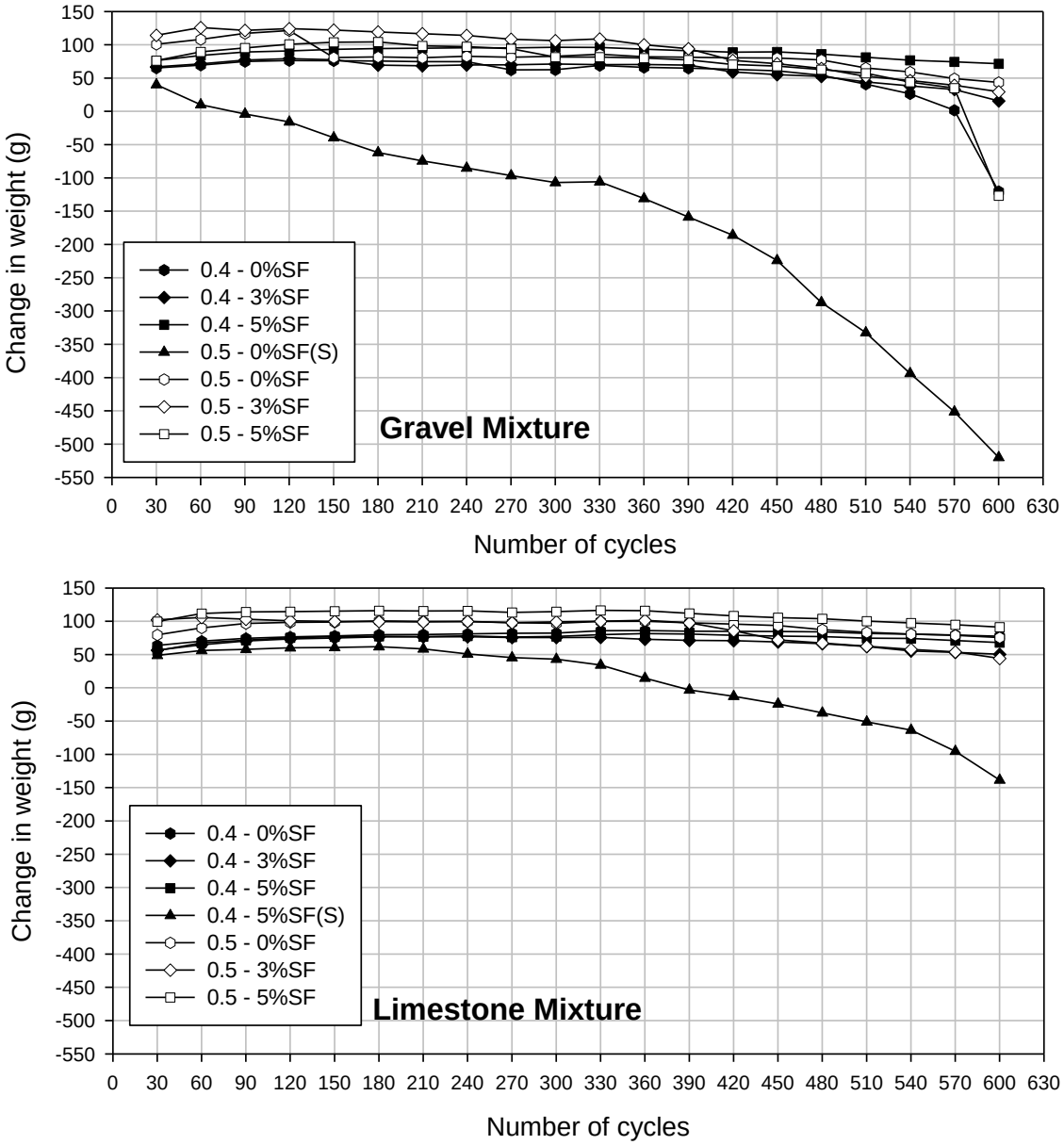

Figure 31. Weight change on the beams for 600 freezing and thawing cycles (0.4-0%SF: w/cm=0.4 with 0% silica fume; 0.4-5%SF(S): w/cm=0.4 with 5% silica fume under salt solution)

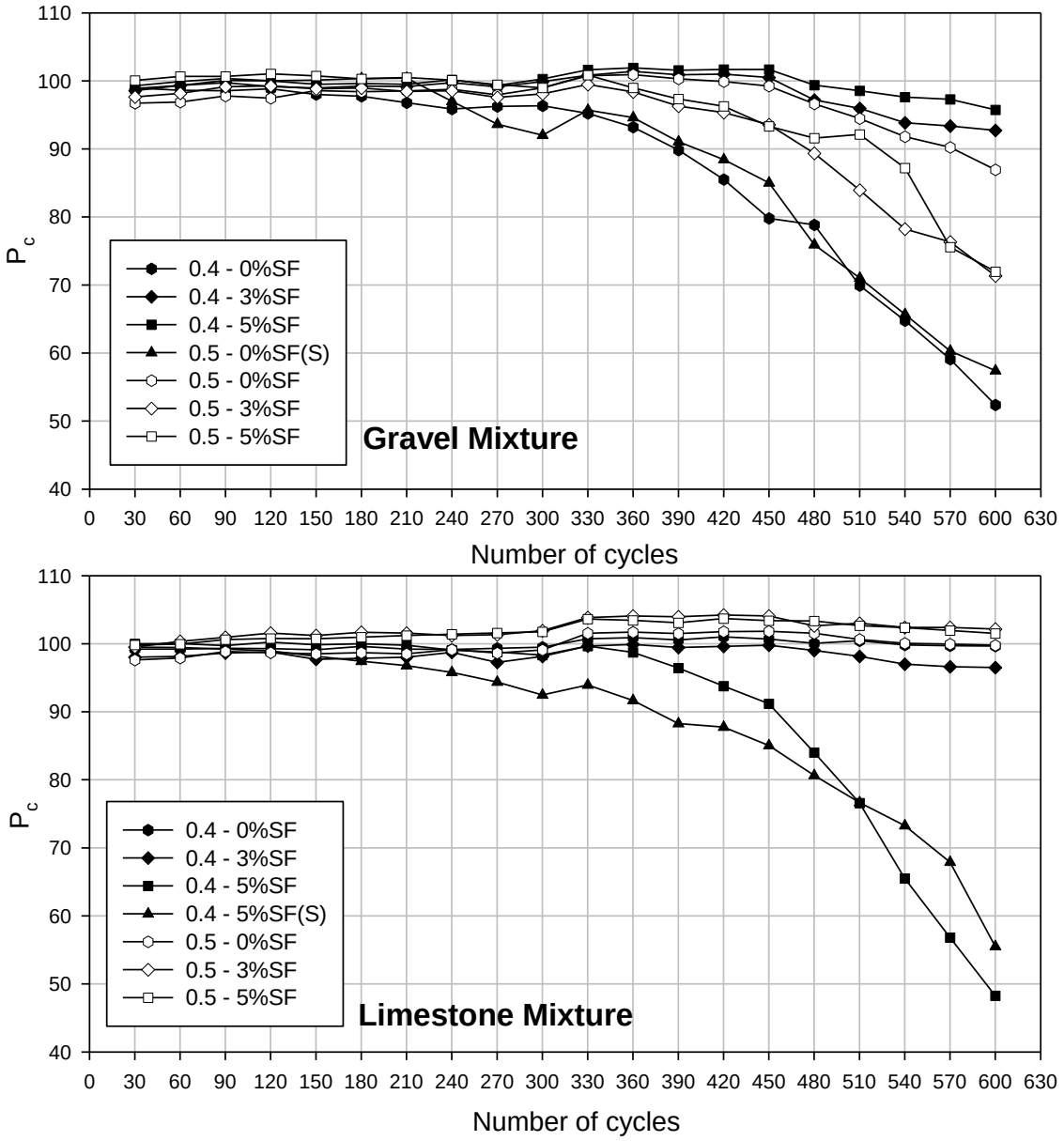

Figure 32. Relative dynamic modulus of elasticity on the beams for 600 freezing and thawing cycles (0.4-0%SF: w/cm=0.4 with 0% silica fume; 0.4-5%SF(S): w/cm=0.4 with 5% silica fume under salt solution)

Distress likely related to the ITZ was observed in the sample as shown in Figure 33. In some cases, the failure surfaces go around aggregate which is consistent with the hypothesis.

Figure 33. Laboratory observation of distress related to the ITZ during freezing and thawing cycle

Concrete beams tested under salt solution were further investigated using silver nitrate to map the distribution of chloride on a cut face perpendicular to the length of the beam. Two slices were cut from each beam. One slice was sprayed with silver nitrate after cyclic testing was completed, and the other was vacuum saturated under salt solution prior spraying.

Some locations show a narrow “white ring” around the aggregate as shown in Figure 34, which indicates the salt solution preferentially penetrated into the ITZ. The limestone aggregates show fewer “white rings” than the sample mixed with gravel. The sample mixed with gravel had a higher w/cm without any silica fume, all factors likely leading to a more dominant ITZ.

Figure 34. Silver nitrate sprayed samples for mapping chloride (a: concrete mixture using gravel; b: concrete mixture using limestone)

If such porous ITZ zones were more saturated with water and/or salt solution than the bulk paste when the concrete was frozen, it is likely that the paste would separate from the aggregate, as is seen in the field. This is supported by examination of the fracture surfaces of slices broken in half. In the gravel, high w/cm case, the aggregate has debonded from the bulk paste, and the silver nitrate is showing some chloride presence in the cavity left behind (top slice in Figure 35). In the other low w/cm sample with silica fume, a similar fracture has propagated through the aggregate rather than around it.

Figure 35. Fracture surface of silver nitrate sprayed samples

SEM analysis was performed on a specimen obtained from a concrete beam which underwent 300 freezing and thawing cycles in a calcium chloride solution. The SEM image is shown in Figure 36, and the lighted area indicates the concentration of the element, which is shown on the upper left corner, on the sample. Both chloride map and calcium map show a lighted area around the aggregate, which indicates the presence of salt solution in the ITZ.

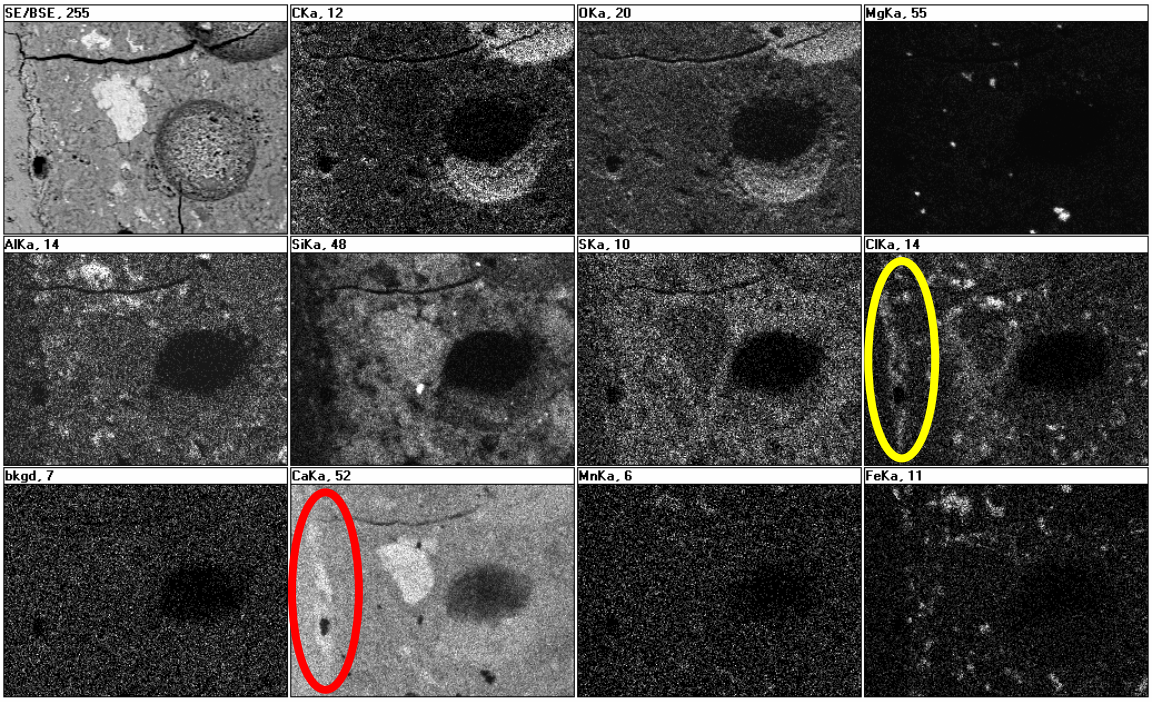

Figure 36. SEM analysis on distressed samples under cyclic freeze thaw in $CaCl_2$ solution

Conclusion and Recommendation

Factors affecting the concrete interfacial transition zone (ITZ) were evaluated in this study. These, include w/cm, aggregate type, and addition of silica fume. Concrete samples were evaluated using an absorption test, air permeability test, cyclic freezing-thawing test and visual observation of surfaces sprayed with silver nitrate.

The tests results show that concrete mixtures with a higher w/cm ratio (0.5) exhibited

higher absorption and higher air permeability. High w/cm samples also exhibited more salt accumulation around aggregate particles, greater distress and greater tendency for cracks to go around the aggregate.

Concrete mixtures with limestone showed significantly higher durability than the gravel mixtures, and that is likely due to lower impact of ITZ compared with gravel.

The collected evidence from the permeability tests and the microscopy all indicated that the ITZ can indeed be contributing to the accelerated deterioration of joints in concrete pavements.

References

Bentz, D.P., Hwang, J.T.G., Hagwood, C., Garboczi, E.J., Snyder, K.A., Buenfeld, N. and Scrivener, K.L.(1995), "Interfacial zone percolation in concrete: Effects of interfacial thickness and aggregate shape," in Microstructure of Cement-Based Systems/Bonding and Interfaces in Cementitious Materials, edited by S. Diamond et. al., (Materials Research Society Vol. 370, Pittsburgh) pp. 437-442

Cwirzen, A., and Penttala, V. (2004). Aggregate-cement paste transition zone properties affecting the salt-frost damage of high-performance concretes. *Cement and Concrete Research*, 35(4), pp. 671-679

G. Prokopski, and J. Halbiniak (2000). Interfacial transition zone in cementitious materials. Cement and Concrete Research, 30 (2000), pp. 579-583

Li, W., Pour-Ghaz, M., Castro, J., and Weiss, W. J., (2011) “Water Absorption and the Critical Degree of Saturation as it relates to Freeze-Thaw Damage in Concrete Pavement Joints,” ASCE Journal of Civil Engineering Materials

Mehta, P. K. Concrete: Structure, Properties, and Materials. Englewood Cliffs, NJ: Prentice-Hall, 1986.

Rossignolo JA (2006), Interfacial interactions in concretes with silica fume and SBR latex, *Construction and Building Materials*, pp. 817-821.

Spragg, R., Castro, J., Li, W., Pour-Ghaz, M., Huang, P., and Weiss, W. J., (2011) “Wetting and Drying of Concrete in the Presence of Deicing Salt Solutions”, Cement and Concrete Composites, Volume 33, Issue 5, May, pp. 535-542

Vivekanandam, K., and Patnaikuni, I. (1997), Transition Zone in High Performance Concrete During Hydration, Cement and Concrete Research, Vol. 27 (6), pp. 817-823.

Zhang, M.H., Lastra, R., and Malhotra, V.M. (1996), Rice-Husk Ash Paste and Concrete: Some Aspects of Hydration and the Microstructure of the Interfacial Zone Between the Aggregate and Paste, Cement and Concrete Research, Vol. 26 (6), pp. 963-977.

CHAPTER 4. INVESTIGATION OF INTERFACIAL ZONE RELATED FREEZING AND THAWING DETERIORATION IN CONCRETE PAVEMENTS

A paper to be submitted to *ACI Materials Journal*

Jiake Zhang and Peter Taylor

Abstract

Sawn joints in concrete pavements appear to be more easily susceptible to deterioration under cyclic freezing and thawing than formed joints and a number of factors may contribute to this. It is hypothesized that the significant difference between the two joints is that in the sawn joints the coarse aggregates, and the interfacial transition zones (ITZ) around them are exposed in the sawn joints but covered by paste in the formed joint. Water and salt solutions can easily penetrate into concrete through the permeable ITZ, which increases the risk of local expansion or dissolution around the aggregate particles at the joint face.

The work described in this paper was performed to evaluate this hypothesis. A range of concrete mixtures were tested in a range of deicing solutions which subjected to cyclic freezing and thawing. The data indicate that this mechanism is feasible, and that improving the quality of the interfacial zone will likely reduce the risk of damage.

Introduction

It has been observed that sawn joints are more easily subject to freeze thaw deterioration than formed joints in concrete pavements. The difference between the sawn joints and formed joints is that the coarse aggregate, and the interfacial transition zones (ITZ) are exposed in the sawn joints but covered by paste in the formed joint (Zhang and Taylor

2012). The ITZ is reported to be more permeable than the bulk paste in concrete (Cwirzen and Penttala 2005). Water or salt solution trapped in the kerf of a sawn joint is therefore more readily absorbed into the matrix and so able to expand during freezing due to ice formation and/or salt crystallization.

One approach to improving the quality of the ITZ is to include silica fume into a mixture. Silica fume is added to concrete to enhance properties, such as to reduce permeability and improve strength. Thomas et al. (1999) reported that chloride diffusivity is significantly lower for concrete containing silica fume compared with plain concrete (Figure 37). Similar conclusions about permeability have been reached by other researchers (ACI 1987; Gjorv et al. 1990; Cwirzen and Penttala 2005). The effects of silica fume are reportedly due to two mechanisms: pozzolanic reactions that convert calcium hydroxide to calcium silicate hydrate, and as a micro-filler that acts as an initiation site for reaction products to form around (Detwiler et al. 2006). Silica fume contents are typically between 5% and 10% by mass of the cementitious material (Kosmatka et al. 2002) which is the range evaluated in this work.

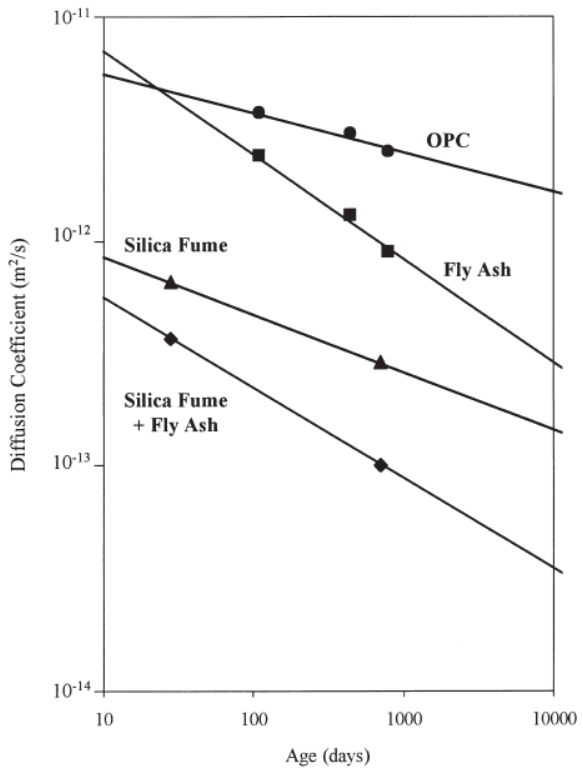

Figure 37. Effect of silica fume on concrete chloride diffusivity (Thomas et al. 1999)

The effect of deicing salts on distress accumulation was evaluated under cyclic freezing and thawing. The salts evaluated were sodium chloride, magnesium chloride, and calcium chloride at concentrations of 3% and saturated. Sutter et al. (2008) reported that mortar cylinders exposed in $MgCl_2$ and $CaCl_2$ solution at 40°F exhibit more distress than those exposed to NaCl solution due to formation of expansive calcium oxychloride. It has been found that deicing solutions result in more distress to concrete at concentrations of about 3% during freezing and thawing than at other values (Verbeck and Klieger 1957). This reportedly due to the salt scaling affect. When deicing solutions freeze, it will form an ice layer covers the concrete surface. The ice layer cracks as temperature continue drops because of thermal expansion mismatch, and concrete cracks when the ice layer propagate (Sun and Scherer 2010).

Li et al. (2012) have reported a clear increase of freeze-thaw related distress with increasing sample saturation above about 86−88%. When the degree of saturation above the critical degree of saturation, the damage initiates during the first freezing and thawing cycle. Sample with the saturation lower than the critical saturation did not show damage, but sample with the saturation above the critical saturation show a rapid distress during cyclic freezing and thawing.

Previous work reported by the authors indicated that exposed ITZ zones are likely contributing to accelerated failure of concrete joints (Zhang and Taylor 2012). The aim of the work reported here was to use different silica fume concentrations in mixtures exposed to freezing and thawing cycles under a range of deicing salts to continue to assess the validity of the hypothesis. The other variable assessed was to compare performance of samples that had been vacuum saturated with similar samples that were soaked in water for several days following 28 days of drying.

Experimental Design

Table 4 summarizes the experimental matrix for this study.

Table 4. Experimental Matrix

Variables	
Water cement ratio	0.38 and 0.45
Binder	0, 5 and 10% silica fume
Moisture content	Vacuum saturated and soaked
Fixed parameters	
Binder content	564 pcy
Air content	6±1%
Coarse aggregate	Round gravel
Fine aggregate	River sand

Two concrete 3" × 4" × 16" beams were prepared from each mixture. All beams were subjected to 3 days wet curing then in air until aged 28 days, when they were sliced into 1 inch thick samples. The selection of a short, wet curing period was to mimic field practice. Sliced samples were soaked in one of the 7 test solutions under vacuum saturation for 24 hours. An extra set of samples was soaked in water for 28 days instead of vacuum saturated. One-inch thick samples, with exposed aggregate faces were chosen to increase the degree of saturation internally for the soaked samples.

Seven solutions were used:

- Water
- 3% or saturated sodium chloride
- 3% or saturated magnesium chloride
- 3% or saturated calcium chloride

After vacuum saturation in the solutions, the samples were subjected to cyclic freezing and thawing using machines set up to run in accordance with ASTM C 666. The samples prepared in 3% solutions were tested in the same solutions. The saturated solution samples were tested in water because some of these solutions will not freeze at the temperatures used in the test.

Samples under test were regularly weighed and photographed, and the number of cycles to achieve a 1% mass loss was recorded.

Results and Discussion

Some fresh concrete properties are summarized in Table 5. All air contents of the fresh concrete mixtures were in a range normally expected to provide protection from freezing and thawing.

Table 5. Fresh concrete properties

Mix ID	w/cm ratio	Silica fume content (%)	Slump (in.)	Air content (%)	Unit weight (pcf)
1	0.45	0	6.0	5.5	147.4
2		5	5.0	7.0	143.6
3		10	3.0	7.0	142.2
4	0.38	0	2.0	6.0	147.0
5		5	1.8	6.3	146.2
6		10	1.0	5.0	146.2

Table 6 summarizes the number of freezing and thawing cycles to reach a 1% mass loss for samples prepared in different solutions.

The samples soaked in water, rather than vacuum saturated, lasted for the longest number of cycles and were still in good condition after 35 cycles. This indicates that the paste systems were able to resist conventional exposure. This is to be expected because the degree of saturation of these samples is unlikely to exceed the critical 85%. In the set of vacuum saturated samples, the samples prepared in saturated magnesium chloride exhibited the least distress under the freezing and thawing test. While this is unexpected, it may be explained by the probability that the solution contained in the sample pores prevented freezing and expansive ice formation.

Consistent with the previous research (Verbeck and Klieger 1957; Valenza and Scherer 2006), the samples prepared in 3% deicing solutions were less durable than prepared in high concentration and water.

Concretes with the lower water to cement ratio (w/cm=0.38) generally performed better, and also were more sensitive to silica fume content (Figure 38), as expected.

Table 6. Number of freezing and thawing cycles when sample exhibited 1% mass loss

w/cm	Silica Fume, %	H_2O (Soak)	H_2O	3% NaCl	Sat. NaCl	3% $MgCl_2$	Sat. $MgCl_2$	3% $CaCl_2$	Sat. $CaCl_2$
0.45	**0**	>35	17	5	18	8	38	7	14
0.45	**5**	>35	11	5	18	14	33	7	15
0.45	**10**	>35	13	5	18	7	29	7	24
0.38	**0**	>35	17	5	16	22	17	7	13
0.38	**5**	>35	11	11	20	14	25	7	15
0.38	**10**	>35	18	19	22	14	36	10	29

Red: <10 cycles, Green: >20 cycles to 1% mass loss

Figure 38. Sample exposed $MgCl_2$ solution during freezing and thawing (Top row: w/cm=0.38, bottom row: w/cm=0.45; left to right: silica fume contents are 10%, 5%, and 0%)

Figure 39 illustrates the surface of the example containing 10% silica fume and prepared in water after 11 freezing and thawing cycles. It can be seen that the paste fraction of the sample has expanded, leaving the surfaces of the coarse aggregate particles below the surface of the mortar. It is likely that this is due to the effects of cyclic freezing and thawing of solution in the paste capillaries, and the deposition of salts in the capillaries. That the sample has expanded rather than crumbled indicates that the expansion is a relatively small strain, but has occurred through the full thickness of the sample. 9% strain in concrete will

built as the absorbed water in the ITZ freezes because of the 9% volume expansion when water freezes, and that equivalents to 9.0×10^4 microstrain in concrete. Liu and McDonald 1978 reported that the strain capacity of concrete is ranging from 50 to 100 microstrain. Thus, the strain from freezing waster in the ITZ of a saturated concrete is extremely higher the strain capacity of concrete.

Also notable in Figure 39 is the number of coarse aggregate particles that have been removed from the sample leaving a clean indent. This is a clear indication that there had been significant damage in the ITZ, because if it were in the paste alone, the surface of the indent would not be smooth but pocked like the exposed surface. Likewise, the aggregates had been carefully selected to be sound under freeze thaw testing, as is confirmed by the lack of distress in the remaining aggregate particles.

Figure 39. Sample exposed in water during freezing and thawing showing paste pushed above the aggregate

Figure 40 illustrates this point further. In this case the sample is from a mixture containing 10% silica fume with w/cm of 0.45 and prepared in 3% NaCl solution after 10

freezing and thawing cycles. In this case a corner of the sample has been removed under freeze-thaw cycling leaving the coarse aggregate cleanly exposed. The limited surface distress in the sample indicates that the bulk paste was able to resist freeze thaw damage for the length of the test. The rough surface of the mortar around the exposed aggregate is typical of a fracture surface, likely set up by the tensile stresses imposed by the expansions occurring in the ITZ around the large aggregate particle. Two possible tensile stresses may contribute to this occurrence as the solution freezes, which are salt crystallization pressure and osmotic pressure. The crystallization pressure is about 374 psi based on equation (Correns 1949):

$$\mathrm{P} = \frac{RT}{V_s} \times \ln \frac{C}{C_s} \tag{4}$$

where

P = crystallization pressure,

R = gas constant (0.082 L-atm/mol K),

T = absolute temperature in K,

V_s = molar volume of solid salt in L/mole, and

C/C_s = the degree of supersaturation where C is the existing solute concentration and C_s is the saturation concentration.

The osmotic pressure is about 160 psi based on Valenza and Scherer (2007) when concrete freezes in a 3% NaCl solution, and the combined pressure is about 534 psi. Typical tensile strength of concrete containing 10% silica fume with w/cm of 0.45 is about 650 psi (Bhanja and Sengupta 2005). Thus, the combined tensile stress from crystallization pressure and osmotic pressure may not be enough to cause the distress on the concrete sample. It is therefore, a chemical dissolution during the freezing and thawing procedure is also

contributing to failure. Some researchers have reported that concrete interfacial transition zone is rich in calcium hydroxide (Mehta 1986; Maso 1996; Cwirzen and Penttala 2005). Calcium hydroxide can be dissolved with the present of deicing salt solution (Sutter et al. 2006). The combined mechanical damage and chemical dissolution will likely cause the coarse aggregate to debond without any paste adhering to it (Figure 41).

Figure 40. Sample exposed in 3% NaCl solution shown washed aggregate on concrete

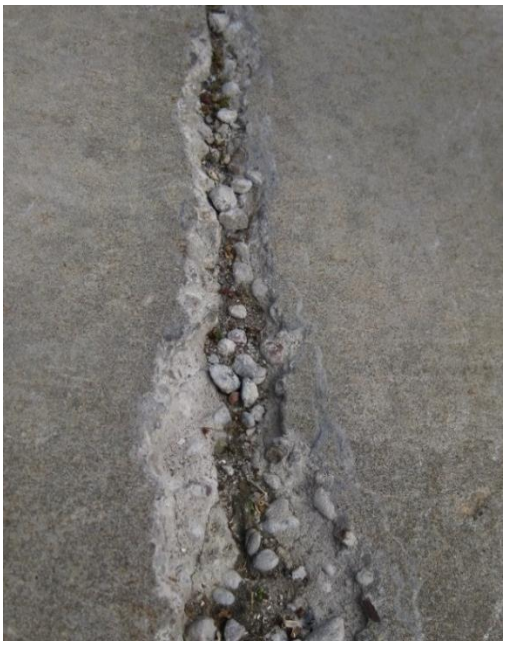

Figure 41. Field observation of joint deterioration

Conclusions and Recommendations

Six concrete mixtures were prepared with different w/cm ratio and silica fume contents. Samples were saturated in seven salt solutions before being subjected to freezing and thawing.

The test data and observations from the samples indicate that the ITZ appears to play an important role in the premature deterioration of joints in concrete pavements. The data also indicate that improving the paste quality helps to reduce the risk or amount of damage.

It is recommended that specifications should be based around the need to provide a high quality paste at the joint face, and extrapolating from this, that every effort should be made to ensure that the mixture is well cured, and protected from a suturing environment.

References

ACI Committee 226. (1987). "Silica fume in concrete." *ACI Material Journal*, Vol. 84, pp. 158-166

Bentz, D.P., Hwang, J.T.G., Hagwood, C., Garboczi, E.J., Snyder, K.A., Buenfeld, N. and Scrivener, K.L., (1995), "Interfacial zone percolation in concrete: Effects of interfacial zone thickness and aggregate shape", *Microstructure of Cement-Based Systeme/Bonding and Interfaces in Cementitious materials*, Vol. 370, pp. 437-442.

Bhanja, S., and Sengupta, B. (2005). "Influence of silica fume on the tensile strength of concrete", *Cement and Concrete Research*, Vol. 35, pp. 743-747.

Cwirzen, A., and Penttala, V. (2005). "Aggregate-cement paste transition zone properties affecting the salt-frost damage of high-performance concretes", *Cement and Concrete Research*, Vol. 35(4), pp. 671-679

Correns, C.W., (1949), "Growth and dissolution of crystals under linear pressure" Discuss Faraday Soc 5:267–71.

Detwiler, R. J., Bhatty, J. I., and Bhattacharja, S., Supplementary Cementing Materials for Use in Blended Cements, Research and Development Bulletin RD112, Portland Cement Association, 1996, 108 pages.

Gjorv, O., Monteiro, P., and Mehta, P. (1990). "Effect of condensed silica fume on the steel-concrete Bond", *ACI Material Journal*, Vol. 87(6), pp. 573-580.

Liu, T.C., and McDonald, J.E., (1978). "Prediction of tensile strain capacity of mass concrete", In *ACI Journal Proceedings*, Vol. 75, No. 5.

Li, W., Pour-Ghaz, M., Castro, J., and Weiss, J., (2012). "Water Absorption and Critical Degree of Saturation Relating to Freeze-Thaw Damage in Concrete Pavement Joints", *Journal of Materials in Civil Engineering*, Vol. 24, pp. 299-307.

Maso, J.C. (1996). *Interfacial Transition Zone in Concrete*, RILEM State-of-the-art Report (E&FN Spon, London).

Mehta, P. K. (1986), *Concrete: Structure, Properties, and Materials*. Englewood Cliffs, NJ: Prentice-Hall.

Paulon, V.A., Molin, D.D., and Monteiro, P.J.M., (2004). "Statistical analysis of the effect of mineral admixtures on the strength of the interfacial transition zone", *Interface Science*, Vol. 24, pp. 339-410.

Thomas, M.D.A, Shehata, M.H., Shashiprakash, S.G., Hopkins, D.S., and Cail, K., (1999), "Use of ternary cementitious systems containing silica fume and fly ash in concrete", *Cement and Concrete Research*, Vol. 29, pp. 1207-1214.

Khedr, S.A., Abou-Zeid, M.N., (1994), "Characteristics of Silica-Fume Concrete", *Journal of Materials in Civil Engineering*, Vol. 6, No. 3, pp. 357-375.

Valenza II JJ, and Scherer G.W., (2006), "Mechanism for Salt Scaling", *Journal of the American Ceramic Society*, Vol. 89, Issue 4, pp. 1161-1179.

Valenza II JJ, and Scherer G.W., (2007), "A review of salt scaling: II. Mechanisms", *Journal of Cement and Concrete Research*, Vol. 37, pp. 1022-1034.

Verbeck, G. and Klieger, P., (1957), "Studies of 'Salt' Scaling of Concrete" *Highway Research Board Bulletin No.150.* Washington, D.C.: Transportation Research Board. 1-13.

Sun, Z., and Scherer, W.G., (2010), "Effect of Air Voids on Salt Scaling and Internal Freezing", *Cement and Concrete Research*, Vol. 40, pp. 260-270.

Sutter, L., Dam, T.V., Peterson, K.R., and Johnston, D.P., (2006). "Long-Term Effects of Magnesium Chloride and Other Concentrated Salt Solutions on Pavement and Structural Portland Cement Concrete", *Journal of the Transportation Research Board*, No.1979, pp. 60-68.

Thaulow, N. and Sahu, S. (2004). "Mechanism of Concrete Deterioration due to Salt Crystallization", *Materials Characterization*, Volume 53, pp. 123-127.

CHAPTER 5. COMPARISON OF PORE SIZES OF CEMENT PASTE AND AGGREGATE USING MERCURY INTRUSION POROSIMETRY

A paper to be submitted to *ASCE Journal of Materials in Civil Engineering*

Jiake Zhang and Peter Taylor

Abstract

The pore size distributions of hardened cement pastes were studied in this research. Mercury intrusion porosimetry (MIP) was utilized in this research to obtain the pore structure of hardened cement pastes with different water to cement (w/cm) ratios and supplementary cementitious materials (SCMs). Paste samples were treated with air dry and oven dry before conducting the MIP test and cyclic freezing and thawing test. The findings were compared with pores sizes that may slow drying, thus increasing the risk of freeze thaw damage similar to that observed in D-cracking aggregates.

Introduction

The work described in this document is part of a large and ongoing project investigating the causes of premature deterioration of sawn joints in concrete pavements in cold regions.

The working hypothesis regarding the cause of damage is that water is penetrating the sawn face of the concrete to a level above 85% saturation, which then results in localized damage when freezing occurs (Fagerlund 1977; Li et al. 2012). The presence of deicing salts containing magnesium and calcium chloride have been shown to exacerbate the distress because they slow or prevent drying of the surface, increasing the saturation in the system.

Recommendations have therefore been made that the quality of the concrete should be improved to be able to resist this harsher environment (Sutter et al. 2008; Villani et al. 2012).

However, as part of the work, it was observed that two samples of concrete, only feet apart were performing very differently. On the one hand a parking lot is showing classic joint deterioration as shown in Figure 42A. On the other hand the adjacent sidewalk is undamaged (Figure 42B). This observation is counter-intuitive because it may be reasonably comfortably assumed that the quality of the pavement concrete is better than that of the sidewalk concrete. It was observed through the winter that the amount and type of salt applied to both surfaces was similar, mainly because of concerns about falling hazards on the sidewalk.

At the same time, work on another project was investigating the role of pore size distribution on the risk of D-cracking in some aggregates.

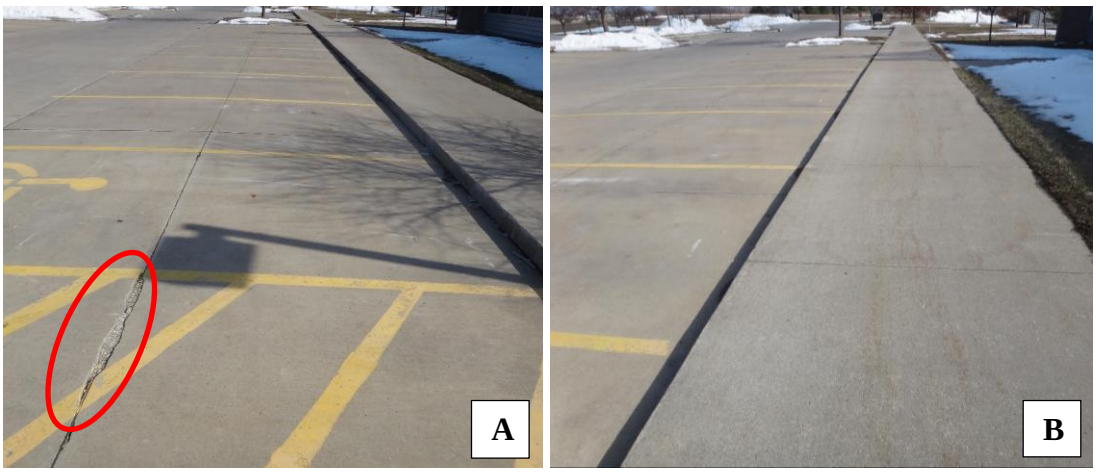

Figure 42. Field observation showing sidewalk performances better than parking lot (A: distressed parking lot, B: undamaged sidewalk)

Both pore structure and porosity of the aggregates influence the frost resistance of concrete. Concrete D-cracking is mainly caused by the delamination or cracking of coarse aggregate within the concrete due to expansion of freezing water within the aggregate pores

(Alexander and Mindess 2005) (Figure 43).

- Aggregates with fine and/or discontinuous pores tend to be durable because water has limited access into the surface of the aggregate. In addition, water in pores that are smaller than 0.1 μm tends not to freeze because of freezing point depression (ACI, 1996).
- Aggregates with coarse pores are also durable because freezing water can easily be expelled without causing significant distress to the aggregate (Pigeon and Pleau 1995).
- Aggregates with intermediate pores are the least durable because significant amounts of water can be absorbed into the aggregate, yet the pore sizes limit the transportation of the water back out when freezing occurs. Water expansion on freezing then set up tensile stresses in the aggregate leading to cracking of the aggregate that propagate into the concrete (Pigeon and Pleau 1995; Marks and Dubberke 1982).

Service records of 15 aggregate types from Iowa and Illinois show that aggregates with pore sizes ranging from 0.04 μm to 0.20 μm are non-durable in pavements (Marks and Dubberke 1982) (Figure 44).

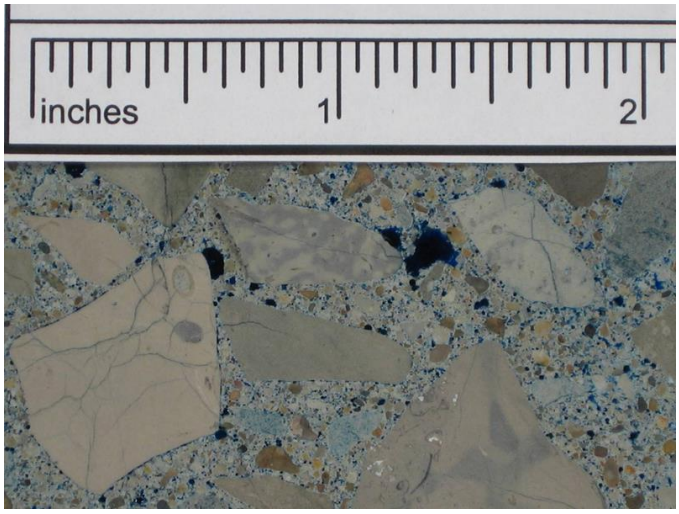

Figure 43. An example of a D-cracking aggregate that has cracked under freeze thaw cycling despite the air-entrained paste remaining in good condition

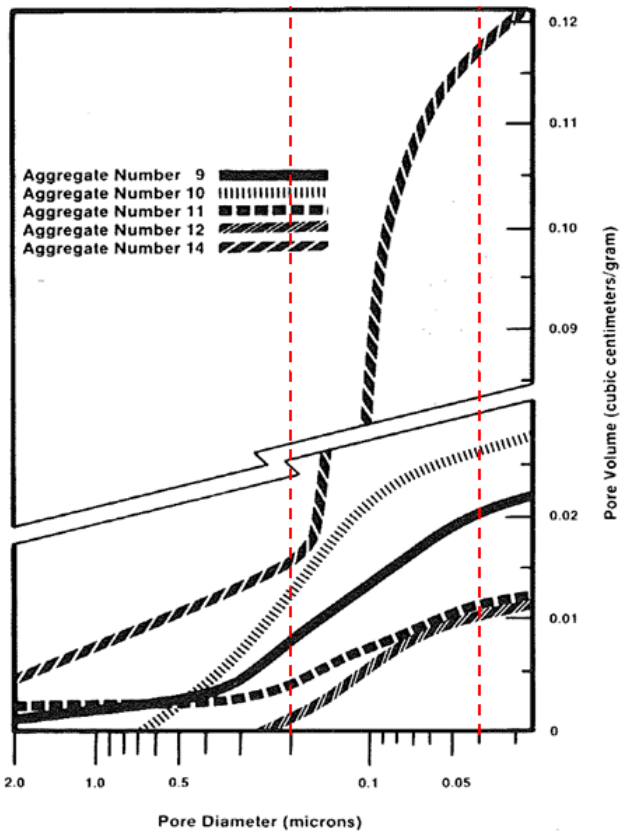

Figure 44. Pore size distribution for a typical D-cracking aggregate (Marks and Dubberke 1982)

Based on the observation that there is a particular range of pore sizes that are critical for risk of aggregate D-cracking, the question was raised whether such a similar phenomenon may be true of cement paste. In this case very high quality pastes would limit ingress of water, while very poor quality of paste would allow water move freely, but intermediate quality paste is at risk of trapping water and thus being more prone to freeze thaw damage. The work reported here discusses an initial investigation into this question.

The capillary pore structure of cement paste is primarily governed by the w/cm of the mixture, because water that is no used in hydration remains in the microstructure, and after evaporation leaves behind so-called capillary pores. The more water in the original mix, the greater the volume of capillary pores while a greater degree of will reduce porosity because

more water is consumed in the reaction (Cook and Hover 1999). Mehta (1986) compared data for hardened cement paste cured for 28 days with a range of w/cm ratios and showed that decreasing w/c resulted in finer and lower porosity.

The addition of supplementary cementitious materials also reportedly reduces the size and volume of capillary pores in hardened cement pastes (Cook and Hover 1999; Chindaprasirt et al. 2005).

Villani et al. (2012) reported that equilibrium relative humidity is above 90% for paste systems with pore diameters in the range of 0.05 μm to 0.10 μm. This means that hardened cement pastes with such pore sizes tend to remain nearly saturated, even at moderate exterior humidity levels. Pores larger than 0.50 μm will tend to allow evaporation at typical environmental humidity and typically do not remain completely filled with water, and so do not incur frost damage (Page and Page 2007).

Mercury intrusion porosimetry (MIP) is a test used to assess the pore structure of porous materials. The method involves squeezing liquid mercury into the surface of a small sample. The pressure required to force the mercury into the sample is a function of the pore system. This relationship is used to assess the distribution of pore sizes in the sample. A limitation of this approach is that pores with a small throat will be reported as the size of the throat (ink bottle effect), which may bias the results toward finer pores than reality (Abell et al. 1999; Cook and Hover 1999). Lange et al. (1994) reported that the pore sizes obtained from backscatter electron (BSE) microscopy were three orders of magnitude larger than the pore sizes obtained from MIP test.

Another limitation of the MIP test is the effect of moisture in cement−based materials

because water remaining in pores will hinder the flow of mercury–thus reporting finer systems than actual (Uchikawa et al. 1991). Air dried samples may therefore appear to be finer than the same sample that has been oven dried. This is to be balanced with the knowledge that oven drying will incur damage in the paste system.

Galle (2001) reported that higher curing temperature results in greater total porosity on hardened cement paste by conducting MIP tests. MIP result of the pore structure of hardened cement paste is significantly affected by the drying method. Because the increased curing temperature causes pore water leaving available space for mercury.

The work reported here is a brief and initial investigation into the pore size distributions in hydrated cement paste systems with different w/cm, SCM types and moisture states. The data collected using MIP is compared with typical data for D-cracking aggregates to assess whether the parameters of the paste system may be playing into the risk of freeze-thaw damage in concrete.

Experimental Design

This research aims at determining the pore sizes of hardened cement pastes with different w/cm ratios and investigating whether adding supplementary cementitious materials (SCMs), such as fly ash and silica fume will change the pore sizes. The data are compared with reported trends for D-cracking aggregates. The matrix of variables is shown in Table 7.

.

Table 7. Experimental Matrix

w/cm	0.30	0.40	0.60
SCM	None	None 20% Class C fly ash 5% silica fume	None
Sample drying	Oven to constant mass	Oven to constant mass	Oven to constant mass or in air dry for 7 days

The materials used in the mixtures were:

- Type I/II portland cement (ASTM C 150)
- Class C fly ash (ASTM C 618)
- Silica fume(ASTM C 989)

Paste samples were machine mixed and then formed into 1 in. diameter by 2 in. high cylinders in plastic bottles. The bottles were inserted into a frame and rotated at 7.5 rpm for 24 hours as shown in Figure 45 in order to minimize the effects of bleeding.

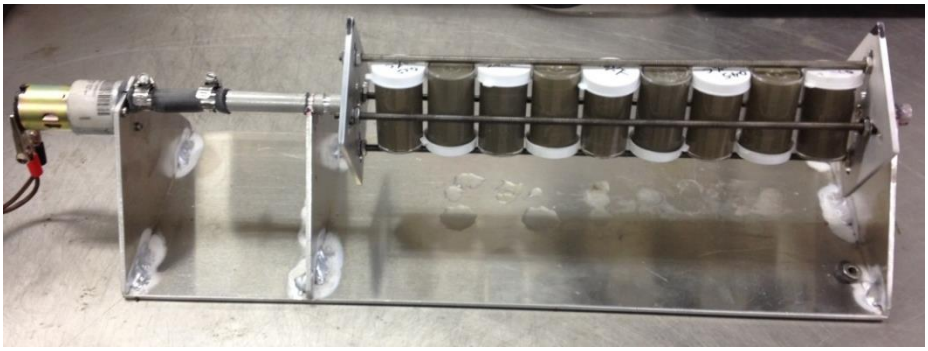

Figure 45. Rotating frame for fresh paste specimens during setting

Air dried samples were kept in their sealed bottles for 28 days at room temperature before being exposed to the air for a further 7 days before testing.

Oven dried samples were kept sealed in the bottles at 75°F until aged 7 days. The lids were then removed and the oven-dried samples were kept in an oven set at 122°F until constant mass was achieved.

Prepared samples were then shipped to a commercial lab for MIP testing using

applied pressures ranging from 0.50 psi to 60,000 psi. The equivalent pore radii were calculated using the Washburn equation:

$$P \times r = -2\gamma \cos\theta \tag{5}$$

where

P = applied pressure,

r = determined pore radius,

γ = mercury surface tension,

θ = contact angle between mercury and the pore wall.

In addition, one additional paste sample was prepared from each mix and subjected to cyclic freezing and thawing under water. Samples were cured with the same procedure as the MIP samples. Freezing and thawing was cycled at one cycle per day between 0 and 40°F. Samples were photographed daily.

Results and Discussion

The data collected are presented in Figure 46 through Figure 51, and discussed in the following paragraphs.

Figure 46 shows the pore size distributions for the oven dried pastes made with plain cement with w/cm ranging from 0.3 to 0.6. The vertical bars in the plot are the range of values normally considered to indicate aggregates at high risk of D-cracking (0.20 to 0.04 µm). As noted in the introduction, evaporation from pores in the range 0.05 to 0.10 µm is unlikely at normal environmental humidity levels. As expected, decreasing w/cm significantly decreases porosity of the systems, as exhibited by the areas under the lines. In addition, decreasing w/cm pushes the peak of each line to the right, indicating that the systems contain finer pore systems. Notable is that the peaks for the 0.3 and 0.4 mixtures are

within the range where drying is difficult. While the 0.6 mixture also has a peak in the same range, the bulk of the curve is to the coarse side of the envelope.

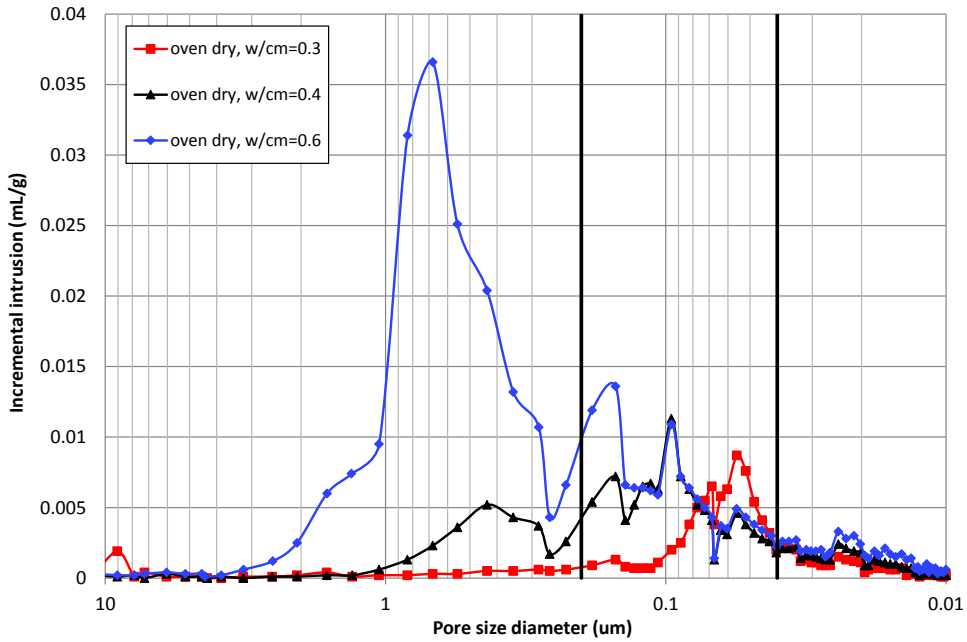

Figure 46. Pore size distribution for samples under oven dry treated

Photographs of similar samples subjected to one freeze thaw cycle are shown in Figure 47. It can be observed that the greatest distress is in the 0.4 w/cm sample. This is consistent with the model that open systems allow water to move freely, while tight systems do not allow sufficient water to enter and the intermediate system allows water to enter but not to leave readily.

Figure 47. Oven dried paste samples with different w/cm ratios after one freeze thaw cycle

Figure 48 compares the data collected in this work and that reported by Mehta (1986). Differences in the samples include 28 day curing by Mehta and 7 days followed by oven drying in this work. The trends between the mixtures are similar, but the systems reported in this work are coarser than those from Mehta. This is to be expected based on the shorter curing period. It is notable that there is a marked difference between the 0.6 w/cm set and the others.

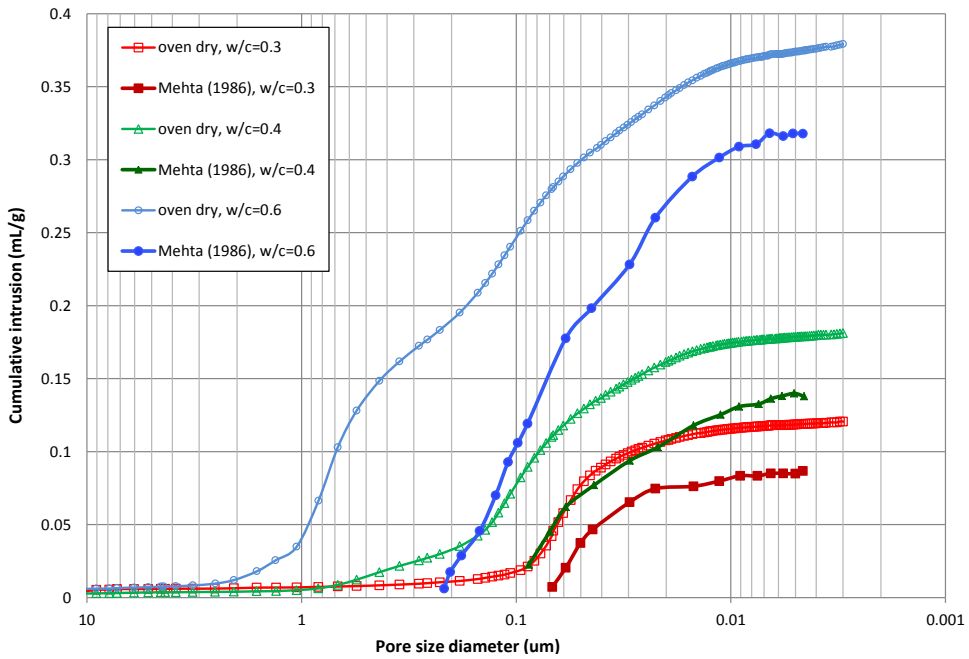

Figure 48. Comparison of the pore sizes from this study (open symbols) with those reported by Mehta (1986) (closed symbols)

Figure 49 provides the pore size distribution of oven dried pastes with w/cm ratio of 0.40 containing different binder systems. No significant differences were observed between the mixtures except the peak in the 0.15 µm range for the fly ash sample that is negligible for the silica fume sample. If the peak at 0.10 µm is considered critical then it may be expected that the silica fume would be at slightly higher risk of distress than the other two.

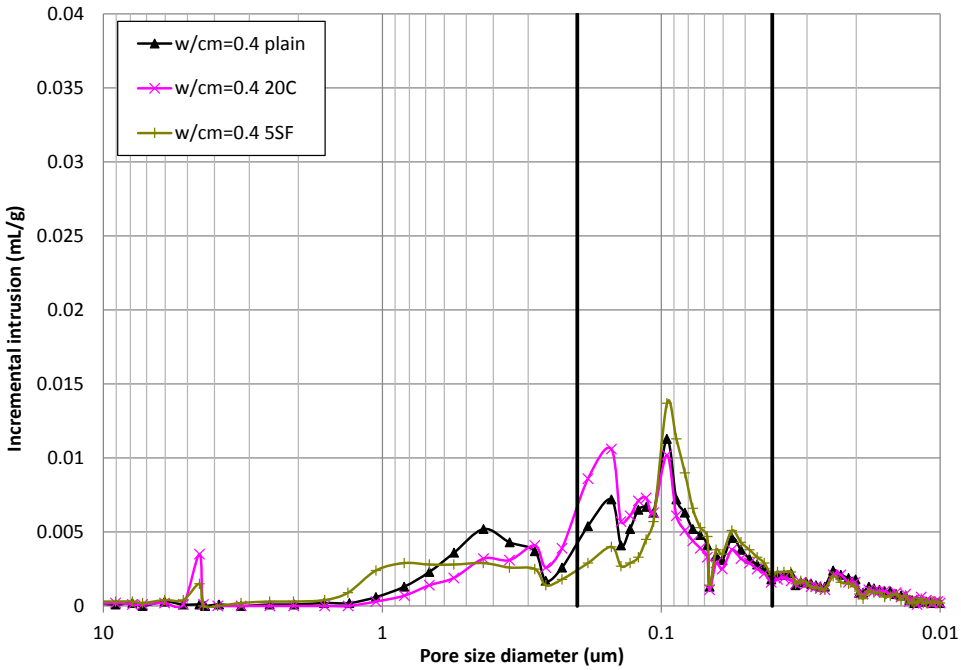

Figure 49. Comparison of the pore size diameter of pastes with different SCMs

Photographs of similar samples subjected to one freeze thaw cycle are shown in Figure 50. The plain sample has the most distress, and sample containing 20% C fly ash has the least distress. However, the pore size distribution data on the three hardened paste samples do not show significant differences. It is possible that there is damage caused by the oven dry treatment which is not detected by the MIP test.

Figure 50. Oven dried paste samples with different SCMs after one freeze thaw cycle

Figure 51 shows the pore size distributions of paste samples with w/cm ratio of 0.60 and treated by oven drying or air drying. The oven dried data shows significantly larger pores and greater porosity than the data from the air dried sample. This reflects the significant effect of water in the pores influencing the information provided by a MIP test.

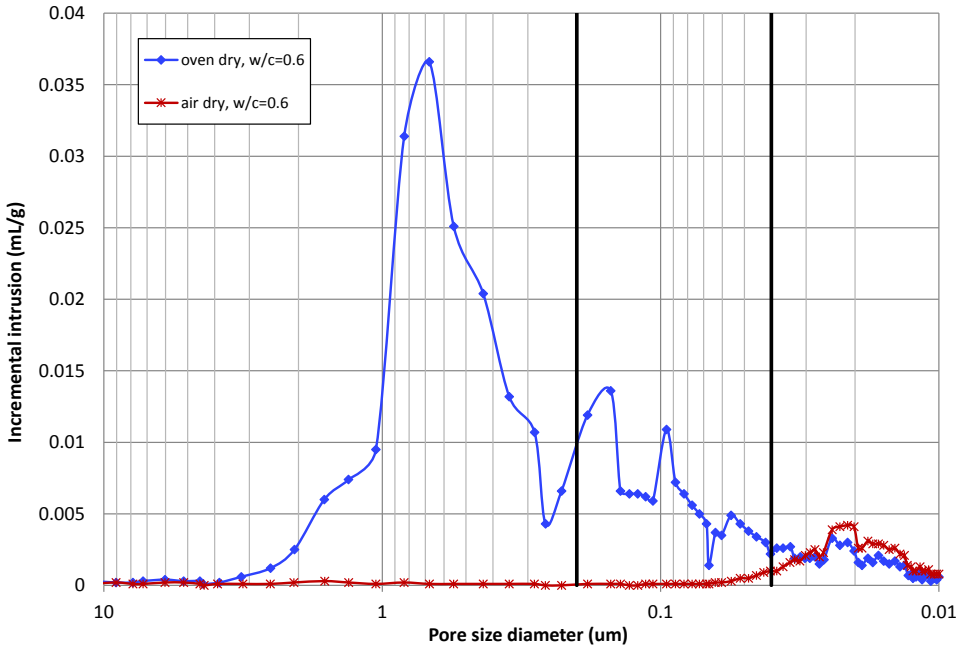

Figure 51. Comparison of reported pore sizes for oven dried and air dried samples with w/cm of 0.60

Figure 52 shows the performance of the paste samples with w/cm ratio of 0.60 and treated by oven or air drying after one freeze thaw cycle. No visible damage is observed in the air dried sample, but the oven dried sample exhibits significant damage. This illustrates the damage incurred by oven drying.

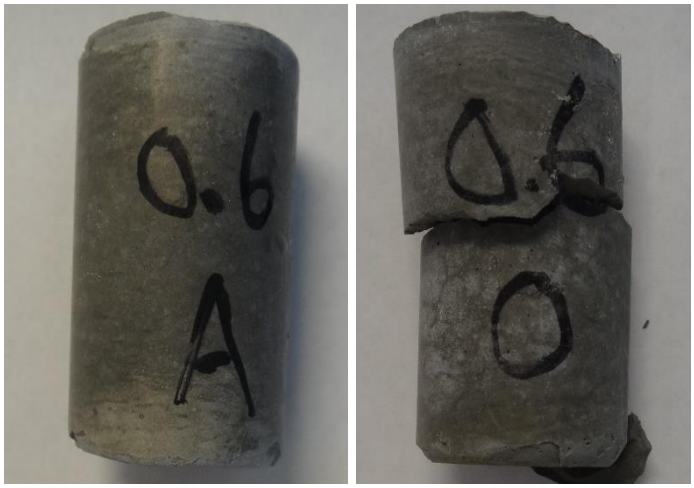

Figure 52. Comparison of freezing and thawing resistance for paste samples treated with different drying conditions

Figure 53 illustrates that good condition of the air dried sample containing fly ash after 5 freeze thaw cycles. This confirms the beneficial effects of fly ash and the reduction in damage with air drying compared to oven drying.

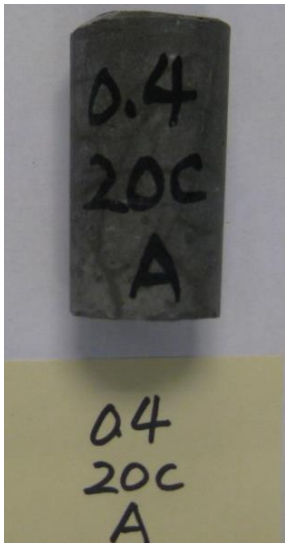

Figure 53. Freezing and thawing resistance for air dried paste sample containing C fly ash at w/cm = 0.4 after 5 cycles

Conclusion

The pore structures of hardened cement pastes with different w/cm ratios and

supplementary cementitious materials (SCMs) were evaluated using mercury intrusion porosimetry (MIP). The findings were compared with pores sizes that may slow drying, thus increasing the risk of freeze thaw damage similar to that observed in D-cracking aggregates. A limited set of freeze thaw tests were also conducted on similar paste samples.

The following observations were made:

- The total porosity increases as w/cm ratio increases, and the median pore size diameter also increases as w/cm ratio increases.
- Paste samples with an intermediate pore size exhibited the least freezing and thawing resistance compared with paste samples with either finer pores or coarser pores.
- Both C fly ash and silica fume improved the freeze / thaw durability of cement paste, but that does not demonstrated from the MIP data.

This is very preliminary work and it is premature to make recommendations based on it other than to suggest that the idea of a pessimum paste pore system for freeze thaw resistance seems to have merit, and warrants further investigation. It is notable that the pessimum appears to fall with the range of typical pavement mixtures.

References

Abell, A.B., Willis, K.L., and Lange, D.A., (1999). “Mercury Intrusion Porosimetry and Image Analysis of Cement-Based Materials”, *Journal of Colloid and Interface Science,* vol. 211, pp. 39-44.

American Concrete Institute (ACI), 1996. “Guide for Use of Normal Weight Aggregate in Concrete”, *ACI Report 221R*.

Alexander, M., and Mindess, S., (2005). *Aggregates in Concrete*, Taylor & Francis Group. 435 pages.

Chindaprasirt, P., Jaturapitakkul, C., and Sinsiri, T., (2005). “Effect of Fly Ash Fineness on Compressive Strength and Pore Size of Blended Cement Paste”, *Cement and Concrete Composites,* Vol. 27, pp. 425-428.

Cook, R.A., and Hover, K.C., (1999). “Mercury Porosimetry of Hardened Cement Pastes”, Cement and Concrete Research, Vol. 29, pp. 933-943.

Fagerlund, G., (1977), “The international cooperative test of the critical degree of saturation method of assessing the freeze/thaw resistance of concrete”, *Materials and Structures*, Vol. 10 (58) pp. 230–251.

Galle, C., (2001). “Effect of Drying on Cement-based Materials Pore Structure as Identified by Mercury Intrusion Porosimetry A Comparative Study between Oven-, Vacuum-, and Freeze-drying.” *Cement and Concrete Research*, Vol. 31, pp. 1467-1477.

Janusz, A., (2010). Investigation of Deicing Chemicals and Their Interaction with Concrete Materials, Master Thesis. West Lafayette. IN: Purdue University.

Lange, D., Jennings, H.M., and Shah, S.P., (1994). “Image Analysis Techniques for Characterization of Pore Structure of Cement-based Materials”, *Cement and Concrete Research*, Vol. 24, pp. 841-853

Li, W., Pour-Ghaz, M., Castro, J., and Weiss, J., (2012) “Water Absorption and Critical Degree of Saturation Relating to Freeze-Thaw Damage in Concrete Pavement Joints”, Journal of Materials in Civil Engineering, Vol. 24, pp. 299-307.

Marks, V.J, and Dubberke, W. (1982). “Durability of Concrete and the Iowa Pore Index Test”, *Transportation Research Record*, Issue 853, pp. 25-30.

Mehta, P. K. (1986). *Concrete: Structure, Properties, and Materials*. Englewood Cliffs, NJ: Prentice-Hall.

Page, C.L., and Page, M.M., (2007). *Durability of Concrete and Cement Composites*, Cambridge, England.

Pigeon, M. and Pleau, R. 1995. *Durability of Concrete in Cold Climates*, E & FN Spon, 244 pp.

Sutter, L., Peterson, K., Julio-Betancourt, G., Hooton, D., Van, D.T., Smith, K. The deleterious chemical effects of concentrated deicing solutions on Portland cement concrete. South Dakota Department of Transportation. Final Report: 2008

Taylor, P. C., S. H. Kosmatka, G. F. Voigt, M. E. Ayers, A. Davis, G. J. Fick, J. Gajda, J. Grove, D. Harrington, B. Kerkhoff, C. Ozyildirim, J. M. Shilstone, K. Smith, S. M. Tarr, P. D. Tennis, T. J. Van Dam, and S. Waalkes. 2006. *Integrated Materials and Construction Practices for Concrete Pavement: A State of the Practice Manual*. FHWA HIF-07-004. Federal Highway Administration, Washington, DC.

Uchikawa, H., Hanehara, S., and Sawaki, D., (1991). “Structure Change of Hardened Mortar by Drying.” *3rd NCB International Seminar (New Dehli-India)*, 4, VIII-1-VIII-12.

Villani, C., Spragg, R., Pour-Ghaz, M. & Weiss, J.W., 2012. The role of deicing salts on the non-linear moisture diffusion coefficient of cementitious materials during drying. In Brandt, A.M., Olek, J., Glinicki, M.A. & Leung, C.K.Y., eds. 10th Tenth International Symposium on Brittle Matrix Composites. Warsaw, 2012. Institute of Fundamental Technological Research PAS.

Winslow, D., and Liu, D., (1990). "The Pore Structure of Paste in Concrete", *Cement and Concrete Research*, Vol. 20, pp. 227-235.

CHAPTER 6. A CASE STUDY OF EVALUATING JOINT PERFORMANCE IN RELATION WITH SUBSURFACE PERMEABILITY IN COLD WEATHER REGION

A paper to be submitted to *Cold Regions Science and Technology*

Jiake Zhang, David White, and Peter Taylor

Abstract

Permeable subsurface layers are important for concrete pavement systems to provide good serviceability. Water that stays in pavement systems introduces problems (e.g., freezing and thawing, degradation of materials, and erosion) that can be avoided by using permeable subsurface layers to drain excess water from the pavement system as quickly as possible. A borehole permeameter was developed at Iowa State University and used in this research to measure the permeability of subsurface layers. This research aims to better understand the relationship between concrete pavement performance and the permeability of subsurface layers. Field tests were conducted on three joints (two sealed and one unsealed) and a middle panel in summer, winter, and spring on a city street in Ames, Iowa. Field tests results indicate that low permeable subsurface layer contributes to joint deterioration, especially under freezing condition. Soil classification tests on the base materials from below the distressed joint and the middle panel show that base material below the joint includes more fines than material below the middle panel, which may cause by material lost from the deteriorated joint.

Laboratory falling head permeability tests on a selected base material under frozen and unfrozen conditions show that permeability decreases as moisture content increases for

both frozen and unfrozen samples, and freezing moist base material significantly reduces the permeability. The petrography test on the distressed core and sound core shown that the distressed core sample has higher w/cm ratio than the sound core sample. Moreover, ettringite was found from the core sample and that may due to the application of de-ice salt on the pavement during the cold seasons.

Introduction

Drainage systems play an important role in good pavement serviceability because water in pavement systems is one of the causes of distress in concrete pavements. Low permeable base may contribute to pavement deterioration by keeping water in the base of pavement or by blocking up the drainage (Stutzman 1999).

Surface water primarily flows into base layers through joints and cracks in pavements. A well-drained base layer is important for keeping water out of pavement systems. Moreover, well designed drainage systems can avoid water related problems in concrete pavements, such as pumping/erosion, faulting, corner cracking, and durability cracking (Rodden 2010). Water is used to measure the permeability of pavement layers when they are not subjected to freezing conditions. The permeability of sufficiently drainable subsurface layers ranges from 0.0529 cm/s to 0.1058 cm/s (150 to 300 ft. /day) (Rodden 2010). The Federal Highway Administration (1992) *Pavement Design Guide* states that to drain 50% of the drainable water in one hour is recommended for the highest class of roads with the greatest amount of traffic and that to drain 50% of the drainable water in two hours is recommended for most highways and freeways.

Because of difficulties with accessing subsurface layers in the field, the traditional

approaches for obtaining in-situ permeability of base layers are either by sampling field material for laboratory permeability tests or using empirical correlations with density and particle size distribution (Richardson 1997). However, these approaches introduce significant variations with in situ permeability either from different laboratory and field boundary conditions or sample disturbance.

Freezing of moist base materials significantly reduces the permeability of subsurface layers. It has been reported that water infiltration rates decrease with increasing water content for wet soils (Kane 1980; Granger et al. 1984). This is due to the increased blockage of soil pores by ice growth (Seyfried 1997). However, the current challenge is to directly measure the permeability of subsurface layers under freezing conditions to determine whether permeability changes are the result of resident ice melting or incoming water freezing. In the past, air has been used as the medium to assess the permeability of frozen soil (Bloomsberg and Wang 1969; Saxton et al. 1993). White et al. (2007) developed an Air Permeameter Test (APT) device that effectively measures the permeability of pavement base foundation materials in the field. However, the APT cannot be placed below pavement to measure the permeability of subsurface layers. However, the relationship between permeability measured by air or by water is not fully understood.

This study presents findings obtained with a new borehole permeameter that uses water to measure the permeability of subsurface layers below pavements. The borehole permeameter is a portable device that can be directly placed in a 6.0 in. core hole. The device has one standpipe with three sections, a top pipe with a 1.4 in. interior diameter; a middle pipe with a 13.0 in. interior diameter; and a bottom pipe with a 5.0 in. interior diameter

(Figure 54). A rubber gasket that is attached to the bottom of the bottom pipe where the device meets the subsurface layer in the 6.0 in. borehole is inflated after seating to seal the space between the device and the pavement. Wedges are used to stabilize the device during testing.

Figure 54. Borehole permeameter

Site Description and Method

Site description

Field tests were conducted in a city street (South Loop Drive) in Ames, Iowa. The street is a two lane street in a research park serving office buildings, and it is approximately ½ mile long. The street was reportedly paved in 1997 in one day using a full width slipform paver running from southwest to northeast.

A typical cross section of the street is shown in Figure 55, and the foundation of the street includes a 6.0 in. special backfill base layer on top of a 6.0 in. special compacted subgrade. The street is 27.0 ft. wide with 7.0 in. thick Portland cement concrete pavement. A

2% slope exists on both directions of the street, and a 4.0 in. perforated subdrain was installed on the left side of the street. There is a storm sewer on the right side of the street.

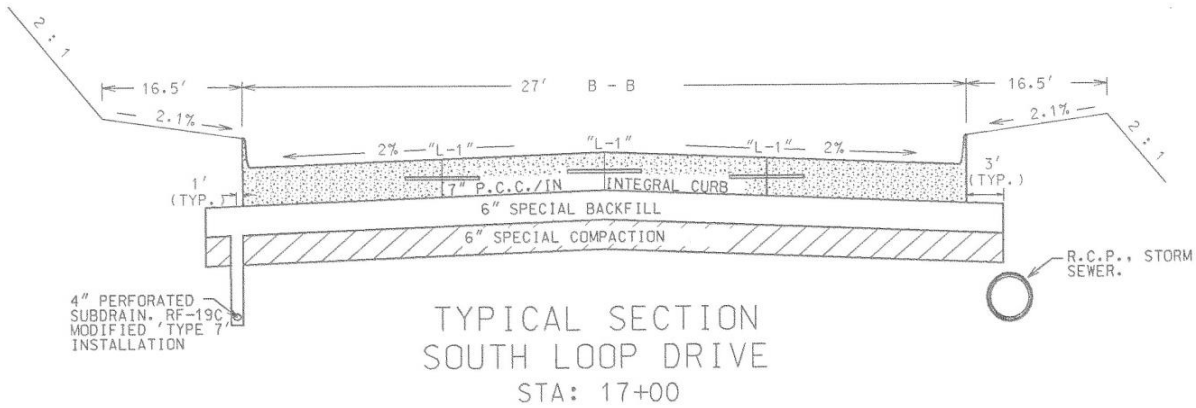

Figure 55. Typical cross section of South Loop Drive

The longitudinal joints were originally unsealed but maintenance crews installed a hot-seal material in some of the joints at some point. It was noted that deterioration was occurring at some joints and an investigation was initiated in 2010.

The extent of the distress was mapped, along with details of where joints had been sealed as shown in Figure 56. Table 8 summarizes the condition of core samples and tested locations on this street. Figure 57 provides the field overview of the distressed joint and a core sample obtained from the distressed joint (Figure 58). Core sample from the distressed joint exhibits bottom up distress, which may cause by impermeable base keeping excess water in the system or water pump up from the ground. Five cores were extracted from the pavement over a period of two years. Core #1 and core #5 were sent for petrographic examination (Figure 56). One core is from a distressed joint, and the other one is from a sound joint. The petrography tests cores were about 13 ft. apart.

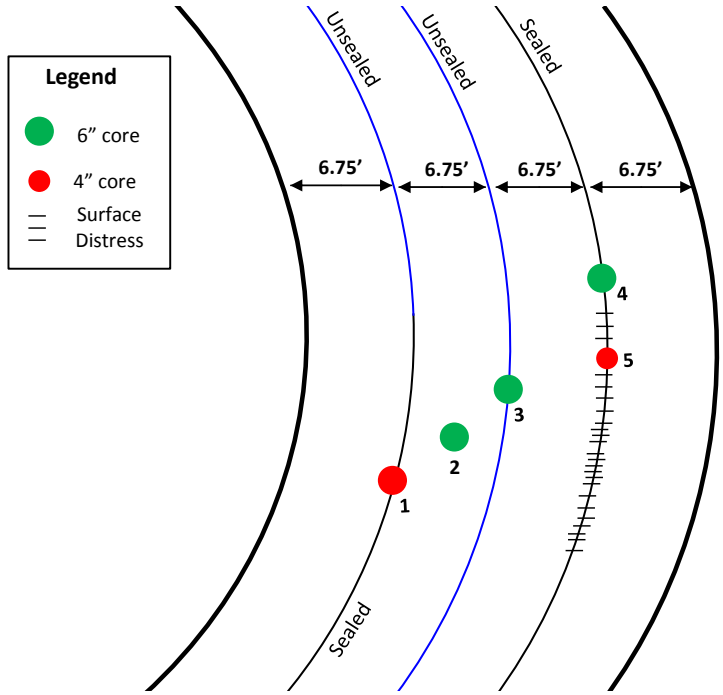

Figure 56. Plan view of coring and distressed locations on South Loop Drive (not to scale)

Table 8. Test locations, descriptions, and tests performed

Core	Location	Joint type	Condition	Borehole size (in.)	Test
1	Joint	Sealed	Sound	6	BP, P
2	Middle panel	—	Sound	6	BP
3	Joint	Unsealed	Sound	6	BP
4	Joint	Sealed	Distressed	4	P
5	Joint	Sealed	Distressed	6	BP

Note: BP = Borehole permeameter and P = Petrography

Figure 57. Field view of core 4 location showing joint distress

Figure 58. Core sample 4 from the distressed joint

One borehole held more than half of the excess water after the permeability test has been completed for more than 2 hours during winter testing (Figure 59), which indicates the subsurface layer cannot drain out excess water efficiently.

Figure 59. Field observation of impermeable subsurface below pavement (2 hours after test completed)

Method

Field permeability tests were conducted at several locations during summer, winter and spring (Figure 56). The permeability test was conducted to provide an indication of the rate of water movement through the base layer of a pavement. Steps to perform the test are as follows:

1. Inserting the device into a 6 in. core hole.
2. Sealing the bottom of the device against the concrete using an inflatable rubber tube.
3. Filling the device with water.
4. Monitoring the rate of water loss from the device over a period of 60 minutes.

Field Tests Results and Discussion

The distance of water loss was recorded based on the marked ruler on the inside of each standpipe. ASTM D6391-06 was followed to obtain the permeability of the subsurface layer. Equation 6 was used to calculate the permeability (*K* in cm/s),

$$K = R_t G_1 \ln(H_1 / H_2) / (t_1 - t_2) \tag{6}$$

where

R_t = Ratio of kinematic viscosity of permeant at temperature of test permeant during time increment t_1 to t_2 to that of water at 20°C (68°F),

d = Effective inside diameter of standpipe (1.4 in. for top standpipe and 13.0 in.for the middle standpipe)

D_1 = Inside diameter of bottom casing (5.0 in. for this device)

a = +1 for impermeable base at b_1,

= 0 for infinite (+20D_1) depth of tested material,

= −1 for permeable base at b_1, and

b_1 = thickness of tested layer between bottom of device and top of underlaying stratum

H_1 = effective head at t_1

H_2 = effective head at t_2

G_1 = $(\pi d^2 / 11 D_1)[1 + a(D_1 / 4b_1)]$

t_1 = time at beginning of increment(s), and

t_2 = time at end of increment(s).

Field borehole permeameter tests results for all locations are summarized in Table 9. Results from the summer tests shown slightly differences on the distressed sealed joint (#4) and sound sealed joint (#1), but the unsealed joint (#3) is significant less permeable than the sealed joints (#1 and #4). The subsurface layer below middle panel is more permeable than the subsurface layer below the joints, which may due to some fine materials from the distressed joint accumulate in the base layer. The permeability tests results from all four locations are low compare with the sufficient permeable base requirement which is ranging from 0.0529 cm/s to 0.1058 cm/s (Rodden 2010). The time to drain more than 50% of drainable water and less than 50% of drainable water were determined using the Pavement Drainage Estimator (PDE) Version 1.04, which was developed by White et al. (2004). Field

permeability measurements indicate that the subsurface layer on this street is insufficient permeable, which is one of the reasons to cause deterioration on the joint.

Table 9. Average hydraulic conductivity by season

Core	**Location**	**Season**	**K (cm/s)**	**K (ft./day)**	**Time to drain ≤ 50% (days)**	**Time to drain ≥ 50% (days)**
1	Joint	summer	0.0022	6.2	5.8	30.8
		winter	0.0007	1.9	18.8	100.4
2	Middle panel	Spring	0.0086	24.5	1.5	7.8
3	Joint	summer	0.0011	3.0	11.9	63.6
		winter	0.0008	2.2	16.2	86.7
4	Joint	summer	0.0020	5.7	6.3	33.5

Figure 60 and Figure 61 provide the permeability tests results on location #1 and #3 from test conducted during summer 2012 and winter 2013. The outside temperature for tests conducted during summer 2012 was around 84°F, and the outside temperature for tests conducted during winter 2013 was around 40°F. The subsurface layer exhibits significant less permeable during winter for both location #1 and #3, which may due to frozen of the trapped water increased the blockage of pores in the subsurface layer. As water accumulates in the system, more freezing and thawing related distresses will be introduced to the pavement.

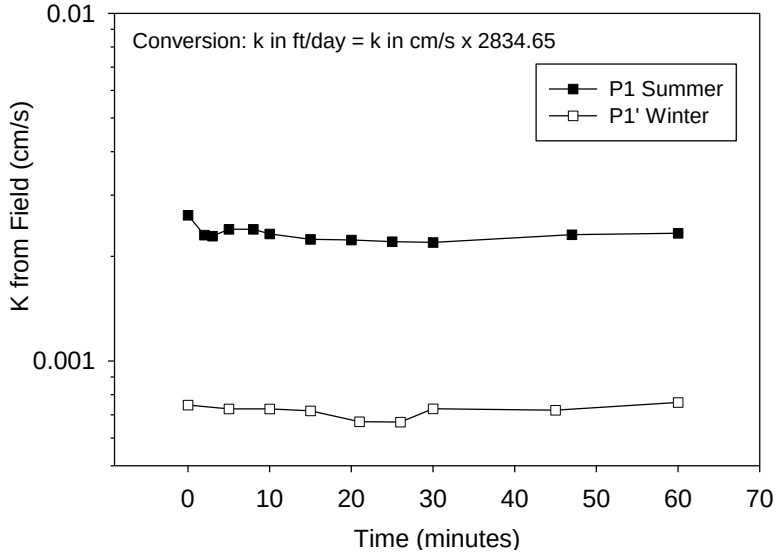

Figure 60. Borehole permeameter test results during summer and winter for location #1

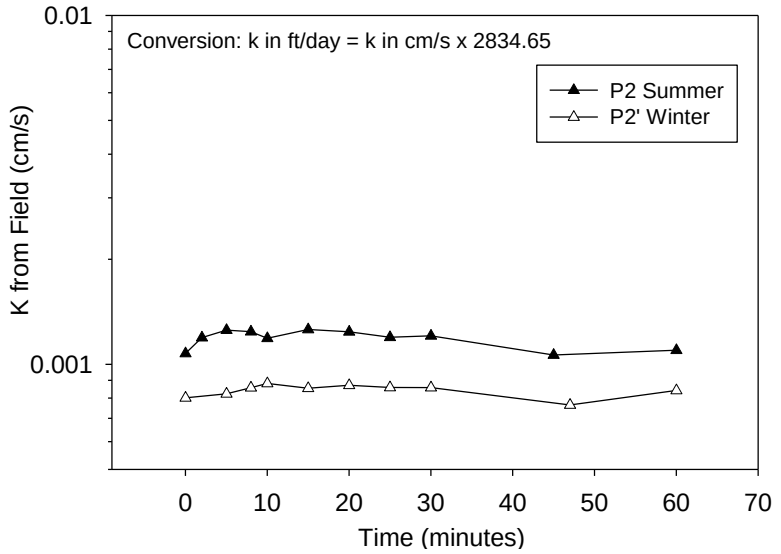

Figure 61. Borehole permeameter test results during summer and winter for location #3

Johnson (2012) measured the freeze-thaw cycles with depth in Plainfield, Iowa during the winter of 2010-2011 (Figure 62). It indicated that most freeze-thaw cycles occur at approximate depth of 0.025 m below the pavement. During the freezing period, water stays in both joints and subsurface layers because of reduced permeability. As temperatures drop, trapped water freezes and increases pressure in the pavement system.

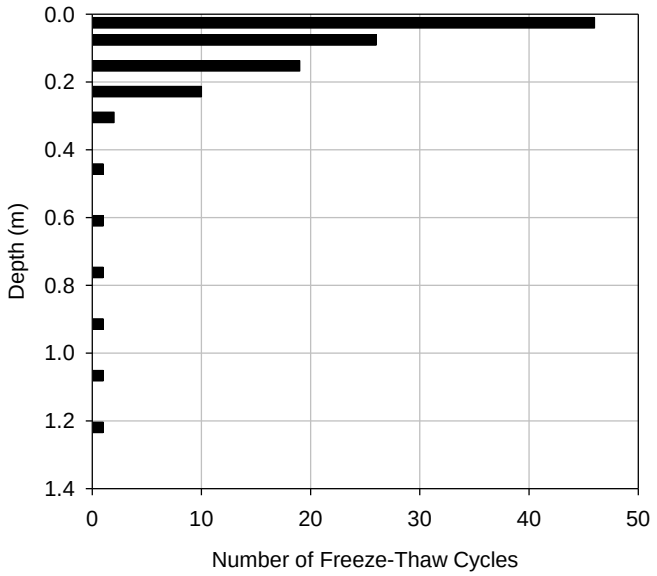

Figure 62. Freeze-thaw cycles in relationship with depth during 2010-2011 winter in Iowa (Johnson 2012)

Laboratory Tests Results and Discussion

Base material was obtained from one core location after permeability tests were completed. Soil classification test was conducted on the base material. Figure 63 and Table 10 provide the soil classification curves for materials sampled from below the joint and from below middle panel, and the gradation limit from Iowa design specification for base material. Materials from both the joint and middle panel contain less than 5% fines (pass No. 200 sieve), which should not bring significant permeability issues. Because Ferguson (1972) reported that the permeability of a material decrease dramatically as fines content above 5%. However, material from below the joint contains significantly more fines than material from the middle panel, which results in the subsurface layer below joint less permeable.

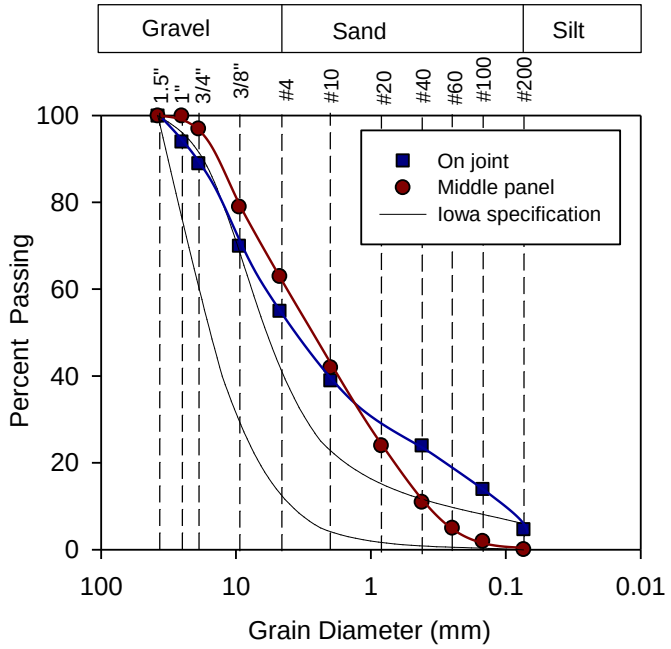

Figure 63. Gradation of base material

Table 10. Comparison of base from Loop Drive with Iowa DOT design specification

Sieve Size	Loop Drive on joint	Loop Drive on middle panel	Iowa design specification
	Percent pass by weight		
38.1 mm (1 ½ in.)	100.0	100.0	100.0
25.4 mm (1 in.)	94.0	100.0	–
12.7 mm (1/2 in.)	80.0	97.0	40.0–80.0
4.76 mm (No. 4)	55.0	63.0	–
2.38 mm (No. 8)	42.0	45.0	5.0–25.0
1.19 mm (No. 16)	32.0	26.0	–
0.297 mm (No. 50)	22.0	7.0	–
0.074 mm (No. 200)	4.7	0.1	0–6.0

The influence of freezing on the permeability of moist base material was evaluated in this research. A selected base material with similar gradation as the base material from below the middle panel was used in the laboratory permeability test (Figure 64). Because limited material can be sampled from the field. Samples were prepared at moisture contents of 0% to 10% with 2% incremental, and then compacted with standard proctor energy. The compacted

samples were frozen for 24 hours before conducting the falling head permeability test. To prevent water freezes during passing through the frozen sample, an anti-freeze windshield wash fluid (freezing point -20°F) was used as the passing medium during the tests (Figure 65). To compare the permeability of the sample under frozen and unfrozen, the falling head permeability test was conducted on the same sample with the same anti-freezing windshield wash fluid after ice was melt.

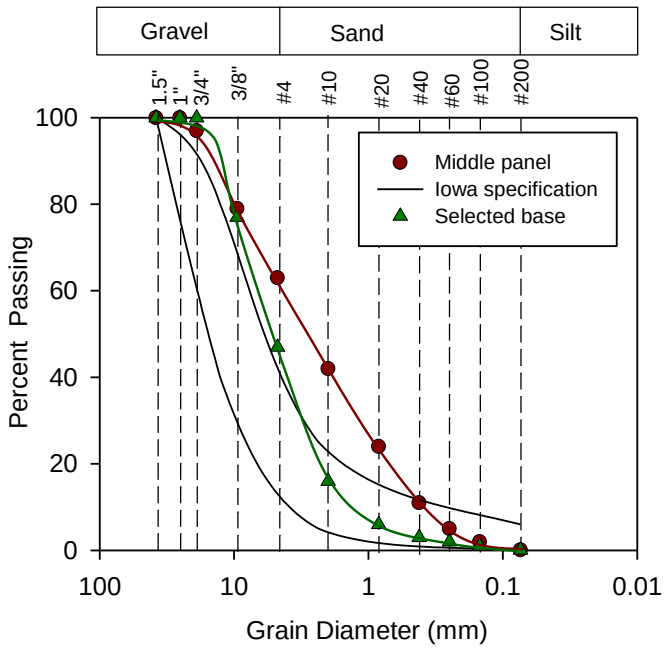

Figure 64. Comparison of gradation curves of selected base material and field material

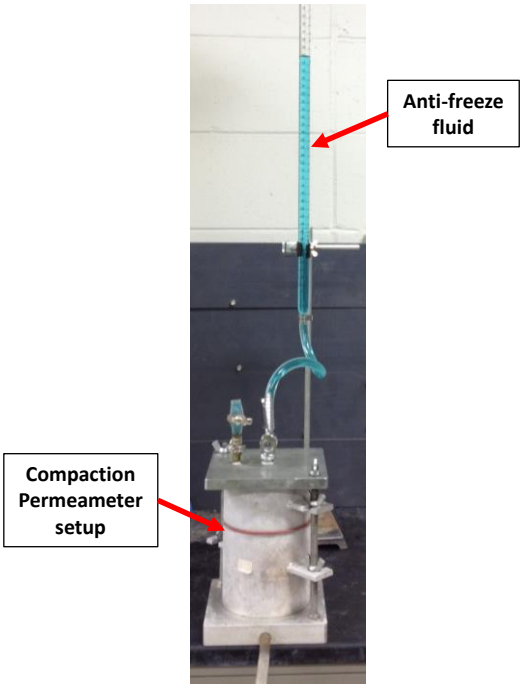

Figure 65. Laboratory falling head permeability test setup

The wet density of the compacted permeability samples increases as moisture content increase, and the maximum dry density of the compacted permeability samples was reached at moisture content around 6% (Figure 66).

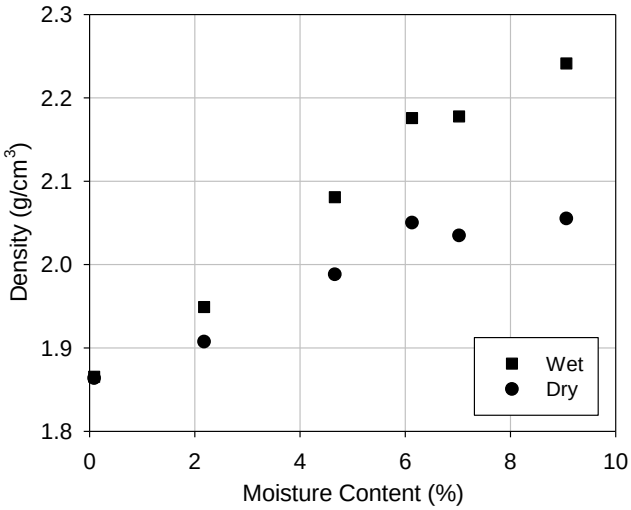

Figure 66. Moisture and density relationship for compacted permeability samples

Falling head permeability tests were conducted on the compacted samples under both

frozen and unfrozen conditions (Figure 67). Permeability decreases as moisture content increases for the samples. Permeability obtained under frozen condition is significantly lower than permeability obtained under unfrozen. This revealed that freezing of the water increases the blockage of pores in the moist samples and the saturated sample almost impermeable when it freezes.

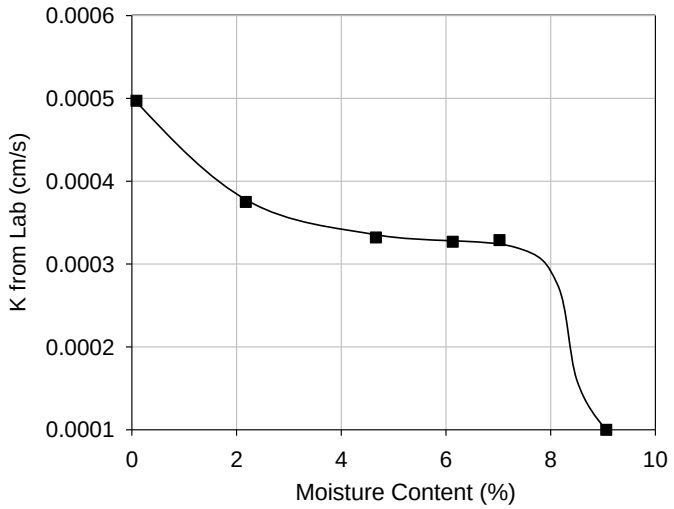

Figure 67. Moisture and permeability relationship under frozen and unfrozen condition

Table 11 and Table 12 summarize the drainage coefficient of the base material based on the permeability obtained from the laboratory tests. The Pavement Drainage Estimator (PDE) Version 1.04 program was used to estimate the time to drain less than 50% and more than 50% of the drainable water. The results indicate that the selected base material is insufficient permeable under both frozen and unfrozen conditions. Higher moisture content causes the sample even less permeable.

Table 11. Estimated drainage coefficient by applying laboratory permeability data under frozen condition

Water content (%)	**Dry density (g/cm^3)**	**Under frozen**		
		K (cm/s)	**Time to drain ≤ 50%**	**Time to drain ≥ 50%**
0.1	1.9	0.0005	25.4 days	136.3 days
2.2	1.9	0.0004	32.4 days	173.5 days
4.7	2.0	0.0003	39.6 days	212.0 days
6.1	2.1	0.0003	39.6 days	212.0 days
7.0	2.0	0.0003	39.6 days	212.0 days
9.1	2.1	0.0002	71.2 days	381.6 days

Table 12. Estimated drainage coefficient by applying laboratory permeability data under unfrozen condition

Water content (%)	**Dry density (g/cm^3)**	**Under unfrozen**		
		K (cm/s)	**Time to drain ≤ 50%**	**Time to drain ≥ 50%**
0.1	1.9	0.0015	8.1 days	43.4 days
2.2	1.9	0.0009	14.8 days	79.5 days
4.7	2.0	0.0006	21.0 days	112.2 days
6.1	2.1	0.0005	23.8 days	127.2 days
7.0	2.0	0.0006	22.3 days	119.3 days
9.1	2.1	0.0006	22.3 days	119.3 days

Petrographic Analysis Results

Petrographic examinations were conducted on two cores from the test location by an independent company. One core is from a distressed joint and the other one is from a sound joint (Figure 68).

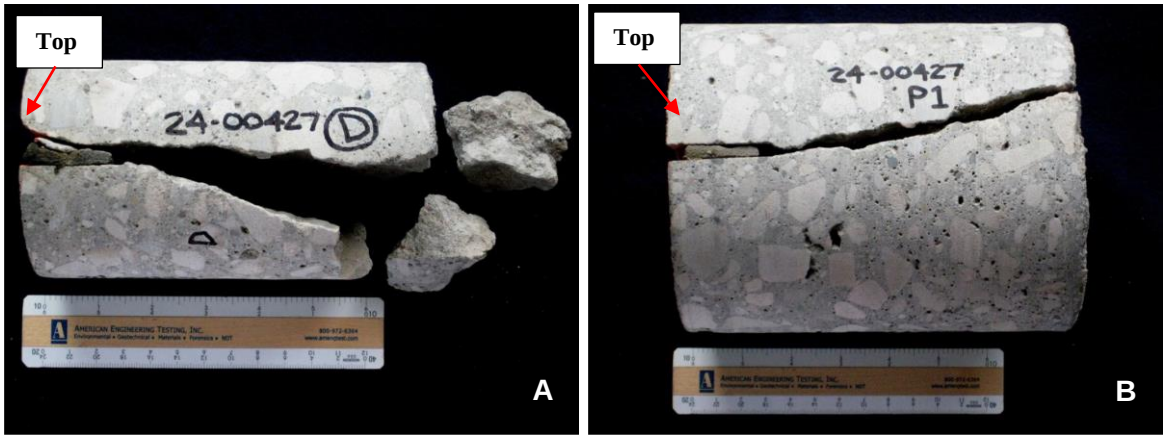

Figure 68. Core samples sent for petrographic examination: (A) distressed joint and (B) sound joint

The full petrographic examination can be summarized as follows (Taylor et al. 2012):

- The original air void systems of both non-distressed core and distressed core were satisfactory, but had been filled with ettringite (see Table 13).
- Both samples contained about 10 to 20% fly ash.
- Some D-cracking was observed, particularly in the distressed sample.
- The w/cm ratio of the undamaged sample was slightly lower than that of the damaged sample.
- Despite the reportedly compromised air void system of sample #1, it is still in reasonable condition.

Table 13. Petrographic data

	Distressed core	**Non-distressed core**
Original air content %	6.7	6.4
Effective air content, %	5.3	4.5
Original spacing factor, in.	0.005	0.007
Effective spacing factor, in.	0.009	0.013
Estimated w/cm	0.42-0.47	0.40-0.45

Conclusions

The primary goal of the work at this location was to assess potential differences

between sound joints and distressed joints in relationship with the subsurface permeability.

The findings from this project proved empirical data that confirms a subsurface layer with low permeability can contribute to joint deterioration. Field permeability tests were conducted in three seasons, and the subsurface layer had the lowest permeability during winter because trapped water in the base freezes. This ice increases the blockage of voids and causes more water to stay in the system so surface water that stays in joints freezes and causes distress. The permeability of all the tested locations are low compare with the sufficient permeable base design requirement. The subsurface layer below the middle panel is relatively permeable compare with the subsurface layer below joints. Because material loss from the joint brings more fines into the subsurface layer which reduces the permeability of subsurface layer.

Laboratory falling head permeability tests results revealed that the permeability of compacted base material reduces as moisture content increases. Freezing of the moist base material causes significant reduction on the permeability.

Petrographic results on the core samples from distressed sample and non-distressed sample indicate that the w/cm ratio and air void system are also the important factor contribute to the distress sample. The abundance of ettringite in the samples is somewhat surprising because the system was free draining, and ettringite is normally an indicator of abundant water continually in contact with the concrete. One possible explanation may be that salts absorbed into the surface of the joint retain water, thus increasing saturation.

References

Bloomsberg, G.L., Wang, S.J., (1969), "Effect of moisture content on permeability of frozen soils", *Proc. American Geophysical Union Pacific Northwest Regional Meeting*. Portland, OR.

Federal Highway Administration. *Drainable Pavement Systems.* Participant Notebook, Demonstration Project 87, FHWA-SA-92-008, U.S. Department of Transportation, March 1992.

Ferguson, E.G., (1972). "Repetitive triaxial compression of granular base course material with variable fines content", PhD Dissertation submitted at Department of Civil Engineering, Iowa State University, Ames, Iowa, USA.

Granger, R.J., Gray, D.M., Dyck, G.E., (1984), "Snowmelt infiltration to frozen Prairie soils", *Canadian Journal of Earth Sciences*, Vol. 23, pp. 669-677.

Johnson, A.E., (2012). "Freeze-thaw performance of pavement foundation materials", Maters thesis submitted at Department of Civil Engineering, Iowa State University, Ames, Iowa, USA.

Kane, D.L., (1980), "Snowmelt infiltration into seasonally frozen soils", *Cold Regions Science and Technology*, Vol. 3, pp. 153-161.

Richardson, N.D., (1997), "Drainability Characteristics of Granular Pavement Base Material", *Journal of Transportation Engineering*, Vol. 123, No. 5, pp. 385-392

Rodden, R., (2010), "Drainable Base Layers Revisited," Tennessee Concrete Pavement Conference.

Saxton, K.E., Kenny, J.F., and McCool, D.K., (1993), "Air permeability to define frozen soil infiltration with variable tillage and residue", *Soil and Water Div. of ASAE*, vol. 36, pp. 1369-1375.

Seyfried, M.S., Murdock, M.D., (1997), "Use of air permeability to estimate infiltrability of frozen soil", *Journal of Hydrology*, vol. 202, pp. 95-107.

Taylor, P., Sutter, L., and Weiss, J., *Investigation of Deterioration of Joints in Concrete Pavements*. InTrans Project 09-361. Final Report: 2012.

White, D.J., Vennapusa, P.K., and Jahren, C.T., *Determination of the Optimum Base Characteristics for Pavements*, Iowa DOT Project TR-482. Final Report: 2004.

White, D.J., Vennapusa, P.K., Suleiman, M.T., and Jahren, C.T., (2007), "An In-situ Device for Rapid Determination of Permeability for Granular Bases", *Geotechnical Testing Journal*, Vol. 30, No. 4.

Stutzman, P.E. (1999), "Deterioration of Iowa Highway Concrete Pavements: A Petrographic Study", *National Institute of Standards and Technology.*

CHAPTER 7. A REVIEW OF MECHANISMS ASSOCIATED WITH PREMATURE JOINT DETERIORATION IN CONCRETE PAVEMENTS

A paper to be submitted to *Construction and Building Materials*

Jiake Zhang and Peter Taylor

Abstract

Joint deterioration has been reported in some cold climate regions. Multiple mechanisms contribute to the deterioration of joint, and this paper reviewed some mechanisms that related to cyclic freezing and thawing. It has been recognized that water in concrete is main issue to cause joint deterioration and possible approach can keep water away from concrete will reduce the risk to cause joint deterioration. Laboratory tests found that the exposed concrete interfacial transition zone accelerates the deterioration of saw joints, because water penetrates into concrete through the permeable interfacial transition zone. The application of deicing salts on concrete pavement brings both physical and chemical deteriorations to concrete. Laboratory tests on the pore structure of hardened cement paste revealed that paste samples with intermediate pore sizes are least freeze thaw durable. Field observations of some deteriorated joints agree with the findings from laboratory work.

Current status of the understanding of the mechanisms to cause joint deterioration is discussed and the future needs that how to improve the durability of joints are also addressed in this paper.

Background

Some sawn joints in concrete pavements exhibit premature deterioration in northern

cold-weather states in the U.S. The deterioration is often first observed as joints showing shadowing, later resulting in significant loss of material (Figure 69). A team of researchers funded by a Transportation Pooled Fund (TPF 5(224)) have been investigating the causes behind this distress and developing recommendations to reduce the risk in new pavement.

Figure 69. Deteriorated joint in concrete pavement

The distress appears to be predominately related to by freezing and thawing of saturated concrete, but the details of how that saturation develops varies between locations. Pressures are developed in a freezing section due to a combination of hydraulic expansion causes by water expansion as it cools below 4°C, salt crystallization and osmotic pressure caused by differentials in salt concentration at the freezing front (Valenza and Scherer 2006). Conventional practice to provide small closely spaced air bubbles in the matrix that provide a space for the expanding fluids to move into. It is also reported that the air bubbles delay the saturation of a paste system, effectively buying additional life time for the pavement (Li et al. 2012). The ACI 318 building code recommends that 6% air is required for concrete with 1 inch nominal maximum aggregate size exposed to sever exposure conditions, such as wet-freeze-thaw conditions, deicers, or other aggressive agents. Similar values are commonly

adopted for pavements.

Another mechanism tied to the interfacial transition zone (ITZ) has been studied by Zhang and Taylor (2012). This model is based on the assumption that solutions trapped in a joint may be preferentially absorbed into the ITZ. Expansion of this solution during freezing will cause stresses expansion that will may typically cause a crack pattern as shown in Figure 70. Such cracking is regularly observed in the field.

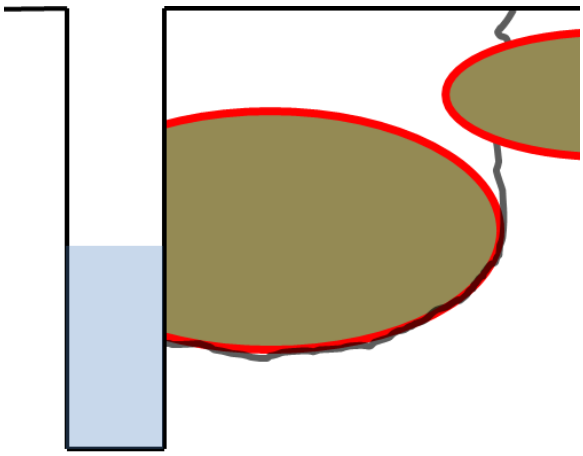

Figure 70. Crack developing out of a saturated ITZ (Zhang and Taylor 2012)

This paper discusses the work conducted in the laboratory and in the field, and summarizes the findings and recommendations developed.

Laboratory Studies

A series of laboratory studies was conducted to investigate the mechanisms that may be related to joint deterioration in concrete pavements, such as the critical degree of saturation on concrete deterioration, influence of deicing salt on concrete deterioration, influence of cyclic freezing and thawing on concrete deterioration, influence of mixture ingredients on paste pore sizes and potential durability.

Influence of Degree of Saturation on Concrete Deterioration

The primary benefit of having air voids in concrete is that it delays the time for concrete to reach a critical degree of saturation (86−88%) (Li et al. 2012), largely because the starting moisture content is lower. The shape of the curve (Figure 71) is the same, just shifted downward with increasing air content, effectively meaning that it will take (potentially) years longer for a given piece of concrete to reach critical moisture content.

Other data presented by Li clearly showed that increasing moisture content significantly reduces resistance to freezing and thawing when moisture content is above about 85% (Figure 74).

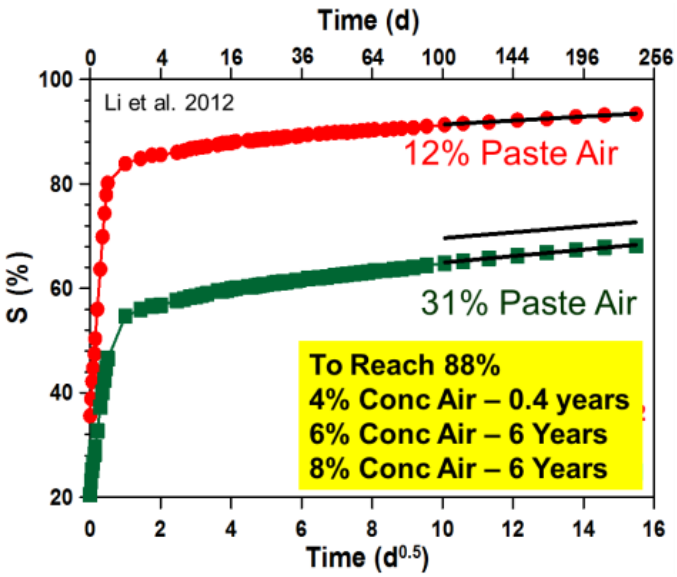

Figure 71. Time to reach the critical degree of saturation for concrete with different air content (Li et al. 2012)

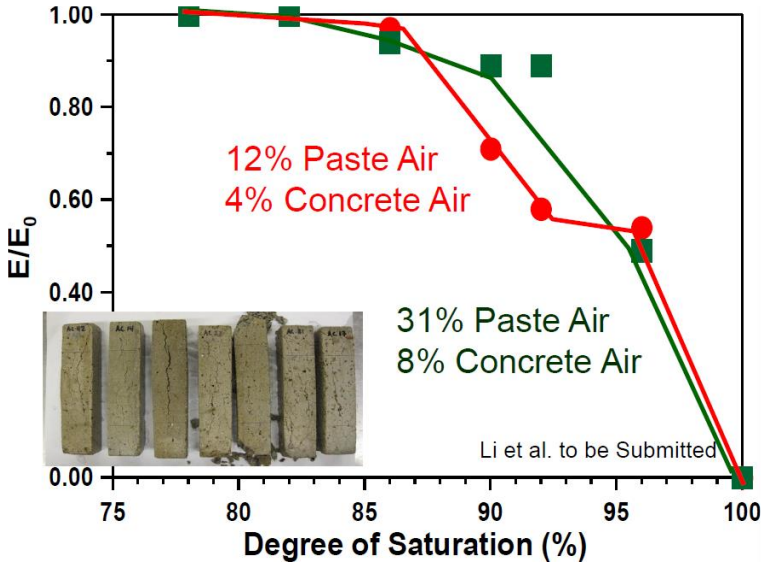

Figure 72. Relationship between degree of saturation and freeze-thaw durability (Li et al. 2012)

Influence of Deicing Salt on Concrete Deterioration

Deicing salts applied to concrete can accelerate concrete deterioration (Lee at al. 2000; Sutter et al. 2008; Darwin et al. 2008) due to both physical and chemical mechanisms. Physical damage due to freezing is considered to be the predominant mechanism. The maximum distress peaks when the concentration of deicing salt is about 3% (Verbeck and Klieger 1957). This is due to glue-spalling affect. When deicing solutions freeze, it will form an ice layer covers the concrete surface. The ice layer cracks as temperature continue drops because of thermal expansion mismatch, and concrete cracks when the ice layer propagate (Sun and Scherer 2010).

A significant contribution of deicing salts is that $CaCl_2$ and $MgCl_2$ both tend to slow or stop drying, depending on their concentration. This is illustrated in Figure 73, which crystals of solid $MgCl_2$ have dissolved in water attracted from the atmosphere in a standard laboratory environment. This phenomenon of salts taking in water from the air is known as

deliquescence.

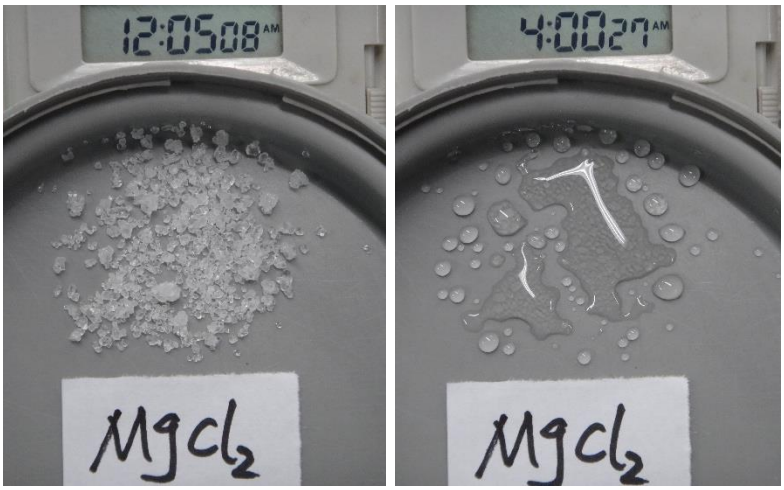

Figure 73. Melting of $MgCl_2$ by attracting water from atmosphere

Chemical reactions between concrete and deicing salts mainly consist of the substitution of hydroxyl ions for chloride ions, resulting in concrete degradation (Sutter et al. 2006). It has been reported that application of chloride solutions on concrete commonly result in decalcification of paste and altered ettringite to chloroaluminate (Lee et al. 2000). The chemical reactions between the chloride salts and concrete are summarized in Table 14.

Table 14. Chemical reactions between deicing salts and concrete (Sutter et al. 2006)

Deicing Salts	**Equations**
Sodium chloride (NaCl)	$2NaCl + Ca(OH)_2 \rightarrow CaCl_2 + 2NaOH$
Calcium chloride ($CaCl_2$)	$CaCl_2 + Ca(OH)_2 + 12H_2O \rightarrow 3CaO{\cdot}CaCl_2{\cdot}15H_2O$
Magnesium chloride ($MgCl_2$)	$MgCl_2 + Ca(OH)_2 \rightarrow CaCl_2 + Mg(OH)_2$
	$MgCl_2$ + C-S-H → $CaCl_2$ + M-S-H

In addition, ettringite growth in air voids is considered by some to reduce freeze thaw resistance (Ouyang and Lane 1999; Stark and Bollmann 2000; Arribas-Colon 2008) (Figure

74). Stark and Bollmann (2000) reported that ettringite can be formed from monosulfate during freezing and thawing cycles (Figure 75).

The mechanisms proposed include expansion due to the ettringite formation, although work by Detwiler et al. 1999 has indicated that expansion and distress occurred before the ettringite was deposited. A second mechanism is that the ability of the air voids to contain the expanding fluid is compromised because they have been filled (Ouyang and Lane 1999). A third alternative is that the smaller pores in the ettringite have a high capillary suction, thus accelerating saturation of the air void spaces and so shortening the life of the concrete (Figure 76) (Stark and Bollmann 2000). It is agreed that ettringite appearing in air voids is a clear indication of abundant water passing through the system because ettringite containing 32 moles of water can only form when adequate water is present.

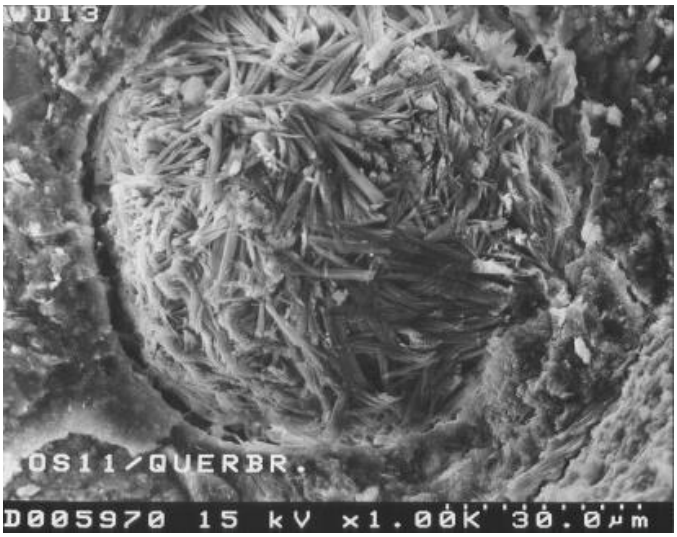

Figure 74. Air voids filled with ettringite in a damaged concrete pavement (Stark and Bollmann 2000)

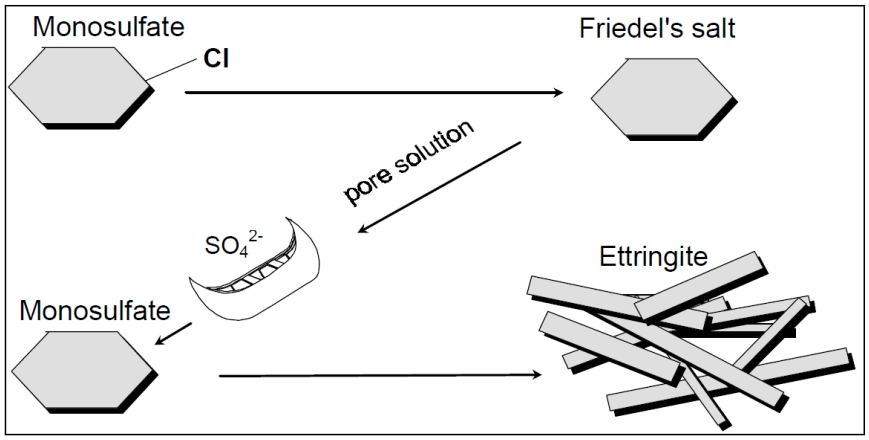

Figure 75. Mechanism to ettringite formation under frost and deicing salts (Stark and Bollmann 2000)

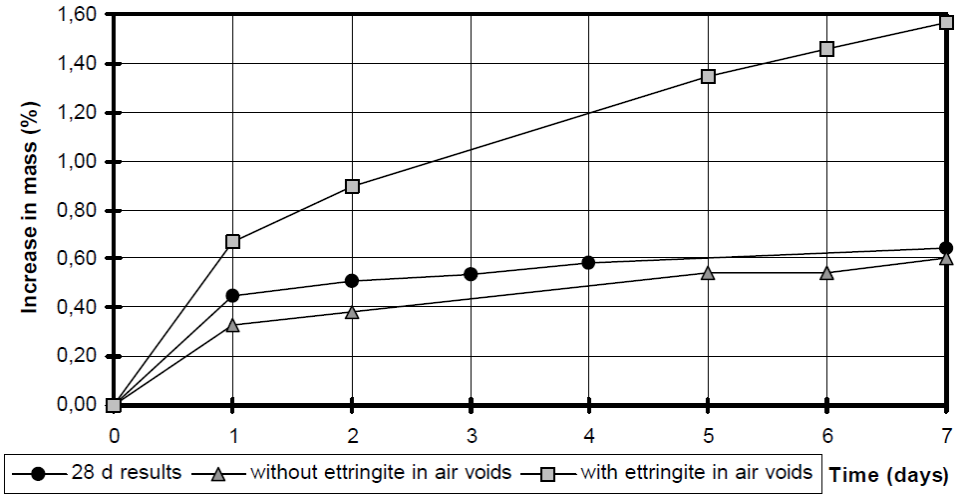

Figure 76. Capillary suction of concrete sample with and without ettringite in air voids (Stark and Bollmann 2000)

Influence of Cyclic Freezing and Thawing on Concrete Deterioration (Taylor et al. 2012)

Table 15 summarizes the four phases of cyclic freezing and thawing tests that were conducted using a modified ASTM C666 method. Each phase evaluated different sets of variables to assess their significance.

Table 15. Mix design for laboratory freezing and thawing test

Phase	Parameters Investigated	Fixed Parameters	Variables	Curing
I	• Air entraining admixture type • Fly ash • Deicing salt • Saw cutting	• Binder content: 624 pcf • Target air content: 7±1% • w/cm: 0.43	• AEA type: vinsol, tall-oil • C fly ash content: 0%, 15% • Solutions in cell: water, 3% NaCl	Half of the samples were cured in water for 14 days before drying and half were sprayed with curing compound when de-molded and left in a laboratory environment
II	• w/cm • Air content • Exposure to salt solution	• Binder content: 564 pcf	• w/cm: 0.4, 0.6 • Target air content: 3%, 6% • Samples were partially immersed in salt solution	7 days wet curing and 21 days drying before cycling started
III	• w/cm • Aggregate type • Silica fume • Saw cutting	• Binder content: 564 pcf • Target air content: 6±1%	• Binder content: 0, 3 and 5% silica fume • w/cm: 0.4, 0.5 • Coarse aggregate: gravel, limestone • One vertical face of each beam was sawn off to expose the aggregates	14 days wet curing and 28 days drying before cycling started
IV	• w/cm • Silica fume • Concentration of deicing salts and types	• Binder content: 564 pcf • Target air content: 6±1%	• Binder content: 0, 5 and 10% silica fume • w/cm: 0.38, 0.45	3 days wet curing and 28 days drying before slicing into 1 in. thick

Findings from this work have been reported elsewhere (Taylor et al. 2012).

Based on the finding of the laboratory freezing and thawing tests, the following conclusions can be drawn:

- Higher w/cm ratio samples gained more solution than the lower w/cm ratio samples during cyclic freezing and thawing tests.

- Distress was clear related to degree of saturation with higher moisture contents leading to greater risk.
- Distress was markedly increased with the use of deicing salts.
- The data from the laboratory tests indicate that the interfacial transition zone can contribute to the accelerated deterioration of joints in concrete pavements.

Influence of Pore Sizes on Paste Freezing and Thawing Durability

The pore structure of cement paste affects water transport and so potential durability of a mixture. This is also reflected in the risk of d-cracking in coarse aggregates where

- A coarse pore structure is durable because water is free to enter or drain from the system.
- A very fine pore structure is also durable because water cannot penetrate into the system.
- However, an intermediate pore structure may potentially at risk because water can enter the pores, but is difficult to evaporate out (Pigeon and Pleau 1995). Such a system then, is at a higher risk of reaching critical saturation leading to damage under freezing and thawing.

The purpose of the work conducted in this study was to look at the parallels between paste porosity and non-durable coarse aggregates.

Mercury intrusion porosimetry (MIP) was utilized to access the pore structure of a set of cement pastes with different w/cm ratios (0.3, 0.35, 0.40, 0.45, and 0.6), supplementary cementitious materials (fly ash, silica fume), and drying treatments (oven dry and air dry) (Zhang and Taylor 2013). Paste samples prepared from the same mixtures were also subjected to freeze-thaw cycles following the same preparing and curing procedures as the samples prepared for the MIP tests. Air dried samples were kept in their sealed bottles for 7 days before conducting the cyclic freezing and thawing test. Oven dried samples were kept

sealed in the bottles at 75˚F until aged 7 days. The lids were then removed and the oven-dried samples were kept in an oven at 122˚F until constant mass was achieved.

The findings that can be drawn from this study include:

- Increasing w/cm ratio increased the total porosity and pore size of hardened cement paste. Most notably the peak pore sizes in the lower w/cm mixtures were within the range indicated as problematic based on the ability to allow water to evaporate from them. The high w/cm mixture had similar peaks in the fine zone, but had a far larger peak on the coarse side, likely meaning that water is able to enter and leave the system readily easily.
- Both C fly ash and silica fume improved the freeze / thaw durability of cement paste, but that does not demonstrated from the MIP data.

There seems to be merit in pursuing this issue further, including finding ways to control the pore size distribution in paste mixtures used in pavement mixtures.

Field Investigations

Field investigations were conducted at multiple sites in Wisconsin, Iowa, Michigan, Illinois and Minnesota to observe the various forms of distress in concrete pavements. Common observations were that:

- In most cases it could be observed that drainage of the system was almost always involved. Locations where distress is occurring commonly exhibited signs of high moisture contents:
    - From below in places with a high water table and no cut-off layer below the slab
    - Trapped in joints because cracks have not opened, preventing drainage out the bottom
    - Held in joints by deicing salts that slow evaporation
    - Distress is more common in sawn joints than in formed joints (Figure 77).

Figure 77. Comparison performance of sawn joint and formed joint

- In many cases where tests were conducted the measured air contents were often lower than desired.
- Distress is commonly concentrated near intersections, likely because of higher salt dosages both because of safety concerns and because salt trucks are working both ways across the intersection.
- Distress seems to be more common in hand placed sections, likely because water has been added to make the mixture more workable, but with the side effect of increasing w/cm and degrading permeability.
- The form of distress varies between states, likely because of different practices with respect to foundation design, drainage detailing and joint sealing.

Cores from three locations were subjected to petrographic analysis and the findings are summarized below (Taylor et al. 2012).

Eau Claire, Wisconsin

One site selected in Wisconsin was at the intersection of First Avenue and Grand Avenue in Eau Claire. Grand Avenue is showing significant deterioration on the joint (Figure 78), but First Avenue is not. Both streets were built in 1997 by different contractors. Cores

were collected for petrographic analysis on this site to investigate why one street was performing well while the other was not.

Figure 78. Grand Avenue in Eau Claire, Wisconsin

Cores were taken from mid-panel locations and at joints in both streets. The concrete in both cores taken from mid-panel appeared to be in good condition. Signs of chemical attack were seen in the distressed joint, likely caused by deicing materials other than NaCl. Both cores from joints did contain ettringite in the air voids. Micrographs clearly show a concentration of cracks near the aggregate from the distress joints (Figure 79).

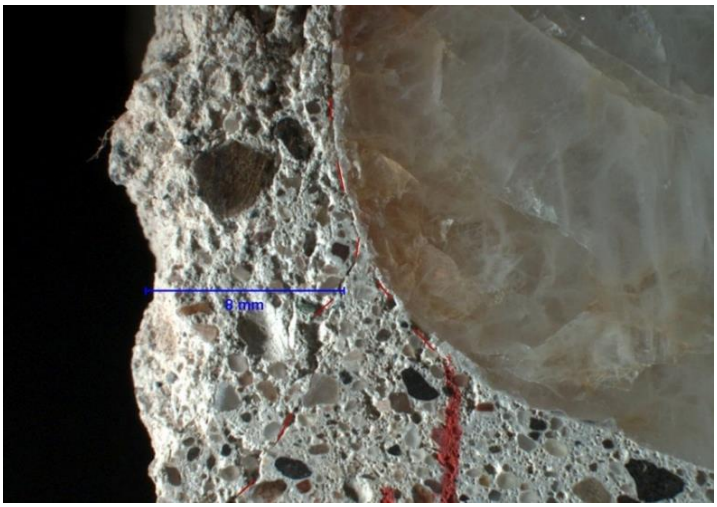

Figure 79. Cracks concentrated adjacent to the coarse aggregate for core sample from Grand Avenue in Eau Claire, Wisconsin (Taylor et al. 2012)

Ames, Iowa

This site is a two lane city street serving an office park in Ames, IA. The street was paved in 1997, and deterioration on one joint was observed in 2010 (Figure 80). Two core samples were taken from adjacent damaged and undamaged joints for petrographic analysis.

Figure 80. Field view of distressed joint

The petrographic results from this site indicate that air void systems in both cores were satisfactory. Some ettringite growth was observed in air-voids in the core from the

distressed joint indicating a high degree of saturation. Later work indicated that permeability of the base was low, and negligible when under freezing conditions (Zhang et al. 2013). It was also noted that after a snow event, the material close to the joint appeared to stay wet for longer than the mid-panel, likely because the deicing salts used would slow drying. Most notable was that the w/cm of the concrete at the distressed joint was higher than that of the non-distressed concrete (0.40-0.45 vs. 0.42-0.47) while air void systems in both cores was satisfactory. The damage is limited to a relatively short section of the road. It was calculated that the volume of concrete reflected by the distress is about the same as that from three truck-loads of material. It is feasible that a change in batching resulted in this volume of concrete not being at the same standard as the rest of the project.

Meeker County, Minnesota

Two cores were taken from Route 12 west of Minneapolis in Meeker County. One core was from a distressed joint and the other core was from a sound joint (Figure 81).

Figure 81. Core samples from Meeker County, Minnesota

The biggest difference between the cores was that the silicone sealant was debonded in the distressed core, and sound in the healthy core. This clearly points to the importance of keeping water out of the joint. In addition the w/c of the distressed cores was also higher than in the other.

Summary

Common observations from the core analyses include:

- Air voids were often filled with ettringite
- Variability in w/cm seems to be associated with risk of distress
- Increasing water content within the concrete is tied to increasing risk of distress

Discussion

If saturation of the microstructure is critical to the performance of a mixture, then it would seem logical to take every effort to reduce the permeability of the paste. This is most easily achieved by the use of a low w/cm and the appropriate inclusion of supplementary cementitious materials. The benefit of a low w/cm is clearly illustrated in the cores reported above, and in the experience of MN DOT that has been incentivizing a w/cm less than 0.40 for several years. Pavements built since this requirement was implemented have shown a marked improvement in performance (Taylor et al. 2012).

This is fundamentally correct because the capillary porosity, and so the permeability, of concrete is strongly dependent on the w/cm ratio as shown in Figure 82. For systems with a w/cm below 0.40 the amount of capillary pores due to unreacted water in well hydrated systems drops markedly (Mindess et al. 2003).

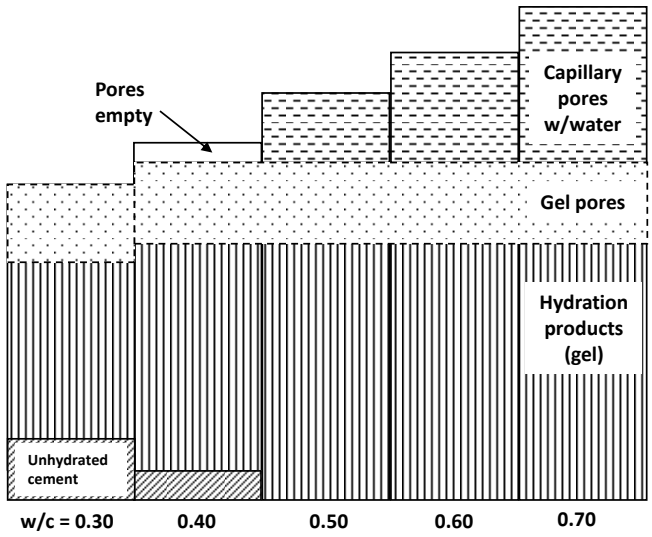

Figure 82. Volume relationship with w/cm ratio for fully hydrated cement paste (Mindess et al. 2003)

In addition, entrained air is known to contribute to the ability of concrete, either by slowing saturation or by provide pressure relief wells for expanding pore solutions. The commonly accepted required air content required for concrete to resist freezing and thawing damage is about 9±1% air by volume of mortar is based on work conducted in the 1950s by Klieger 1952. Recent research has indicated that this number is still appropriate for current materials (Ley et al. 2012). However, this is for the concrete in its final place. Modern mixtures seem to be less stable, meaning that the risk of losing significant amounts of air during placing is high. Requirements should therefore be based on measurement behind the paver, or at a minimum, with regular measurement of losses during processing.

Another approach that may be considered is to reduce permeability of the concrete at the joint face is to consider use of penetrating sealants in the joint. It has been reported that the durability of joints in concrete pavements is improved by applying sealants penetrating sealants (Golias et al. 2012). Further work is needed to define how sealants can be qualified or assessed. There are also questions about when they should be applied; when the concrete

is new or after some distress is observed, and if so – how much distress can be accommodated?

It has been observed in discussions with practitioners that the quality of inspection is also closely tied to the longevity of a pavement. One site was inspected where the only difference between distressed and sound sections was that the former was not inspected during constructed, while the latter was provided with very close scrutiny. All other parameters were nominally the same including design details, specification, materials provider and contractor.

Recommendations

Based on the findings thus far, the following recommendations are made:

- w/cm should be less than 0.40.
- Air content in the concrete in place should be greater than 5% (or spacing factor <0.08 inch).
- Detailing should ensure that water is allowed to leave the joints.
- Penetrating sealants applied to the joint faces may be considered

Future Needs

The greatest need stemming from this work is a better understanding of how to specify and select penetrating sealers. This work is ongoing.

Other details that have been raised in the discussion above include:

- What is the real contribution of ettringite-filled air-voids to the distress?
- How can moisture content be measured in small local zones near joint faces in real time?
- Does cementitious chemistry affect performance?

References

ACI Committee 318, Building Code Requirements for Structure Concrete and Commentary, ACI 318-99, ACI Committee 318 Report, American Concrete Institute, Farmington Hills, Michigan, 1999.

Arribas-Colon, M.D.M., (2008). *Investigation of Premature Distress around Joints in PCC Pavements.* Master's Thesis, Purdue University, West Lafayette, Indiana.

Darwin, D., Browning, J., Gong, L., and Hughes, R.S., (2008). "Effects of Deicers on Concrete Deterioration", *ACI Materials Journal*, Vol. 105, No. 6. pp. 622-627.

Detwiler, R. J., and Powers-Couche, L. J., (1999), "Effects of Sulfates in Concrete on Their Resistance to Freezing and Thawing", Special Publication 177-15. American Concrete Institute, Farmington Hills, Mich., pp. 219–247.

Golias, M., Castro, J., Peled, A., Nantung, T., Tao, B., and Weiss, W.J., (2012), "Can Soy Methyl Esters Improve Concrete Pavement Joint Durability?" *Transportation Research Record: Journal of the Transportation Research Board*, No. 2290, Transportation Research Board of the National Academies, Washington, D.C., pp. 60-68.

Klieger, P., (1952), "Studies of the Effect of Entrained Air on the Strength and Durability of Concrete Made with Various Maximum Size of Aggregate", Research Department Bulletin RX040, Portland Cement Association.

Lay, T., Cook, D., and Fick, G., Concrete Pavement Mixture Design and Analysis (MDA): Effect of Aggregate Systems on Concrete Properties. InTrans Project 09-353. Technical Report: 2012.

Lee, H., Cody, D.R., Cody, M.A., and Spry, G.P., (2000). "Effects of Various Deicing Chemicals on Pavement Concrete Deterioration", Mid-Continent Transportation Symposium Proceedings, pp. 151-155.

Li, W., Pour-Ghaz, M., Castro, J., and Weiss, J., (2012). "Water Absorption and Critical Degree of Saturation Relating to Freeze-Thaw Damage in Concrete Pavement Joints", *Journal of Materials in Civil Engineering*, Vol. 24, pp. 299-307.

Mindess, S., Young. J. F. and Darwin, D., (2003). Concrete. 2nd Edition, Prentice-Hall, Inc., Englewood Cliffs, NJ.

Ouyang, C., and Lane, O.J., (1999). "Effect of Infilling of Air Voids by Ettringite on Resistance of Concretes to Freezing and Thawing", *ACI Special Publication*, Vol. 177, pp. 249-262.

Pigeon, M. and Pleau, R. 1995. Durability of Concrete in Cold Climates, E & FN Spon, 244 pp.

Sutter, L., Peterson, K., Julio-Betancourt, G., Hooton, D., Van D.T., Smith, K., "The Deleterious Chemical Effects of Concentrated Deicing Solutions on Portland Cement Concrete." South Dakota Department of Transportation. Final report: 2008.

Sutter, L., Dam, T.V., Peterson, K.R., and Johnston, D.P., (2006). "Long-Term Effects of Magnesium Chloride and Other Concentrated Salt Solutions on Pavement and Structural Portland Cement Concrete", *Journal of the Transportation Research Board*, No.1979, pp. 60-68.

Sun, Z., and Scherer, W.G., (2010), "Effect of Air Voids on Salt Scaling and Internal Freezing", Cement and Concrete Research, Vol. 40, pp. 260-270.

Stark, J., Bollmann, K. (2000). Delayed ettringite formation in concrete. Nordic Concrete Research Publications, 23, 4-28.

Taylor, P., Sutter, L., and Weiss, J., Investigation of Deterioration of Joints in Concrete Pavements. InTrans Project 09-361. Final Report: 2012.

Verbeck, G. and Klieger, P., (1957). "Studies of 'Salt' Scaling of Concrete" Highway Research Board Bulletin No.150. Washington, D.C.: Transportation Research Board. 1-13.

Valenza II JJ, and Scherer G.W., (2006), "Mechanism for Salt Scaling", *Journal of the American Ceramic Society*, Vol. 89, Issue 4, pp. 1161-1179.

Zhang, J. and Taylor, P., (2012), "Investigation of the Effect of the Interfacial Zone on Joint Deterioration of Concrete Pavements", International Conference on Long-Life Concrete Pavements, Seattle.

Zhang, J. and Taylor, P., (2013), "Comparison of Pore Sizes of Cement Paste and Aggregate Using Mercury Intrusion Porosimetry", will submit to ASCE Journal of Materials in Civil Engineering.

Zhang, J. White, D.J., and Taylor, P., (2013), "A Case Study of Evaluating Joint Performance in Relation with Subsurface Permeability in Cold Weather Region", will submit to Cold Regions Science and Technology.

CHAPTER 8. GENERAL CONCLUSIONS

This dissertation provides results of work conducted investigating mechanisms that cause premature joint deterioration in concrete pavements. Both laboratory studies and field tests were conducted to identify the mechanisms of joint deterioration. Laboratory studies included freezing and thawing tests on concrete beams to evaluate the influences of water to cement (w/cm) ratio, aggregate type, air content, and silica fume on concrete frost durability. Mercury intrusion porosimetry (MIP) tests were conducted on hardened cement paste samples with different w/cm ratios and with added supplementary cementitious materials (SCMs) to compare pore sizes with pore structures of nondurable aggregates. A field investigation was conducted on a local street in Ames, Iowa to investigate the relationship between joint performance and subsurface permeability.

Conclusions

The interfacial transition zone (ITZ) appears to play an important role in the freeze thaw resistance of joints in concrete pavements. The mechanism is of distress is likely due to dissolution of the ITZ in cold conditions into salt solutions that have penetrated the ITZ layer. Laboratory tests show that concrete samples with higher w/cm ratio exhibited higher absorption and permeability than samples with lower w/cm ratios. Samples with higher w/cm ratios exhibited more salt accumulation around aggregate particles, greater distress and greater tendency for cracks to go around the aggregate.

Concrete samples mixed with limestone aggregate appeared to be more durable than concrete samples mixed with gravel likely because bond between the paste and the aggregate was improved. The laboratory studies showed that the ITZ can contribute to accelerated

deterioration of joints in concrete pavements.

Measured pore size distributions were in the range that likely allow water to be absorbed into the microstructure but evaporation rates on drying are slow, so increasing saturation and risk of damage under freezing conditions. The pore distributions were similar to those of aggregates known to be prone to D-cracking. As expected, both pore sizes and total porosity of hardened cement paste increases with increasing w/cm ratio. Both Class C fly ash and silica fume improved the freeze/thaw resistance of cement paste.

Field investigations found that the distressed joint is likely related to a combination of ponding, salts collecting in the joint, and differential permeability between joint faces. Field permeability tests results indicate that permeability of the base was low, and negligible under freezing conditions. It was also noted that after a snow event, the material close to the joint appeared to stay wet for longer than the mid-panel, likely because the deicing salts would slow drying rates. Most notable was that the w/cm of the concrete at the distressed joint was higher than that of the non-distressed concrete (0.40-0.45 vs. 0.42-0.47) while air void systems in both cores were satisfactory. Some ettringite growth was observed in air-voids in the core from the distressed joint indicating a high degree of saturation.

Recommendations for Future Work

The following are recommendations for future research:

- Practical approaches to controlling the effect of the concrete interfacial transition zone need to be investigated.
- The effect of paste pore size distribution on water movement should be investigated further.

- The real contribution of ettringite-filled air-voids to distress needs to be better understood.
- Develop possible approaches to measure the moisture content of concrete in small local zones near joint faces in real time.
- The benefits of different sealants, and methods to evaluate their quality needs to be better understood.

ACKNOWLEDGEMENTS

First and foremost, many people deserve my greatest gratitude which cannot be expressed in a few words. I must give my deepest appreciation to my major professors Dr. Peter Taylor and Dr. David White who provided guidance and supervision through varies means during this research. This dissertation could not have been be completed without their valuable help along with that of Dr. Christine White. I would like to thank Dr. Kejin Wang, Dr. Halil Ceylan, and Dr. Tom Rudolphi who served as my committee members throughout the study, and their invaluable comments and suggestions have greatly improved the quality of the study.

The financial support from Federal Highway Administration (FHWA) and Transportation Pooled Found (TRF) are greatly appreciated. Special thanks go to Bob Steffes and the other PCC lab staff for helping me with the laboratory tests.

I would like to express my eternal appreciation towards my parents who have always been there for me with unconditional support and encouragement. Thank you for being ever so understanding and supportive. Your encouragement has pushed me to become a better student and researcher.

Last, but in no sense least, I would like to thank my dear friends and colleagues. Your companionship made my days at Iowa State University more enjoyable and fruitful. I wish you all the best in everything you do and hope our paths can cross again.